Dissertation

zur Erlangung des Doktorgrades

der Fakultät für Chemie und Pharmazie der

Ludwig-Maximilians-Universität München

Molecular imaging and radionuclide therapy in non-thyroidal tumors after mesenchymal stem cell- mediated sodium/iodide symporter (NIS) gene transfer

von

Kerstin Knoop
aus Darmstadt

2014

Erklärung

Diese Dissertation wurde im Sinne von § 7 der Promotionsordnung vom 28. November 2011 von Frau Professor Dr. C. Spitzweg betreut und von Herrn Professor Dr. E. Wagner vor der Fakultät für Chemie und Pharmazie vertreten.

Eidesstattliche Versicherung

Diese Dissertation wurde eigenständig und ohne unerlaubte Hilfe erarbeitet.

München, ...

.....

Dissertation eingereicht am	28.03.2014
1. Gutachter:	Prof. Dr. Ernst Wagner
2. Gutachterin:	Prof. Dr. Christine Spitzweg
Mündliche Prüfung am	08.05.2014

Meiner Familie

The Answer to the Ultimate Question of Life, the Universe and Everything is 42.

(The Hitchhiker´s Guide to the Galaxy by Douglas Adams)

Table of contents

1 Introduction 1

1.1 Cancer gene therapy 1

1.2 Tumor biology 2

1.2.1 Role of tumor stroma in tumor biology 2

1.2.2 Role of chemokines in tumor development 4

1.3 Mesenchymal stem cells (MSC) 5

1.3.1 Characterization of MSCs 5

1.3.2 MSCs as gene transfer vehicles 6

1.4 The sodium iodide symporter (NIS) 9

1.4.1 Characterization of the sodium iodide symporter (NIS) 9

1.4.2 The sodium iodide symporter as theranostic gene 10

1.5 Aims of the thesis 14

2 Chapter 1 Image-guided, tumor stroma-targeted ^{131}I therapy of hepatocellular cancer after systemic mesenchymal stem cell-mediated NIS gene delivery 15

2.1 Abstract 16

2.2 Introduction 17

2.3 Methods 19

2.4 Results 24

2.5 Discussion 32

2.6 Acknowledgements 36

3 Chapter 2 Stromal targeting of sodium iodide symporter using mesenchymal stem cells allows enhanced imaging and therapy of hepatocellular carcinoma 37

3.1 Abstract 38

3.2 Introduction 39

3.3 Methods 41

3.4 Results 44

3.5 Discussion 52

3.6 Acknowledgements 56

4 Chapter 3 Effective ^{131}I therapy after mesenchymal stem cell-mediated stromal targeting of the sodium iodide symporter in an orthotopic hepatocellular cancer model 57

4.1 Abstract 58

4.2 Introduction 59

4.3 Material and methods 61

4.4 Results 64

4.5 Discussion 70

4.6 Acknowledgements 70
5 Chapter 4 Mesenchymal stelm cell (MSC)-mediated, tumor stroma-targeted radioiodine therapy of metastatic colon cancer using the sodium iodide symporter (NIS) as theranostic gene 74
5.1 Translational Relevance 75
5.2 Abstract 76
5.3 Introduction 77
5.4 Material and methods 79
5.5 Results 82
5.6 Discussion 89
5.7 Acknowledgements 93
6 Summary 94
7 Publications 97
7.1 Original papers 97
7.2 Manuscripts in preparation 97
7.3 Oral Presentations 98
7.4 Poster Presentations 99
7.5 Awards 101
8 References 102
9 Acknowledgments 114

1 Introduction

1.1 Cancer gene therapy

Cancer comprises more than 100 diseases with diverse phenotypes that ultimately lead to approximately 13% of all human deaths worldwide. Cancer, referred to as a malignant neoplasm, is characterized by uncontrolled and abnormal growth of cells. These cells are able to spread locally or through the bloodstream and lymphatic system to other parts of the body. In general, malignant cancers cause significant morbidity and are lethal to the host if not treated.

Based on its complex biology, the field of cancer research has investigated numerous therapeutic approaches. One major field is gene therapy, which was first evaluated in 1972, and has become more and more popular over the last 20 years. Gene therapy consists of the introduction of genetic material into cells for a therapeutic purpose. The initial aim of the gene therapy field was the correction of inherited genetic diseases by providing to the targeted cells a functional copy of the deficient gene responsible for the disease (Touchefeu *et al.* 2010). One central issue associated with gene therapy approaches is the method used for delivery of the therapy gene. Gene delivery can occur by two main classes of methods – viral and non-viral systems. The viral method makes use of recombinant viruses as gene delivery vehicles which bind to their host cells and specifically introduce their genetic material into these cells as part of their replication cycle. Most viral vector approaches have focused on adenovirus, adeno-associated virus, retrovirus, herpes simplex virus and pox virus. The major hurdles of effective oncolytic virotherapy, in particular after systemic application, have been antiviral immune responses, inefficient viral spread within the tumor and significant virus pooling in the liver, reducing the levels of viable virus reaching the tumor resulting in limited transduction efficiency (Cattaneo *et al.* 2008).

Non-viral gene delivery systems include the use of DNA-complexes. The DNA carriers used include: oligonucleotides, liposomes, dendrimers and inorganic nanoparticles. These are all generally polycationic molecules that are able to build a stable complex with the negatively charged therapeutic nucleic acid based on electrostatic interaction to avoid enzymatic degradation by nucleases in the blood stream and destabilization by electrostatic interactions with serum proteins (Burke and Pun 2008). The surface of these complexes is often modified in a chemical or biological way for specific or active targeting.

More recently the concept of stem cell driven therapy has been included in the field of non-viral gene delivery methods. Stem cells have the intrinsic ability to “home” to growing tumors and are hypoimmunogenic. Therefore, they can be used as a “Trojan Horse” to deliver gene therapy deep into tumor environments. They can also serve as carriers for nanoparticles to

allow cell tracking and simultaneous cancer detection. This thesis focused on the potential use of engineered mesenchymal stem cells as therapy vehicles for the treatment of solid tumors.

1.2 Tumor biology

1.2.1 Role of tumor stroma in tumor biology

The hallmarks of cancer constitute an organizing principle that provides a logical framework for understanding the remarkable diversity of neoplastic diseases. They include sustaining proliferative signaling, evading growth suppressors, resting cell death, enabling replicative immortality, inducing angiogenesis and activating invasion and metastasis (Hanahan and Weinberg 2000; 2011). But importantly, tumor cells are only able to exist within a complex tumor environment called tumor stroma. The tumor stroma is composed of various compartments and cell types including endothelial cells, pericytes, fibroblasts, infiltrating leukocytes, which are all embedded in an extensive extracellular matrix (ECM). Many of the characteristics of tumors detailed above are provided in part by interaction of the tumor stroma with the cancer cells.

The most prominent cell type in the tumor stroma are cancer-associated fibroblasts (CAF). They belong to the tumor-associated mesenchymal stem cell types and have their origin from resident local fibroblasts or bone marrow-derived progenitor cells. Because of their different origins, CAFs show high heterogeneity in marker expression, but the expression of α-smooth muscle actin (α-SMA), platelet-derived growth factor (PDGF) receptor and fibroblast specific protein (FSP)-1 is found to overlap in most tumor types (Anderberg *et al.* 2009; Sugimoto *et al.* 2006). Tumor cells can be directly stimulated by CAFs via production of various growth factors [hepatocyte growth factors (HGF), epidermal growth factor (EGF)], hormones and cytokines [stromal-derived factor (SDF)-1α (CXCL12), interleukin-6 (IL6)] in a context-dependent manner (Bhowmick *et al.* 2004; Engels *et al.* 2012; Olumi *et al.* 1999; Orimo *et al.* 2005; Orimo and Weinberg 2006). CAFs can also stimulate tumor growth through production of insulin-like growth factor-1 and -2 that in turn stimulate proliferation and promote tumor cell survival. CAFs also express collagen A, which is essential for construction of the ECM, resulting in a stronger general structure of the stroma and resulting in a physical barrier for lymphocytes and macrophages, as well as chemotherapeutical reagents (Engels *et al.* 2012; Li *et al.* 2007). Stem and progenitor cells from the bone marrow are now seen as important factors in tumor progression in that they can act as a key source for tumor-associated stromal cells (Hanahan and Weinberg 2000; 2011). The progenitor cells migrate into the tumor and differentiate into various stromal cell types.

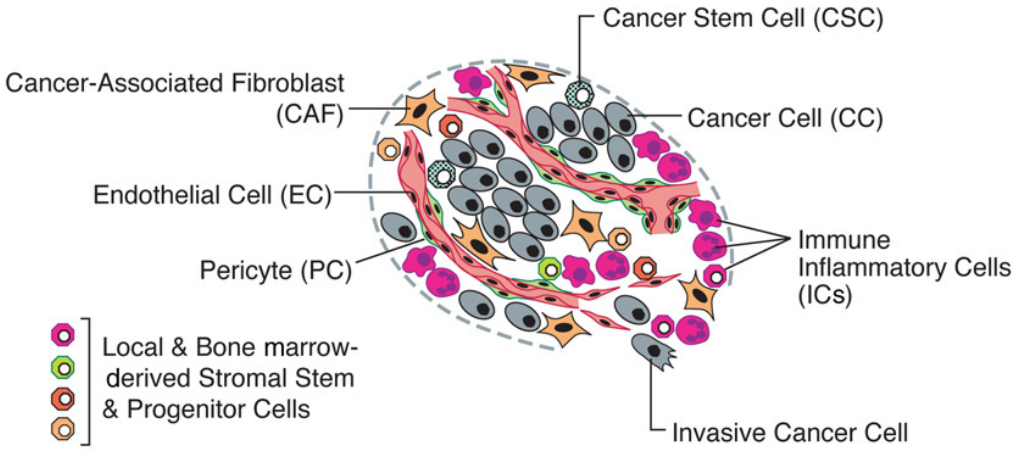

Figure 1 Schematic illustration of the tumor microenvironment in most solid tumors. The parenchyma and stroma of tumors contain distinct cell types and subtypes that collectively enable tumor growth and progression. The immune inflammatory cells present in tumors can include both tumor-promoting as well as tumor-killing subclasses (Hanahan and Weinberg 2011).

Thus the tumor stroma is essential for tumor initiation, growth and progression. Angiogenesis is induced early during the development of invasive cancers and is a key factor in tumor growth, because the supply of oxygen and nutrients has to be ensured. The interaction between the tumor stroma and cancer cells stimulates the expression of proangiogenic factors including vascular endothelial growth factor (VEGF), CXCL12 and matrix-remodeling protein matrix metalloproteinases (MMP)-2 and MMP9, which are essential for blood vessel development. VEGF is involved in orchestrating new blood vessel growth during embryonic and postnatal development. In adults it is responsible for homeostatic survival of endothelial cells and is regulated by hypoxia as well as by oncogene signaling (Hanahan and Weinberg 2000; 2011). The blood vessels produced within tumors are abnormal in their function and have a leaky structure, which allows molecules to freely traverse between the interstitial space and blood capillaries.

The second important component for tumor progression is suppression of an immune response. The tumor tissue produces many chemokines like CCL2 and CSF1 which result in an immune response of the body (Mueller and Fusenig 2004). Especially tumor associated-macrophages (TAM) play an important role in tumor progression. They exhibit some anti-tumorigenic proteins, but also express growth factors like VEGF, HGF, PDGF, TGFβ, and cytokines such as TNFα and IL8. In contrast, TAM also secretes MMP2 and MMP9 resulting in a proangiogenic and prometastatic effect (Bhowmick and Moses 2005; Gao and Mittal 2009; Mueller and Fusenig 2004). The invasion of lymphocytes, dendritic cells, neutrophils, eosinophils, mast cells and monocytes leads to enhanced tumor progression.

1.2.2 Role of chemokines in tumor development

Chemokines are chemotactic cytokines that cause the directed migration of leukocytes and are induced by inflammatory cytokines and growth factors (Tanaka *et al.* 2005). Chemokine signaling results in transcription of target genes, which are involved in cell invasion, motility, interactions with the ECM and survival (Viola *et al.* 2012). Chemokines are responsible for the recruitment of immune cells to organize the anti-tumor or inflammatory response via a chemokine gradient (Balkwill 2004). Chemokines are also able to sustain tumor survival, promote progression and drive metastasis. For example, the chemokine CCL5, also called RANTES (regulated on activation, normal T-cell expressed and secreted), is normally involved in inflammation and is expressed by inflammatory tissue. In tumors, CCL5 has been shown to play an important role in tumor progression and invasion, and is also involved in the recruitment of tumor-associated macrophages (TAM) (Nelson *et al.* 1993; Von Luettichau *et al.* 1996). CCL5 expression is found in many tumor entities such as melanoma, prostate cancer, Hodgkin´s lymphoma and breast cancer (Fischer *et al.* 2003; Konig *et al.* 2004; Luboshits *et al.* 1999; Mrowietz *et al.* 1999). CCL5 signals through the chemokine receptors CCR1, CCR3 and CCR5 (Tanaka *et al.* 2005).

A pro-malignant activity of CCL5 was identified in experimental breast cancer models. Soria *et al.* showed high expression of CCL5 and CCL2 in breast tumor cells at primary tumor sites as well as in metastases, whereas only minimal expression was found in normal breast epithelial cells. These data indicate that CCL2 and CCL5 expression is needed in the course of malignant transformation and suggest the important role of chemokines in breast cancer development and progression (Soria *et al.* 2012). Furthermore, in a murine pancreatic tumor model and a breast cancer mouse model inhibition of the CCR5 receptor resulted in a reduction of CCL5 production and thereby reduced growth of tumor and metastases (Stormes *et al.* 2005; Tan *et al.* 2009).

Importantly for the focus of this thesis, CCL5 is not only expressed by tumor cells, Karnoub *et al.* have also shown an induction of CCL5 by mesenchymal stem cells in a breast cancer mouse model. Breast cancer cells were found to stimulate the *de novo* secretion of CCL5 from mesenchymal stem cells, which then acts in a paracrine fashion on cancer cells to enhance their motility, invasion and metastasis (Karnoub *et al.* 2007).

1.3 Mesenchymal stem cells (MSC)

1.3.1 Characterization of MSCs

*S*tem cells have unlimited self-renewal capacity and are able to produce more differentiated progenitors (embryonic and adult stem cells). Bone marrow-derived stem cells are the best characterised and most accessible type of adult stem cells. They can be subdivided into haematopoietic stem cells that produce progenitors for all types of mature blood cells, and mesenchymal stem cells (MSC). The term “mesenchymal” as opposed to “epithelial” or “parenchymal” defines a progenitor cell with fusiform shape and able to actively move. MSCs are multipotent progenitors with the ability to differentiate into cells of mesenchymal tissue including bone cartilage, fat, tendon, muscle and marrow stroma (Pittenger 2008). They play an important role in retention and reconstruction of the tissue integrity in the course of normal cell turnover as well as in wound healing. They are easy to isolate from the bone marrow, the main source of MSCs (0.01% - 0.001%), but they can also be extracted from blood or fat (Korbling and Estrov 2003; Kumar *et al.* 2008).

One major issue associated with MSCs is their identification as no specific marker or simple assay is currently available. The “International Society of Cellular Therapy” has defined the hallmarks of MSCs, which include their ability to adhere to plastic, a fibroblast-like morphology, and the ability to undergo differentiation toward chondrogenic, adipogenic and osteoplastic lineages. MSC should show positive staining for markers such as CD29, CD44, CD73, CD90, CD106, but they should be negative for markers of the hematopoietic lineage, including the lipopolysaccharide receptor CD14, CD34 and the leukocyte common antigen CD45 (Pittenger 2008). Furthermore, MSCs should express low levels of the major histocompatibility complex (MHC) I, and should lack expression of MHC II as well as the costimulatory molecules CD80, CD86 and CD40 (Kumar *et al.* 2008).

MSCs play an important role in tissue repair based on their ability to differentiate into various cell types and through paracrine signalling, which generally lead to reduced inflammation, enhanced angiogenesis and the induction of cell migration and proliferation (Gnecchi *et al.* 2008). They secrete many known mediators of tissue repair including growth factors, cytokines and chemokines, specifically VEGF, PDGF, HGF and TGF-β and thereby facilitate the recruitment of fibroblasts and host stem cells (Hocking and Gibran 2010). The potential of MSCs to differentiate into required cell types was shown by Conrad *et al.* in a murine lymphatic edema model resulting in the formation of lymphoendothelial cells for a functional lymphatic vasculature after systemic MSC injection (Conrad *et al.* 2009).

1.3.2 MSCs as gene transfer vehicles

The following properties make MSCs ideal therapeutic cellular carriers: they are relatively easy to isolate and expand *in vitro*, they show easy handling for *ex vivo* genetic modification; autologous transplantation in patients is possible (overcome issues of host immune responses) and they also show hypoimmunogenicity (and are thus also suitable for allogenic transplantations) (Tang *et al.* 2010). The migration behaviour and distribution pattern of MSCs show clear differences in healthy versus tumor-bearing mice. After systemic injection in healthy mice MSCs are predominantly found in lung at an early stage and later in spleen as well as thymus, lymph nodes, skin, brain, salivary glands, intestine and sometimes also in the bone marrow (Pereira *et al.* 1998; Von Luttichau *et al.* 2005). After systemic injection into mice bearing solid tumors, MSCs show strong preferential migration towards sites of inflammation, injury and cancer. This tropism of MSCs for tumors is thought to result from the fundamental role that MSCs play in the context of tissue repair. However, some recruitment to non-tumor tissues may also occur.

Tumors have been described as sites of tissue damage or “wounds that never heal”, as well as sites of potential inflammatory cytokine and chemokine production. These properties are thought to underlie the general tumor tropism for MSCs (Dvorak 1986). In a pancreatic insulinoma mouse model, Direkze *et al.* demonstrated that 25% of fibroblasts in the tumor stroma were of bone marrow origin (Direkze *et al.* 2004). A series of animal studies have demonstrated selective homing of MSCs to gliomas (Dai *et al.* 2007), pulmonary metastases of lung cancer (Mohr *et al.* 2008), breast cancer metastases (Dwyer and Kerin 2010), ovarian cancer (Komarova *et al.* 2006) and melanoma (Studeny *et al.* 2004). It is thought that MSCs play important roles in the later stages of stromal development as regulators of desmoplastic reactions (Hall *et al.* 2007). To date, the exact mechanisms involved in MSC homing into tumors is not completely understood, but it is assumed that the biology is similar to that seen in leukocyte recruitment. MSC adhesion to the vascular endothelium is an early step in homing of circulating MSCs to tumor tissue. High levels of TNF-α have been reported in tumor tissue, which is essential for the upregulation of vascular cell adhesion molecule-1 (VCAM-1) and other key molecules needed for efficient recruitment to endothelial cells. Similar effects can be triggered by IL-1β and IFN-γ (Teo *et al.* 2012; Uchibori *et al.* 2013).

In this context, the following cytokine/receptor pairs and ECM proteins are thought to play a role: SDF-1/CXC chemokine receptor-4 (CXCR4), monocyte chemotactic protein-1/chemokine (C-C motif) receptor 2; hepatocyte growth factor/c-met and vascular endothelial growth facor (VEGF)/VEGF receptor (Dwyer *et al.* 2007; Forte *et al.* 2006; Menon *et al.* 2007; Schichor *et al.* 2006; Son *et al.* 2006).

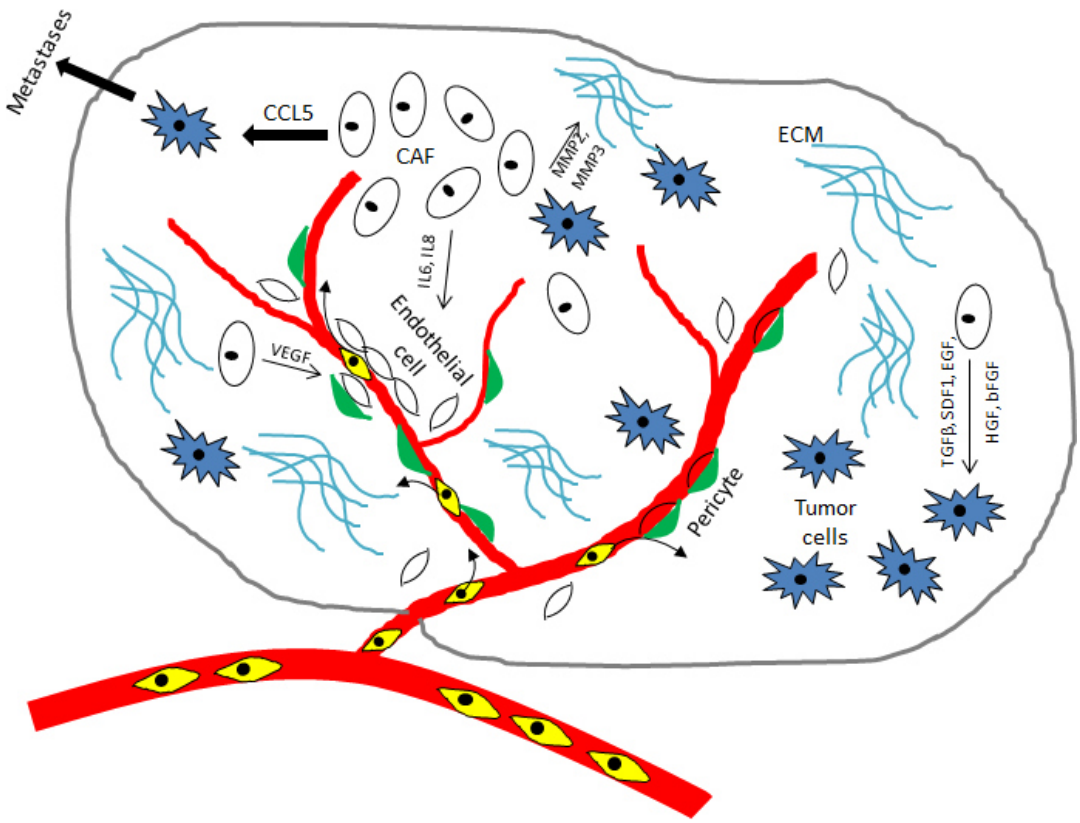

Figure 2 Interactions of MSCs with the tumor microenvironment. Tumors produce various chemokines similar to the process of wound healing or inflammation and thereby stimulate MSC recruitment from the bone marrow as well as from the blood stream in to the tumor stroma. ECM – extra cellular matrix; CAF – cancer associated fibroblasts (Based on the thesis of Zischek 2009)

Based on the inherent ability of MSCs to migrate to tumors while avoiding immune clearance, they represent promising gene delivery vehicles. The main challenge is to ensure that MSCs retain their fundamental properties of migration, differentiation and hypoimmunogenicity after genetic modification. To date, in the cancer gene therapy field, MSCs have been used as gene delivery vehicles for suicide-, apoptosis-, anti-angiogenesis-, immune-stimulatory genes and oncolytic viral vectors (Chen *et al.* 2008; Dwyer *et al.* 2011; Loebinger *et al.* 2009a; Niess *et al.* 2011; Ren *et al.* 2008; Zischek *et al.* 2009).

Conrad *et al.* used MSCs stably transfected with a reporter or therapeutic transgene under the control of the angiogenesis-specific Tie2 promoter which resulted in selective transgene expression in angiogenic “hot spots” in tumors. MSCs stably transfected with the therapeutic gene herpes simplex virus thymidine kinase (HSV-TK) under the control of the Tie2 promoter/enhancer were recruited to the vasculature of spontaneous breast cancer tumors or orthotopic pancreatic tumors and developed endothelial-like characteristics. Treatment with the prodrug ganciclovir (GCV) resulted in a significant reduction of primary tumor growth and an improved survival in both tumor models (Conrad *et al.* 2011; Zischek *et al.* 2009).

In another tumor stroma-specific approach, MSC stably expressing HSV-TK under the control of the tumor stroma-specific CCL5 promoter showed significant reduction of the primary tumor growth and dramatically reduced the incidence of metastases in an orthotopic pancreatic tumor model (Conrad *et al.* 2011; Zischek *et al.* 2009). A direct comparison of the Tie2 and CCL5 targeting strategies in an orthotopic model of hepatocellular carcinoma showed a suppression in tumor growth in both cases, but the CCL5 approach was more effective (Niess *et al.* 2011).

In another experimental approach, Kim *et al.* used human umbilical cord-blood derived MSCs (UCB-MSC) as gene transfer vehicles for glioma therapy. UCB-MSCs were engineered to deliver a secretable trimeric form of tumor necrosis factor-related apoptosis-inducing ligand (stTRAIL) via adenoviral transduction mediated by cell-permeable peptides. Intratumoral injection of engineered UCB-MSC with TRAIL resulted in a significantly inhibited tumor growth and improved survival of glioma-bearing mice (Kim *et al.* 2008). In a more recent study, MSC were transduced with a lentiviral vector encoding stTRAIL and used for treatment in a HCC xenograft mouse model. After subcutaneous injection, MSC-TRAIL localized to the tumors, inhibited tumor growth and thereby significantly improved survival (Deng *et al.* 2014).

The goal of this thesis was evaluation of MSCs as gene delivery vehicles for a tumor-targeted expression of a theranostic gene. Based on its dual function as reporter and therapy gene, the sodium iodide symporter (NIS) was used initially for noninvasive imaging of MSC recruitment and whole body biodistribution as well as localization, level and duration of NIS expression after systemic application of NIS-transduced MSCs. In parallel, the accumulation and therapeutic efficacy of ^{131}I was examined in the context of systemic MSC-mediated NIS gene transfer.

1.4 The sodium iodide symporter (NIS)

1.4.1 Characterization of the sodium iodide symporter (NIS)

The sodium iodide symporter (NIS) is responsible for active uptake of iodide into the thyroid gland. It belongs to the sodium/solute symporter family (SSF) or solute carrier family 5 (SCLA5A). NIS is an intrinsic plasma membrane glycoprotein with 13 transmembrane domains and mediates the active transport of iodide via the basolateral membrane into thyroid follicular cells. The symporter cotransports one I^- anion against its electrochemical gradient together with two Na^+ ions along their electrochemical gradient. The functionality of NIS is dependent on the electrochemical sodium gradient that is maintained by the oubain-sensitive Na^+/K^+ ATPase pump. NIS expression is mainly regulated by thyroid stimulating hormone (TSH), which initiates a G-protein-mediated signalling cascade at the TSH receptor resulting in an increase of NIS mRNA and protein in thyroid follicular cells. TSH also regulates the post-transcriptional phosphorylation and plasma membrane targeting of NIS (Riedel *et al.* 2001). The process of iodide organification describes the oxidation of iodide by the thyroid peroxidase (TPO) in the presence of H_2O_2 and the covalent binding to the tyrosyl residues of thyroglobulin (Tg). The iodinated tyrosyl residues couple the thyroid hormones tri-iodithyronine (T3) and tetra-iodothyronine (T4) and store them in the colloid space until Tg is taken up in thyroid follicular cells and hormones are released into the blood stream. Once there, they play important roles in metabolism, growth and maturation of various organ systems, especially at the nervous system (Hingorani *et al.* 2010; Spitzweg and Morris 2002).

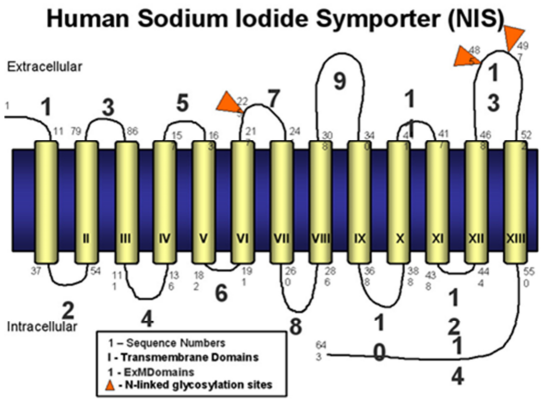

Figure 3 Schematic illustration of the sodium iodide symporter (NIS). With permission reproduced from Spitzweg *et al.* (2002)

Apart from the thyroid gland, NIS is also normally expressed in the stomach, salivary glands and lactating mammary glands. The endogenous NIS expression in extra-thyroidal tissues is not regulated by TSH and is present at a lower level than in the thyroid gland (Spitzweg and Morris 2002). NIS-mediated iodide transport can be inhibited by the Na^+/K^+-ATPase inhibitor ouabain, as well as perchlorate (ClO_4^-) and thiocyanate (SCN^-) (Spitzweg and Morris 2002).

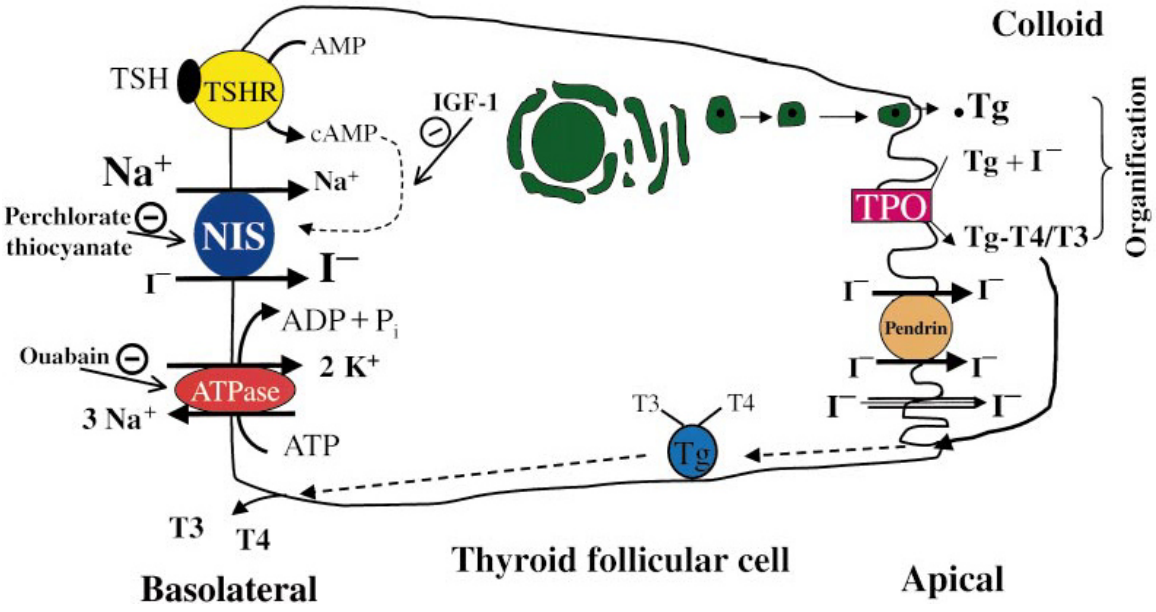

Figure 4 Schematic illustration of a thyroid follicular cell showing the key aspects of thyroid iodine transport and thyroid hormone synthesis. With permission by (Spitzweg and Morris 2002).

1.4.2 The sodium iodide symporter as theranostic gene

NIS represents one of the oldest and most successful targets for molecular imaging and targeted radionuclide therapy. In differentiated thyroid carcinomas functional NIS expression allows postoperative localization and ablation of the thyroid remnant as well as metastases. This has been successfully used for more than 70 years in the management of thyroid cancer patients. Due to organification of therapeutic radioiodine in follicular thyroid cancer cells the tumoral iodide retention time is substantially prolonged leading to sufficiently high tumor absorbed doses of ^{131}I thereby providing clinicians with the most effective form of systemic anticancer radiotherapy available today. In the routine management of patients with differentiated thyroid cancer, radioiodine whole body imaging is able to visualize local and metastatic residual or recurrent disease and quantification of tracer uptake allows for exact dosimetric calculations of tumor absorbed doses for ^{131}I before therapeutic ^{131}I application, thereby aiming at maximal therapeutic efficacy at minimal toxicity in a personalized manner. NIS-based thyroid cancer radioiodine therapy is a clinically already approved anticancer therapy with a well-understood therapeutic window and safety profile (Hingorani *et al.* 2010; Spitzweg *et al.* 2001b; Spitzweg and Morris 2002).

Cloning and characterization of the NIS gene has provided us with a powerful new reporter and therapy gene that allowed the development of a promising cytoreductive gene therapy strategy based on targeted NIS gene transfer in extrathyroidal tumors followed by the diagnostic or therapeutic application of radionuclides. It gives us the possibility to investigate

its expression and regulation in thyroidal and non-thyroidal tissues. In its dual role as diagnostic and therapeutic gene, NIS has many advantages for the use in cancer gene therapy strategies:

1. Normal human gene and protein: NIS expression in cancer cells is unlikely to be toxic or to elicit a significant immune response that could limit its efficacy.
2. Its dual function: NIS as reporter gene allows non-invasive imaging of functional NIS expression by ^{123}I-scintigraphy, ^{123}I-SPECT or ^{124}I-PET-imaging, as well as exact dosimetric calculations before proceeding therapeutic application of ^{131}I.
3. High degree of specificity: Extrathyroidal NIS expression is very low not causing significant morbidity after ^{131}I application, as known from the extensive experience with radioiodine therapy in thyroid cancer.
4. High degree of efficacy: The NIS-based radioiodine therapy in thyroid cancer is already in clinical use with a well-understood therapeutic window and safety profile.
5. High bystander effect: The NIS gene therapy concept is associated with a substantial bystander effect based on the crossfire effect of the beta-emitter ^{131}I with a path length of up to 2.4 mm. A bystander effect is desirable for any kind of gene therapy, because it reduces the level of transduction efficiency required for a therapeutic response.

One of the main advantages of the NIS gene is its applicability as a reporter gene that may be employed for real-time non-invasive assessment of biodistribution, gene expression and replication of various vector systems. Moreover, it mediates the transport of readily available radionuclides, such as ^{123}I, ^{124}I, ^{125}I, ^{131}I, ^{99m}Tc, ^{188}Re, ^{211}At or ^{18}F-TFB. Several investigators have studied the potential of NIS as reporter gene in various applications, demonstrating that *in vivo* imaging of radioiodine accumulation correlates well with the results of *ex vivo* gamma counter measurements as well as NIS mRNA and protein analyses (Dwyer *et al.* 2005a; Dwyer and Kerin 2010; Richard-Fiardo *et al.* 2012; Spitzweg *et al.* 2000; Willhauck *et al.* 2007b; Willhauck *et al.* 2008a; Willhauck *et al.* 2008c). ^{123}I-scintigraphy, ^{123}I-SPECT (single-photon emission computed tomography) and ^{124}I-PET (positron emission tomography) imaging were usually used in preclinical imaging experiments. Nuclear imaging modalities, such as SPECT or PET, reveal the 3-dimensional distribution of radiopharmaceuticals and combine excellent sensitivity and high resolution with excellent tissue penetration as compared to 2-dimensional gamma camera imaging (Grunwald *et al.* 2013c; Klutz *et al.* 2011a; Richard-Fiardo *et al.* 2012). For exact anatomical identification of tracer uptake regions, especially in orthotopic and metastatic tumor models with small tumors, images can be correlated with CT (computer tomography) or MRT (magnetic resonance tomography).

In pioneering studies by J.C. Morris and C. Spitzweg, the NIS gene therapy concept was first evaluated in a subcutaneous prostate cancer model in mice. Using a replication-incompetent adenovirus, where NIS is driven by the prostate-specific antigen (PSA) promoter to achieve prostate-specific iodide accumulation, they achieved a significant therapeutic effect after radioiodine application (Spitzweg *et al.* 2000; Spitzweg *et al.* 1999). To this end, the NIS gene therapy concept was evaluated in other non-thyroidal tumor models. For this purpose, tissue-specific promoters were investigated such as alpha-fetoprotein (AFP) promoter, carinoembryonic antigen (CEA) promoter and the calcitonin promoter for specific NIS expression in liver, colon and medullary thyroid cancer cells, respectively (Cengic *et al.* 2005; Scholz *et al.* 2005; Willhauck *et al.* 2008c). After the proof of principle of the NIS gene therapy concept, the next step was further preclinical evaluation in several animal models like rats and beagle dogs before a first phase I clinical study was initiated on radioiodine therapy of locally recurrent prostate cancer after local NIS gene transfer (Barton *et al.* 2008; Dwyer *et al.* 2005b).

The next critical step towards clinical application of the NIS gene therapy concept has to be the evaluation of gene transfer methods that allow sufficient tumor-selective transgene expression levels not only after local but also after systemic application to reach metastases.

Therefore, various non-viral gene delivery systems have been evaluated until now. Delivering genes to target organs with synthetic vectors is a vital alternative to virus-based methods. For systemic delivery polycationic molecules are used to condense DNA into sub-micrometer particles termed polyplexes, which are efficiently internalized into cells, while DNA is protected from nucleases. Several polycations, like polyethylenimine (PEI), bear an intrinsic endosomic mechanism, which allows the transition of the polyplex from the endosome to the cytoplasm (Meyer and Wagner 2006). Non-viral vectors can easily synthesized and convince especially by their absent immunogenicity and enhanced biocompatibility. Using biodegradable branched polycations complexed with a NIS-expressing plasmid, Klutz *et al.* demonstrated iodide accumulation in subcutaneous HCC xenograft tumors in nude mice after intravenous injection. The iodide uptake activity was further high enough for a significant therapeutic effect of ^{131}I resulting in an improved survival (Klutz *et al.* 2009). In a more recent study, tumor-selective iodide uptake and therapeutic efficacy of radioiodine was observed in a HCC xenograft mouse model after systemic injection of novel polyplexes based on linear polyethylenimine (LPEI), shielded by polyethylenglycol (PEG) and coupled with an epidermal growth factor receptor-specific ligand GE11 (LPEI-PEG-GE11) which were complexed with a NIS expressing plasmid resulting in active ligand-mediated tumor targeting (Klutz *et al.* 2011a).

Adenovirus Type 5 (Ad5) is one of the most powerful gene vectors in gene therapy approaches. Its cellular internalization depends on the presences of the Coxsackie- and

Adenovirus Receptor (CAR), which is known to be down-regulated especially in aggressive, metastatic cancers. Genetically engineered replication-selective adenoviruses represent very efficient gene transfer vehicles with the advantage of potentiating therapeutic efficacy of gene therapy by its own oncolytic activity (Duffy *et al.* 2012). Due to limited virus spread in the tumor, virotherapy is ideally combined with therapeutic genes that are associated with a bystander effect. In a study of Grünwald *et al.*, a replication-competent adenovirus was used in which the E1a gene is driven by the mouse alpha-fetoprotein promoter and the human NIS gene is inserted in the E3 region (Ad5-E1/AFP-E3/NIS). Three days after intratumoral virus injection, HCC xenografts accumulated approximately 25% ID/g ^{123}I as shown by scintigraphy. A single intratumoral injection of Ad5-E1/AFP-E3/NIS (virotherapy) resulted in a significant reduction of tumor growth and prolonged survival, as compared to injection of saline. Combination of oncolytic virotherapy with radioiodine treatment (radiovirotherapy) led to an additional reduction of tumor growth that resulted in markedly improved survival as compared to virotherapy alone (Grunwald *et al.* 2013a). In a next step to reduce the adenoviral liver pooling and thereby increase tumor-selective targeting of the adenovirus after systemic application, the negatively charged Ad was coated with cationic PAMAM (Poly(amidoamine)) dendrimers by non-covalent charge interaction. To further improve shielding and targeting we physically coated replication-selective adenoviruses carrying the NIS gene with a conjugate consisting of cationic poly(amidoamine) (PAMAM) dendrimer linked to the peptidic, epidermal growth factor receptor (EGFR)-specific ligand GE11. Systemic injection of the uncoated adenovirus in a liver cancer xenograft mouse model led to high levels of NIS expression in the liver due to hepatic sequestration, which were significantly reduced after coating as demonstrated by ^{123}I-scintigraphy. Evasion from liver pooling resulted in decreased hepatotoxicity and increased transduction efficiency in peripheral xenograft tumors. A significantly enhanced oncolytic effect was observed following systemic application of dendrimer-coated adenovirus that was further increased by additional treatment with a therapeutic dose of ^{131}I (Grunwald *et al.* 2013b).

1.5 Aims of the thesis

Mesenchymal stem cells are currently under investigation as potential clinical therapeutic carriers due to their tumor-selective homing capacity, high lineage plasticity and minimal ethical concerns associated with their isolation and use. In this thesis MSCs were used for tumor targeted NIS gene delivery, where NIS expression was driven by two different promoters. The diagnostic and therapeutic potential of the NIS gene has been widely described in various tumor models by the use of viral and non-viral gene delivery techniques. As a logical consequence after the proof-of-principle studies, the next step towards clinical development is the evaluation of systemic gene delivery systems. Here, MSCs are evaluated as promising gene delivery vehicles after systemic application for a tumor targeted NIS expression.

In the first step we established and characterized human MSCs that were stably transfected with NIS under the control of the unspecific cytomegalovirus (CMV) promoter. The iodide uptake activity of the NIS expressing MSCs was first analysed *in vitro* and confirmed by western blot analysis. In addition, a clonogenic assay was performed to determine whether ^{131}I sequestered by NIS-expressing MSCs would be able to kill adjacent hepatocellular cancer (HCC) cells in cocultures through the crossfire effect of ^{131}I. *In vivo*, the efficacy and therapeutic potential of MSC-mediated NIS gene transfer was studied in a subcutaneous HCC xenograft mouse model after systemic injection.

Following proof-of-principle of MSC-mediated NIS gene delivery, in the next step, we aimed at enhancing tumor stroma-specificity of MSC-mediated NIS gene delivery by application of a tumor stroma specific promoter. For this purpose, MSCs were stably transfected with a NIS expressing plasmid, in which NIS was driven by the tumor stroma specific CCL5/RANTES promoter (RANTES-NIS-MSC). Tumor-specificity and therapeutic efficacy of ^{131}I were evaluated after systemic application of RANTES-NIS-MSC in the subcutaneous HCC xenograft mouse model as well as in an orthotopic HCC xenograft model in nude mice using radioiodine imaging (^{123}I-scintigraphy and ^{124}I-PET) as well as MR imaging for tumor growth control in the orthotopic tumor model.

In the final step, tumor-specificity and therapeutic efficacy of MSC-mediated NIS gene delivery was evaluated in a metastasis model. To this end, a hepatic colon cancer metastases model was established based on intrasplenic tumor cell injection. After systemic injection of NIS-expressing MSCs under the control of the CCL5 promoter, the NIS-mediated iodide uptake activity and the therapeutic potential of radioiodine were analysed using gamma camera and PET imaging as well as MR imaging for tumor growth control at the therapy studies.

2 Chapter 1

Image-guided, tumor stroma-targeted ^{131}I therapy of hepatocellular cancer after systemic mesenchymal stem cell-mediated NIS gene delivery

Kerstin Knoop[1], Marie Kolokythas[1], Kathrin Klutz[1], Michael J. Willhauck[1], Nathalie Wunderlich[1], Dan Draganovici[2], Christian Zach[3], Franz Josef Gildehaus[3], Guido Böning[3], Burkhard Göke[1], Ernst Wagner[4], Peter J. Nelson[2], Christine Spitzweg[1]

Department of Internal Medicine II[1], Clinical Biochemistry Group, Medical Policlinic[2], Department of Nuclear Medicine[3,] Department of Pharmacy, Center of Drug Research, Pharmaceutical Biology-Biotechnology[4], Ludwig-Maximilians-University, Munich, Germany

2.1 Abstract

Due to its dual role as reporter and therapy gene, the sodium iodide symporter (NIS) allows non-invasive imaging of functional NIS expression by ^{123}I-scintigraphy or ^{124}I-PET imaging before the application of a therapeutic dose of ^{131}I. NIS expression provides a novel mechanism for the evaluation of mesenchymal stem cells (MSCs) as gene delivery vehicles for tumor therapy.

In the current study we stably transfected bone marrow-derived CD34$^-$ MSCs with NIS cDNA (NIS-MSC), which revealed high levels of functional NIS protein expression. In mixed populations of NIS-MSCs and hepatocellular cancer (HCC) cells clonogenic assays showed a 55% reduction of HCC cell survival after ^{131}I application. We then investigated body distribution of NIS-MSCs by ^{123}I-scintigraphy and ^{124}I-PET imaging following i.v. injection of NIS-MSCs in a HCC xenograft mouse model demonstrating active MSC recruitment into the tumor stroma which was confirmed by immunohistochemistry and *ex vivo* gamma counter analysis. Three cycles of systemic MSC-mediated NIS gene delivery followed by ^{131}I application resulted in a significant delay in tumor growth.

Our results demonstrate tumor-specific accumulation and therapeutic efficacy of radioiodine after MSC-mediated NIS gene delivery in HCC tumors, opening the prospect of NIS-mediated radionuclide therapy of metastatic cancer using MSCs as gene delivery vehicles.

2.2 Introduction

Mesenchymal stem cells (MSC) are pluripotent progenitor cells with high proliferative and self renewal capacity, which play a key role in maintenance and regeneration of diverse tissues based on their ability to differentiate into cells of connective tissue lineages, including bone, fat, cartilage and muscle (Fritz and Jorgensen 2008; Pittenger *et al.* 1999; Studeny *et al.* 2004). In the course of tissue injury, or during chronic inflammation, MSCs can contribute to tissue remodeling by their mobilization and subsequent recruitment to the site of injury. While the exact mechanisms by which circulating progenitor cells home to remodeling tissues remain unclear, it is thought that chemokine biology and integrins underlie tissue-specific homing of stem cells (Conrad *et al.* 2007; Von Luttichau *et al.* 2005).

Tumors are composed of malignant tumor cells and the “benign” tumor stromal compartment that includes blood vessels, infiltrating inflammatory cells, extracellular matrix and stromal fibroblasts. This tumor stroma plays a key role in tumor growth, tumor angiogenesis and metastatic potential of a tumor, and has therefore become an important target for tumor therapy (Fritz and Jorgensen 2008; Studeny *et al.* 2004). The process of tumor stroma formation is similar to that seen in wound healing which results in tissue remodeling with recruitment and high proliferation of mesenchymal cells. We and others have shown that MSCs are actively recruited to growing tumor stroma where they differentiate into diverse tumor stroma-associated cell types including cells that comprise the tumor vasculature and stromal fibroblast-like cells (Conrad *et al.* 2007; Nakamizo *et al.* 2005; Pittenger *et al.* 1999; Spaeth *et al.* 2009; Studeny *et al.* 2004; Zischek *et al.* 2009). Based on their intrinsic tumor homing capacity, MSCs have gained attention as potential vehicles for delivering therapeutic genes to tumor environments after systemic application, potentially providing a means to deliver therapeutic genes not only to the primary tumor, but also to tumor metastases. A series of recent reports have provided the proof of principle of MSC-mediated gene delivery demonstrating successful tumor-selective engraftment of *ex vivo* transduced MSCs (Loebinger *et al.* 2009a; Nakamizo *et al.* 2005; Studeny *et al.* 2002; Studeny *et al.* 2004; Xin *et al.* 2007; Zischek *et al.* 2009).

NIS, an intrinsic transmembrane glycoprotein with 13 putative transmembrane domains, is responsible for the ability of thyroidal cells to concentrate iodide, the first and rate-limiting step in the process of thyroid hormonogenesis, which can be effectively blocked by the competitive inhibitor perchlorate ($NaClO_4$) (Hingorani *et al.* ; Spitzweg and Morris 2002). Due to its expression in follicular cell-derived thyroid cancer cells, NIS provides the molecular basis for the diagnostic and therapeutic application of radioiodine, which has been successfully used for more than 70 years for the treatment of thyroid cancer patients, and represents the most effective form of systemic anticancer radiotherapy available today

(Spitzweg and Morris 2002). Since its cloning in 1996, the NIS gene has been identified and characterized as a therapeutic gene for the treatment of thyroidal or extrathyroidal tumors following selective NIS gene transfer into tumor cells. This allows the therapeutic application of radioiodine and alternative radionuclides, such as ^{188}Re and ^{211}At (Hingorani *et al.* ; Spitzweg and Morris 2002; Willhauck *et al.* 2007b; Willhauck *et al.* 2008a). NIS also represents one of the most promising reporter genes available, which allows direct noninvasive imaging of functional NIS expression by ^{123}I-scintigraphy and ^{124}I-PET imaging, as well as exact dosimetric calculations before proceeding to therapeutic application of ^{131}I (Dingli *et al.* 2003b; Groot-Wassink *et al.* 2004; Spitzweg and Morris 2002). NIS has many characteristics of an optimal reporter and therapy gene, as it is a non-immunogenic protein with a well-defined body biodistribution and expression, that mediates the transport of readily available radionuclides, such as ^{131}I, ^{123}I, ^{125}I, ^{124}I, ^{99m}Tc, ^{188}Re or ^{211}At (Hingorani *et al.* ; Spitzweg and Morris 2002).

The field of gene therapy has made considerable strides in the last decade through the development of new vector systems, including engineered MSCs, and an increasing repertoire of therapeutic genes. The application of NIS in its role as reporter gene allows detailed characterization and direct monitoring of *in vivo* vector biodistribution as well as localization, level, and duration of transgene expression after viral or non-viral gene delivery. These are recognized as critical elements in the design of clinical gene therapy trials (Baril *et al.* ; Dingli *et al.* 2003b; Spitzweg and Morris 2002). Several research groups, including our own, have demonstrated the potential of NIS as reporter gene in various applications, demonstrating that *in vivo* imaging of radioiodine accumulation by ^{123}I- or ^{99m}Tc-scintigraphy as well as ^{123}I-SPECT/CT fusion imaging correlates well with the results of *ex vivo* gamma counter measurements as well as NIS mRNA and protein analysis (Blechacz *et al.* 2006; Carlson *et al.* 2009; Goel *et al.* 2007; Klutz *et al.* 2009; Merron *et al.* 2007; Spitzweg *et al.* 2007; Trujillo *et al.* ; Willhauck *et al.* 2007a). In addition, PET imaging using ^{124}I provides significant advantages for exact localization and quantitative analysis of NIS-mediated radioiodine accumulation due to enhanced resolution and sensitivity (Dingli *et al.* 2006; Groot-Wassink *et al.* 2004).

In the current study, we applied MSCs as gene delivery vehicles for tumor-targeted NIS gene expression in a hepatoma mouse model. Based on its dual function as reporter and therapy gene, NIS was used initially for noninvasive imaging of MSC recruitment and whole body biodistribution as well as localization, level and duration of NIS expression after systemic application of NIS-transduced MSCs. The therapeutic capacity of ^{131}I therapy was subsequently evaluated after systemic administration of NIS expressing MSCs.

2.3 Methods

Cell culture

The MSCs used express CD73 and CD105, but lack the myelogenic markers CD34, CD14, CD45, and MHC class II and are thus difficult to define (Conrad *et al.* 2002; Thalmeier and Huss 2001). A clonal cell line derived from SV40 large T antigen immortalized MSCs from human bone marrow was used for the outlined studies (Thalmeier and Huss 2001). The cells grow adherently and continuously in cell culture and retain significant pluripotency (Conrad *et al.* 2002; Thalmeier and Huss 2001). MSCs were cultured in RPMI (Invitrogen, Life Technologies Inc., Paisley, UK) supplemented with 10% fetal bovine serum (v/v; PAA, Pasching, Austria) and 1% penicillin/streptomycin.

For animal experiments the human hepatocellular carcinoma cell line Huh7 (JCRB 0403) was cultured in DMEM/F12 (Invitrogen, Darmstadt, Germany) supplemented with 10% fetal bovine serum (v/v; PAA), 5% L-Glutamine (GibcoBRL, Karlsruhe, Germany) and 1% penicillin/streptomycin.

For *in vitro* studies, the hepatocellular carcinoma HepG2 cell line (ATCC-HB-8065) was cultured in RPMI (Invitrogen) supplemented with 10% fetal bovine serum (v/v; PAA) and 1% penicillin/streptomycin.

All cell lines were maintained at 37°C and 5% CO_2 in an incubator with 95% humidity.

Stable transfection of mesenchymal stem cells

Wild-type MSCs (WT-MSCs) were stably transfected with the expression vector CMV-NIS-pcDNA3 (full length NIS cDNA coupled to the cytomegalovirus (CMV) promoter, kindly provided by Dr. S.M. Jhiang, Ohio, State University, Columbus, OH) using LipofectAMINE Plus reagent (Invitrogen) under serum-free conditions according to the manufacturer's recommendations. After transfections, cells were incubated for 24 h in regular growth medium. Selection was performed with 0.5 mg/ml geneticin (Invitrogen) in RPMI medium containing 10% fetal bovine serum and 1% penicillin/streptomycin. Surviving clones were isolated and subjected to screening for iodide uptake activity (see below). The stably transfected cell line with the highest levels of iodide accumulation among approximately 60 colonies screened was termed NIS-MSC and used for the experiments.

^{125}I uptake assay

Following transfection, iodide uptake of NIS-MSCs was determined at steady-state conditions as described previously (Spitzweg *et al.* 1999). Results were normalized to cell survival measured by cell viability assay (see below) and expressed as cpm/A 490 nm.

Cell viability assay

Cell viability was measured using the commercially available MTS assay (Promega Corp., Mannheim, Germany) according to the manufacturer's recommendations as described previously (Spitzweg *et al.* 1999).

In vitro clonogenic assay

HepG2 cells cocultured with NIS-MSCs or WT-MSCs were incubated for 7 h with 29.6 MBq (0.8 mCi) ^{131}I in Hank's balanced salt solution (HBSS, GibcoBRL) supplemented with 10 µM NaI and 10 mM HEPES (pH 7.3) at 37°C. After incubation with ^{131}I, the MSCs were separately removed by incubation with 1% trypsin in PBS for 1 min, which did not affect attachment of HepG2 cells. Thereafter, HepG2 cells were detached by incubation with 0.05% trypsin/0.02% EDTA in PBS for 10 min at 37°C. The HCC cells were then plated at cell densities of 50, 100, 250, 500, 750, 1000 und 2000 cells/well in 12-well plates. Two weeks later, after colony development, cells were fixed with methanol, stained with crystal violet, and HCC colonies containing more than 50 cells were counted. Parallel experiments were performed using HBSS without ^{131}I and all values were adjusted for plating efficiency. The percentage of survival represents the percentage of cell colonies after ^{131}I treatment, compared with mock treatment with HBSS. Purity of HepG2 cells after selective trypsinization was confirmed by phase-contrast microscopy and by immunofluorescence analysis using cell type-specific antibodies (vimentin and keratin) in parallel experiments.

Membrane preparation and Western Blot analysis

Membrane protein was prepared from NIS-MSC and WT-MSC cells followed by Western blot analysis as described previously (Spitzweg *et al.* 1999). A mouse monoclonal NIS-specific antibody (kindly provided by J.C. Morris, Division of Endocrinology, Mayo Clinic and Medical School, Rochester, MN) was applied at a dilution of 1:1000. As loading controls, the blots were reprobed with a monoclonal antibody directed against β-actin (Sigma).

Establishment of Huh7 xenograft tumors

Huh7 xenograft tumors were established in female CD1 nu/nu mice (Charles River, Sulzfeld, Germany) by s.c. injection of 5 x 10^6 Huh7 cells suspended in 100 µl PBS into the flank region. The animals were maintained under specific pathogen-free conditions with access to mouse chow and water *ad libitum*. The experimental protocol was approved by the regional governmental commission for animals (Regierung von Oberbayern).

MSC application and radioiodine biodistribution studies in vivo

Experiments were initiated when the implanted tumors reached a diameter of 3 to 5 mm, after a 10-day pretreatment with intraperitoneal (i.p.) injections of 2 µg L-T4/d (Henning, Sanofi-Aventis, Germany), diluted in 100 µl PBS, to suppress thyroidal iodide uptake. WT-MSCs or NIS-MSCs were applied via the tail vein at a concentration of 5 x 10^5 cells/500µl. Two groups of mice were established and treated as follows: (a) three i.v. applications of NIS-MSC in four day intervals (n=24); (b) three i.v. applications of WT-MSC in four day intervals (n=9). As an additional control, in a subset of mice injected with NIS-MSC (n=9) the specific NIS-inhibitor sodium-perchlorate ($NaClO_4$, 2 mg per mouse) was injected i.p. 30 min prior to ^{123}I administration. 72 h after the last MSC application, 18.5 MBq (0.5 mCi) ^{123}I was injected i.p. and iodide biodistribution was assessed using a gamma camera equipped with UXHR collimator (Ecam, Siemens, Germany) as described previously (Willhauck *et al.* 2007b; Willhauck *et al.* 2008a). Regions of interest were quantified and expressed as a fraction of the total amount of applied radionuclide per gram tumor tissue (after postmortem weighing). The retention time within the tumor was determined by serial scanning after radionuclide injection. Dosimetric calculations were done according to the concept of medical internal radiation dose, with the dosis factor of RADAR-group (www.dosisinfo-radar.com).

In an additional group of mice injected with NIS-MSCs (n=5), radioiodine biodistribution was also monitored using ^{124}I-PET imaging after i.v. injection of 20 MBq ^{124}I. PET imaging was performed as described previously (Groot-Wassink *et al.* 2004; Rominger *et al.*). In brief, PET data were acquired in list-mode format over 40 min on a Siemens Inveon P120 microPET (Siemens Medical Solutions, Munich, Germany). Dynamic emission recordings acquired in list mode were reconstructed using a combined reconstructing algorithm with two OSEM3D iterations as described by Rominger *et al.* (Rominger *et al.*).

Analysis of radioiodine biodistribution ex vivo

For *ex vivo* biodistribution studies, mice were injected with NIS-MSCs (n=8) or WT-MSCs (n=3) as described above followed by i.p. injection of 18.5 MBq (0.5 mCi) ^{123}I. A subset of NIS-MSC injected mice (n=3) were treated with $NaClO_4$ prior to ^{123}I administration as an additional control. Five hours after ^{123}I injection, mice were sacrificed and organs of interest were dissected, weighed and ^{123}I accumulation was measured in a gamma counter. Results were reported as percentage of injected dose per organ (% ID/organ).

Analysis of NIS mRNA expression using quantitative real-time PCR

Total RNA was isolated from Huh7 tumors or other tissues using the RNeasy Mini Kit (Qiagen, Hilden, Germany) according to the manufacturer's recommendations and quantitative real-time PCR (qPCR) was performed as described previously (Klutz *et al.*

2009).

Immunohistochemical analysis of NIS protein and SV40 large T antigen expression

Immunohistochemical staining of paraffin-embedded tissue sections derived from Huh7 tumors after i.v. MSC application was performed as described previously (Spitzweg *et al.* 2007). As primary antibodies, the mouse monoclonal NIS-specific antibody (see above) or the mouse monoclonal anti-SV40 large T Ag antibody (Calbiochem/Merck, Darmstadt, Germany) were used at a dilution of 1:1000 and 1:2000, respectively.

Radioiodine therapy study in vivo

Following a 10-day L-T4 pretreatment as described above, two groups of mice were established receiving 55.5 MBq ^{131}I 48 h after the last of three NIS-MSC (n=15) or WT-MSC (n=15) applications in two-day-intervals (each 5 x 10^5 cells/500 µl PBS), respectively. This cycle was repeated once 24 h after the last ^{131}I application. 24 h after these two treatment cycles one additional MSC (5 x 10^5 cells) injection was administered followed by a third ^{131}I (55.5 MBq) injection 48 later. As control, one further group of mice were treated with saline instead of ^{131}I after injection of NIS-MSC (n=15). A further control group was injected with saline only (n=15). Tumor sizes were measured before treatment and daily thereafter for up to seven weeks. Tumor volume was estimated using the equation: tumor volume = length x width x height x 0.52. Mice were sacrificed when tumors started to necrotize, exceed a tumor volume of 1500 mm^3, in case of weight loss of more than 10%, or impairment of breathing as well as drinking and eating behavior.

Experiments were repeated twice and tumor volumes are expressed as mean of 15 mice per group.

Indirect immunofluorescence assay

Indirect immunofluorescence analysis using a Ki67-specific antibody and an antibody against CD31 was performed on frozen sections as described previously (Willhauck *et al.* 2007b). Immunostainings that had to be compared quantitatively were captured at identical illumination conditions, with identical exposure time and system settings for digital image processing.

Quantification of cellular proliferation (percentage of Ki67 positive cells in the tumor) and blood vessel density (percentage of CD31 positive area in the tumor) was performed by evaluation of 10 high power fields per tumor (6 animals per group) using ImageJ software (NIH, USA).

Results are presented as means ± standard deviation, statistical significance was calculated using students t-test.

Statistical methods

All *in vitro* experiments were carried out in triplicates. Results are represented as mean ± SD of triplicates. Statistical significance of *in vitro* experiments was tested using Student´s t test. Statistical significance of *in vivo* experiments has been calculated using Man-Whitney U test.

2.4 Results

In vitro characterization of MSCs stably expressing NIS

After stable transfection of immortalized human bone marrow derived $CD34^-$ MSCs with a NIS expressing plasmid (CMV-NIS-pcDNA3) (NIS-MSC), the transfected cells showed a 12-fold increase in NIS-mediated iodide uptake activity, which could be blocked upon treatment with the NIS-specific competitive inhibitor perchlorate (Fig. 1a). In contrast, in WT-MSCs no perchlorate-sensitive iodide uptake above background level was observed.

NIS protein expression in NIS-transfected MSCs was confirmed by Western blot analysis using a mouse monoclonal NIS-specific antibody (Fig. 1b). The antibody recognizes the carboxy-terminus of human NIS and revealed a major band of a molecular mass of approximately 80-90 kDa in NIS-MSCs, which was not detected in WT-MSCs.

A time course of iodide uptake in NIS-MSCs and WT-MSCs showed that in NIS-MSCs, iodide accumulation reached half-maximal levels within 10-15 min and became saturated at 40-50 min (Fig. 1c). No NIS-specific iodide accumulation above background level was observed in WT-MSCs.

A clonogenic assay was then performed to determine whether ^{131}I sequestered by NIS-MSCs would be able to kill adjacent HCC cells in cocultures through the crossfire effect of ^{131}I (Fig. 1d). NIS-MSCs or WT-MSCs cocultured with HCC cells were incubated in HBSS containing 29.6 MBq ^{131}I for 7 h. HCC cells, cocultured with WT-MSCs (ratio 1:1) showed no significant cell killing after incubation with ^{131}I. In contrast, in cocultures of HCC cells and NIS-MSCs (ratio 1:1), HCC cells, which have no iodide uptake activity per se, a 55% reduction in cell survival was seen (Fig. 1d).

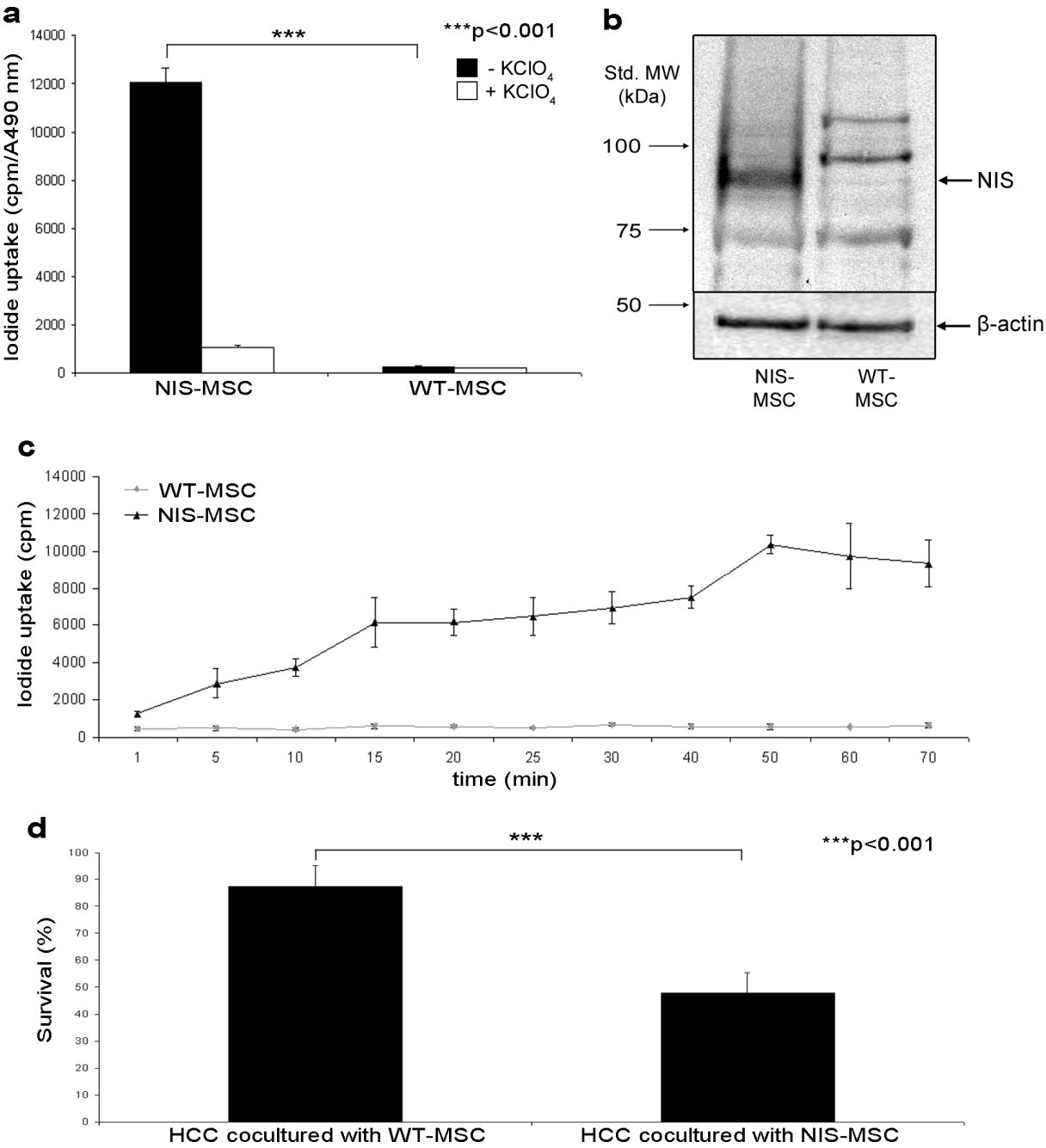

Figure 1 *In vitro* analysis of MSCs stably expressing NIS. ^{125}I uptake was measured in NIS-MSCs compared to WT-MSCs (Fig. 1a). NIS-MSCs showed a 12-fold increase in perchlorate-sensitive ^{125}I accumulation. In contrast, no perchlorate-sensitive iodide uptake above background level was observed in WT-MSCs (Fig. 1a) ($p<0.001$). Analysis of NIS protein expression in NIS-MSCs as compared to WT-MSCs by Western Blot analysis (Fig. 1b). NIS protein was detected as a major band of a molecular mass of 80-90 kDa which was not detected in WT-MSCs (Fig. 1b). MW, molecular weight. Time course of iodide uptake in NIS-MSCs and WT-MSCs (Fig. 1c). Iodide accumulation reached half-maximal levels in NIS-MSCs within 10-15 min and became saturated at 40-50 min, while WT-MSCs showed no iodide accumulation (Fig. 1c). In an in vitro clonogenic assay mixed populations of WT-MSCs and HCC cells as well as NIS-MSCs and HCC cells (ratio 1:1) were exposed to 29.6 MBq ^{131}I (Fig. 1d). In HCC cells cocultured with NIS-MSCs a 55% reduction of cell survival was measured, whereas HCC cells cocultured with WT-MSCs survived the ^{131}I incubation to almost 100% (Fig. 1d) ($p<0.001$). Results represent means of three plated cell densities ± SD (100, 500 and 1000 cells per well).

In vivo radioiodine biodistribution studies

In nude mice harboring HCC xenografts 5 x 10^5 NIS- or WT-MSCs were injected i.v. via the tail vein three times in four day intervals. 72 h following the last MSC injection, 18.5 MBq ^{123}I was administered and radioiodine distribution was monitored using a gamma camera. While no significant iodide accumulation was detected in tumors after application of WT-MSC (Fig. 2c), significant iodide accumulation was observed in 74 % of Huh7 tumors following NIS-MSC application, in addition to physiologic iodide accumulation in thyroid gland, stomach and bladder (Fig. 2a). As determined by serial scanning, a maximum of approximately 7% to 9% ID/g ^{123}I was accumulated after application of NIS-MSCs with a biological half-life of 4 h. Considering a tumor mass of 1g and an effective half-life of 3 h for ^{131}I, a tumor absorbed dose of 43.7 ± 7.7 mGy/MBq ^{131}I was calculated (Fig. 2d). To confirm that tumoral iodide uptake was mediated by functional NIS expression, a subset of NIS-MSC injected mice received $NaClO_4$ 30 minutes prior to ^{123}I administration. In all experiments, a single injection of 2 mg $NaClO_4$ completely blocked tumoral iodide accumulation in addition to abolishing iodide uptake in stomach and thyroid gland (Fig. 2b).

In a subset of mice, radioiodine biodistribution was also monitored using ^{124}I-PET imaging after i.v. injection of 20 MBq ^{124}I (Figs. 2e,f). Three-dimensional data were generated using iterative reconstructions of list-mode data (0-40 min), which gave better anatomical definition. Significant tumor-selective iodide accumulation was observed following NIS-MSC application thereby confirming the findings of the planar gamma camera imaging, but allowing a more detailed three-dimensional analysis of tumoral iodide accumulation. One hour after iodide application a maximum tumoral iodide uptake of approximately 5-7% ID/g was measured.

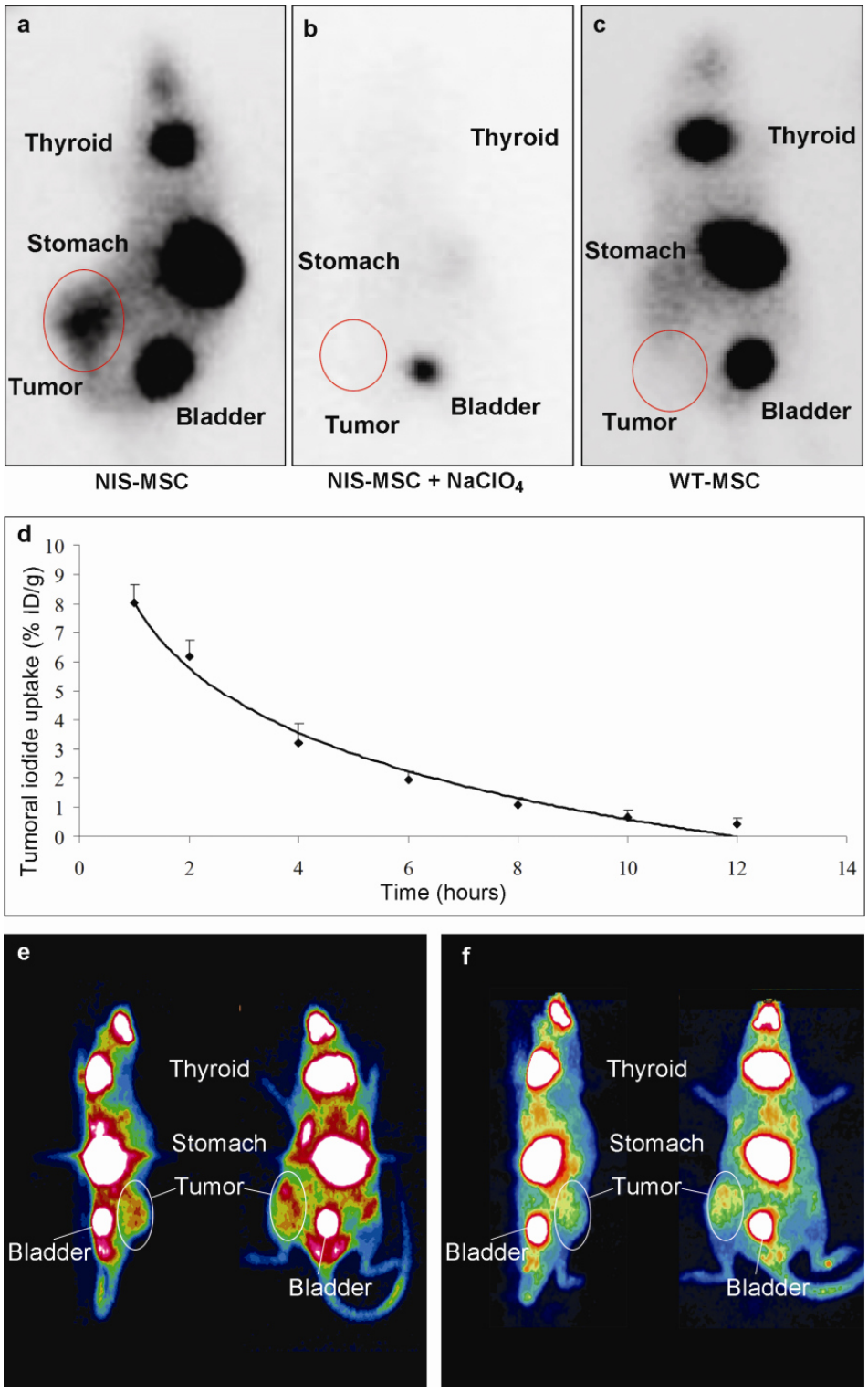

Figure 2 ^{123}I gamma camera imaging of mice harboring Huh7 tumors after MSC-mediated NIS gene delivery three hours following ^{123}I administration (Fig. 2a-c). After three i.v. applications of NIS-MSCs significant tumor-specific iodide accumulation was induced (7-9 % ID/g ^{123}I) (Fig. 2a), which was completely abolished upon pretreatment with $NaClO_4$ (Fig. 2b). In contrast, mice injected with WT-MSCs showed no tumoral iodide uptake (Fig. 2c). Iodide was also accumulated physiologically in thyroid, stomach and bladder (Fig. 2a, c). Time course of ^{123}I accumulation in Huh7 tumors after three i.v. NIS-MSC applications followed by injection of 18.5 MBq ^{123}I as determined by serial scanning (Fig. 2d). Maximum tumoral radioiodine uptake was 7-9% ID/g tumor with an average effective half-life of 3 h for ^{131}I. ^{124}I PET imaging of mice harboring Huh7 tumors after MSC-mediated NIS gene delivery (Fig. 2e, f). After three i.v. applications of NIS-MSCs significant tumor-specific iodide accumulation was confirmed by PET imaging (left: sagittal slice orientation, right: coronal slice orientation).

Ex vivo radioiodine biodistribution studies

Ex vivo biodistribution studies confirmed significant iodide uptake in tumors following three systemic i.v. applications of NIS-MSCs resulting in a tumoral iodide uptake of 2.5% to 3% ID/organ ^{123}I 5 hours after radioiodine injection. In contrast, mice injected with WT-MSCs showed no significant tumoral iodide uptake. No significant iodide uptake levels were observed in the non-target organs lung, liver, spleen or kidney (Fig. 3). In both groups, the thyroid gland and the stomach accumulated approximately 40% and 39% ^{123}I ID/organ resulting from endogenous expression of NIS in thyroid and stomach. It is important to point out that due to the exquisite regulation of thyroidal NIS expression by thyroid-stimulating hormone (TSH), ^{123}I accumulation in the thyroid gland can effectively be downregulated by thyroid hormone treatment as shown in humans (Wapnir *et al.* 2004). In addition, iodide accumulation in the stomach is mostly a result from pooling of gastric juices, which is more prominent in mouse experiments than usually seen in humans due to the anesthesia for a prolonged period during imaging procedure (Klutz *et al.* 2009; Spitzweg and Morris 2002) (data not shown). Administration of perchlorate in mice injected with NIS-MSCs significantly blocked iodide uptake in tumors and in physiologically NIS-expression tissues including thyroid gland and stomach (Fig. 3).

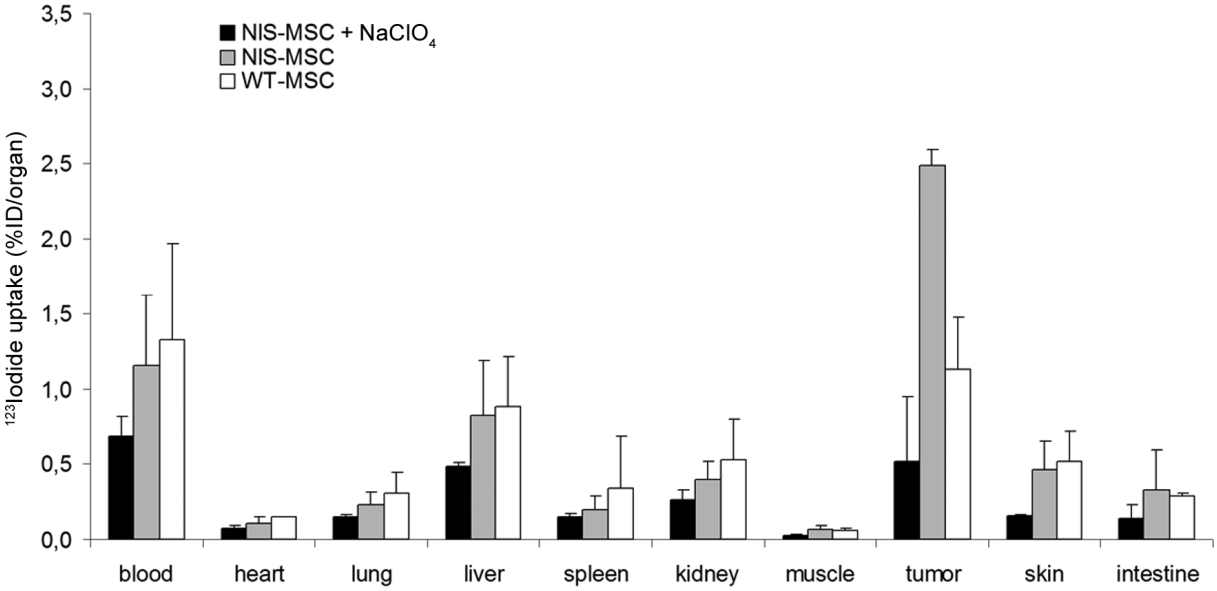

Figure 3 Evaluation of iodide biodistribution *ex vivo* five hours following injection of 18.5 MBq ^{123}I. Tumors in NIS-MSC-injected mice showed high perchlorate-sensitive iodide uptake activity (approx. 2.5-3% ID/organ), while no significant iodide accumulation was measured in tumors after injection of WT-MSCs or in nontarget organs. Results are reported as percent of injected dose per organ ± SD.

Analysis of NIS mRNA expression by qPCR

In order to assess the relative NIS mRNA expression after systemic MSC application, mRNA from tumors and control tissues was extracted and analyzed by qPCR with NIS-specific oligonucleotide primers. While low levels of NIS mRNA expression were detected in tumors

after WT-MSC administration, significant levels of NIS mRNA were detected in tumors of mice following systemic NIS-MSC injection (Fig. 4). As expected, administration of the competitive NIS inhibitor perchlorate had no influence on NIS mRNA expression in tumors treated with NIS-MSCs. In other organs, including liver, lung, kidneys and spleen no significant NIS mRNA expression was observed after systemic NIS-MSC injection.

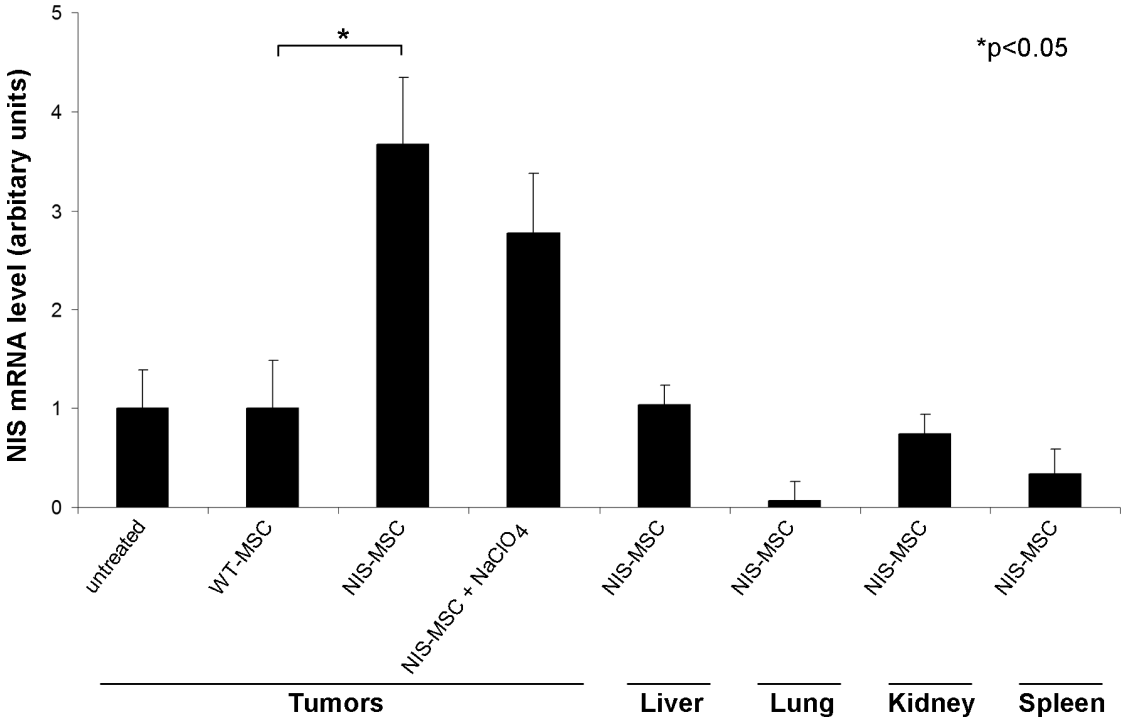

Figure 4 Analysis of NIS mRNA expression in Huh7 tumors and non-target organs by qPCR. While only a low background level of NIS mRNA expression was detected in untreated tumors (which was set as one arbitrary unit) or tumors injected with WT-MSC, significant levels of NIS mRNA expression were induced in Huh7 tumors after three applications of NIS-MSCs with or without $NaClO_4$ pretreatment ($p<0.05$). In addition, no significant NIS mRNA expression was detected in non-target organs after three applications of NIS-MSCs. Results are reported as NIS/GAPDH ratios.

Immunohistochemical analysis of NIS protein expression in Huh7 tumors

To better determine MSC distribution, tumor specimens were immunohistochemically stained with NIS- and SV40 large T Ag-specific antibodies. SV40 large T Ag was used to immortalize the MSC and could thus be used for *ex vivo* detection of the adoptively transferred MSC. NIS-specific immunoreactivity was detected throughout the tumor stroma with most prominent staining in areas neighboring blood vessels in tumors of mice that were injected with NIS-MSCs (Fig. 5a, arrows). Distribution of NIS-specific immunoreactivity was similar to the localization of SV40 large T Ag (Fig 5b). Lungs, liver, and kidneys showed no detectable NIS or SV40 large T Ag immunoreactivity (data not shown). In contrast, strong accumulation of SV40 large T Ag-expressing cells was observed in the spleens of mice after administration of NIS-MSCs (Fig. 5f), while no NIS-specific immunoreactivity was detected (Fig. 5e). WT-

MSC-injected mice showed no significant NIS protein expression in tumors (Fig. 5c) and other organs like lungs, liver, kidneys or spleen (Fig. 5g). However, after WT-MSC application SV40 large T Ag-specific immunoreactivity was widely detectable in implanted Huh7 tumors (Fig. 5d) as well as in spleen (Fig. 5h) demonstrating efficient MSC recruitment into the tumor stroma after systemic application. The presence of MSC in the spleen may result either from the direct recruitment of the cells [6], or from active filtration of the exogenously applied MSC from the peripheral circulation.

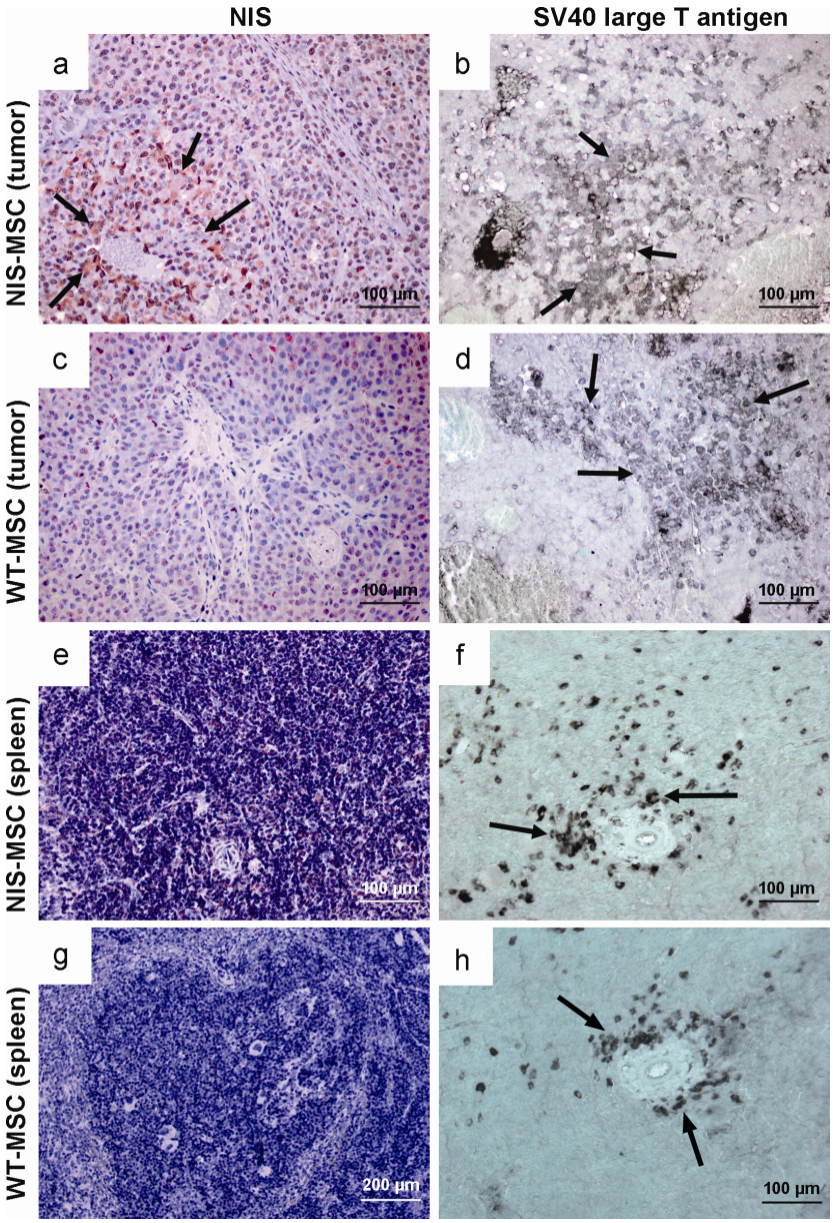

Figure 5 Immunohistochemical staining of Huh7 tumors after application of NIS-MSCs (Figs. 5a, b) or WT-MSCs (Figs. 5c, d). After application of NIS-MSCs Huh7 tumors revealed NIS-specific immunoreactivity throughout the tumor stroma, which was most prominent in the vicinity of blood vessels (Fig. 5a), with a similar distribution of SV40 large T Ag-positive cells (Fig. 5b). After application of WT-MSCs no NIS-specific immunoreactivity was detected in Huh7 tumors (Fig. 5c), while strong cytoplasmic SV40 large T Ag-staining was detected, in particular in the vicinity of blood vessels (Fig. 5d). Other organs like lung, liver, and kidneys showed no detectable NIS protein expression and no SV40 large T Ag staining (data not shown). In contrast, strong accumulation of SV40 large T Ag-expressing cells was detected in the spleen of mice that were injected with NIS-MSCs (Fig. 5f) or WT-MSC (Fig. 5h), while no NIS-specific immunoreactivity was detected (Figs. 5e, g).

Radioiodine therapy studies in vivo after MSC-mediated systemic NIS gene transfer

The effect of therapeutic ^{131}I was then evaluated in concert with application of NIS-MSC. The ^{131}I therapy regime was optimized using small groups of mice (n = 4) and showed the best results when mice were treated with three cycles of NIS engineered MSCs followed by ^{131}I

application (data not shown). Mice treated with NIS-MSCs followed by application of saline or mice treated with WT-MSCs followed by application of ^{131}I , or saline treated mice all showed an exponential tumor growth. In contrast, NIS-transduced (NIS-MSCs) and ^{131}I-treated tumors showed a significant delay in tumor growth (p=0.001703 (NaCl) and p=0.008103 (WT-MSC)) (Fig. 6a). Mice showed no major adverse effects of radionuclide or MSC treatment in terms of lethargy or respiratory failure.

Upon completion of the therapy study, mice were sacrificed and tumors were dissected and processed for immunfluorescence analysis. Immunfluorescence analysis using a Ki67-specific antibody (green) and an antibody against CD31 (red, labelling blood vessels) showed striking differences between mice treated with NIS-MSC/^{131}I (Fig. 6b) and mice treated with WT-MSC/^{131}I (Fig. 6c) as well as mice treated with NIS-MSC/NaCl (Fig. 6d). Control tumors showed a Ki67-index of approx. 45 ± 8.7% and a mean vessel density of 5 ± 0.45%, whereas tumors treated with NIS-MSC and ^{131}I exhibited a lower intratumoral blood vessel density of 1.85 ± 0.25% and a proliferation index of 25 ± 4.1% after ^{131}I therapy.

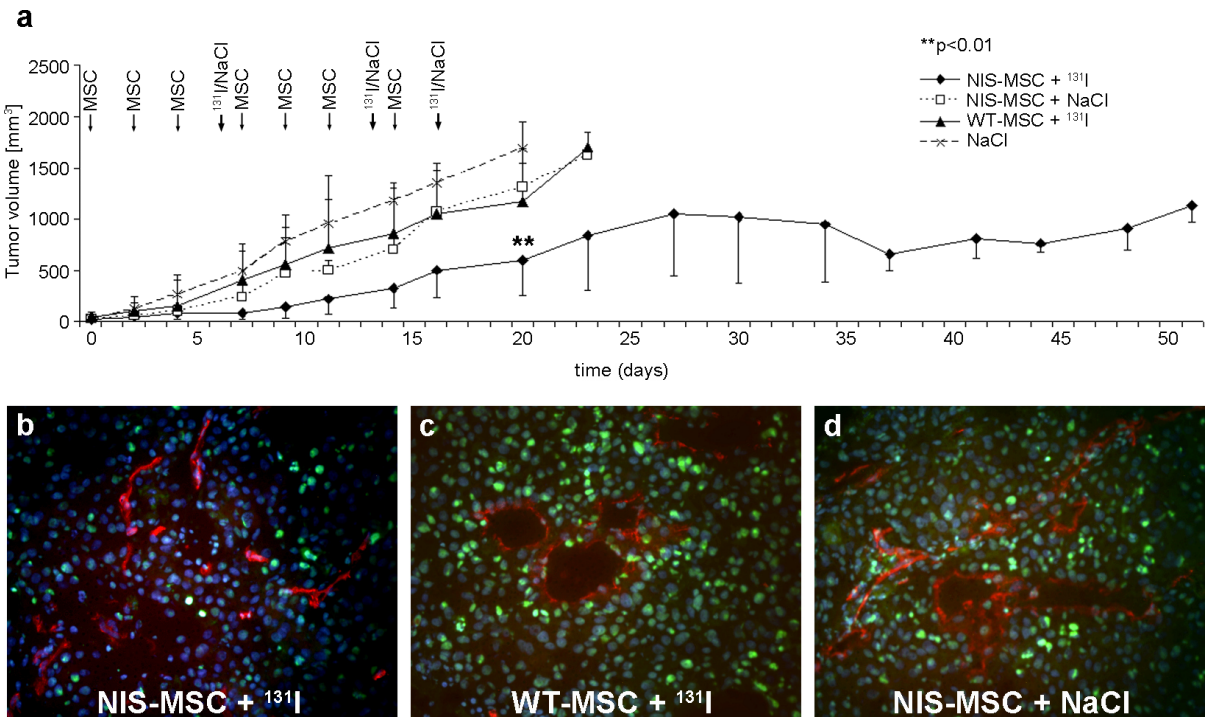

Figure 6 Two groups of mice were established receiving 55.5 MBq ^{131}I 48 h after the last of three NIS-MSC (n=15) or WT-MSC (n=15) applications in two-day-intervals, respectively. This cycle was repeated once 24 h after the last ^{131}I application. 24 h after these two treatment cycles, one additional MSC injection was administered followed by a third ^{131}I (55.5 MBq) injection 48 later. ^{131}I therapy after NIS-MSC application resulted in a significant delay in tumor growth as compared with the control groups, that were injected with WT-MSC followed by ^{131}I (p=0.008103; n=15), with NIS-MSC followed by saline (p=0.001703; n=15) or with saline only (n=15) (Fig. 6a). Immunofluorescence analysis using a Ki67-specific antibody (green) and an antibody against CD31 (red, labeling blood vessels) showed decreased proliferation (Ki67, 25 ± 4.1 %) and reduced blood vessel density (CD31, 1.85 ± 0.25%) in tumors of mice treated with NIS-MSC followed by ^{131}I treatment (Fig. 6b) as compared to tumors of mice injected with WT-MSC and ^{131}I (Fig. 6c) or mice treated with NIS-MSC and saline (Fig. 6d) (Ki67, 45 ± 8.7%; CD31, 5 ± 0.45%). Slides were counterstained with Hoechst Nuclear stain. Magnification 200x.

2.5 Discussion

NIS represents one of the oldest and most successful targets for molecular imaging. Cloning of the NIS gene has provided a versatile new reporter and therapy gene which has paved the way for the development of a novel cancer gene therapy strategy based on NIS-mediated radionuclide imaging and therapy (Hingorani *et al.* ; Spitzweg and Morris 2002). In previous studies in a prostate cancer model, we made use of a prostate-specific promoter to drive tissue-specific NIS expression after *ex vivo* NIS transduction of prostate cancer cells or local adenoviral *in vivo* NIS gene transfer. This approach demonstrated a significant therapeutic effect after application of ^{131}I or alternative radionuclides, such as ^{188}Re and ^{211}At (Kakinuma *et al.* 2003; Spitzweg *et al.* 2001a; Spitzweg *et al.* 2000; Spitzweg *et al.* 1999; Willhauck *et al.* 2007b; Willhauck *et al.* 2008a). Our work in the prostate cancer model and subsequent work in other tumor models, including medullary thyroid, colon and hepatocellular cancer (Dwyer *et al.* 2005a; Dwyer *et al.* 2005b; Herve *et al.* 2008; Klutz *et al.* 2009; Li *et al.* ; Peerlinck *et al.* 2009; Scholz *et al.* 2005; Spitzweg *et al.* 2007; Willhauck *et al.* 2007b; Willhauck *et al.* 2008c), have demonstrated the potential of NIS as a combined reporter and therapy gene.

One of the major hurdles for safe clinical application of the NIS gene-based therapy concept is optimal tumor targeting, with low toxicity, and high transduction efficiency for gene delivery vectors, with the ultimate aim of systemic vector application for the treatment of metastatic disease.

Relatively few studies have investigated NIS-targeted radionuclide therapy of metastatic cancer after systemic NIS gene delivery. The application of an oncolytic measles virus or an oncolytic vesicular stomatitis virus in a multiple myeloma mouse model was found to allow the monitoring of virus replication by radioiodine gamma camera or SPECT imaging as well as stimulation of oncolytic potency of the virus by combination with ^{131}I therapy (Dingli *et al.* 2004; Goel *et al.* 2007). In a recent study, we used NIS as reporter and therapy gene to demonstrate the high potential of synthetic polymeric vectors based on pseudodendritic oligoamines with high intrinsic tumor affinity for tumor-specific delivery of the NIS gene. After intravenous application of NIS polyplexes in a syngeneic neuroblastoma mouse model, NIS-mediated radioiodine accumulation was mainly restricted to the tumor, and sufficiently high for a significant delay of tumor growth (Klutz *et al.* 2009).

In the current study we utilized MSCs as gene delivery vehicles for tumor-targeted NIS gene delivery in a human hepatocellular cancer xenograft mouse model. Previous studies have shown that MSCs can efficiently migrate and engraft into the tumor stroma of tumor lesions representing the basis for the paradigm of the “Trojan horse” approach in which MSCs are used as shuttle vectors for delivery of therapeutic genes into critical parts of growing tumors (Conrad *et al.* 2011; Studeny *et al.* 2004). In a mouse model it was shown that MSCs

expressing TRAIL can provide targeted delivery of this pro-apoptotic agent to breast cancer metastases to the lung (Loebinger *et al.* 2009a). Similarly, MSCs transduced to express IFNβ or the immunostimulatory chemokine CX3CL1 have been shown to provide an antitumor effect in various murine cancer models, including glioma (Nakamizo *et al.* 2005), breast (Studeny *et al.* 2004), melanoma (Studeny *et al.* 2002) and colorectal cancer (Xin *et al.* 2007). In two previous studies we have demonstrated active homing of herpes simplex virus type 1 thymidine kinase (HSV-Tk)-transduced MSCs into primary pancreatic or breast cancer tumor stroma that resulted in significant reduction of tumor growth and in one case reduced incidence of metastases after application of ganciclovir (Conrad *et al.* 2011; Zischek *et al.* 2009).

Here MSCs stably transfected with NIS under control of the CMV promoter (NIS-MSC) revealed high levels of functional NIS protein expression that resulted in a 55% reduction of survival of HCC cells when cocultured with NIS-MSCs in an ^{131}I *in vitro* clonogenic assay. This demonstrated a significant bystander effect based on the crossfire effect of the β-emitter ^{131}I with a path length of up to 2.4 mm. Following systemic application of NIS-MSCs via the tail vein, 74% of implanted HCC tumors showed tumor-specific ^{123}I accumulation as imaged by gamma camera scintigraphy with accumulation of approx. 7% to 9% ID/g, and a biological half-life of 4 hours. In contrast, control mice showed no tumoral radioiodine uptake, confirming that the observed iodide accumulation in the tumors was mediated by functional NIS expression. *In vivo* ^{123}I-scintigraphic imaging confirmed by *ex vivo* biodistribution experiments revealed significant tumoral radioiodine accumulation. No iodide uptake was measured in nontarget organs, including liver, lungs, spleen or kidneys. Tumoral NIS expression was further verified by real time qPCR as well as NIS-specific immunoreactivity, which showed expression throughout the tumor stroma with most prominent staining in areas neighboring blood vessels. Interestingly, SV40 large T Ag immunostaining revealed strong accumulation of MSCs in the spleen without detection of NIS-specific immunoreactivity or iodide accumulation. These data suggest that MSCs were recruited to the spleen but did not undergo the same program of differentiation and activation, and therefore did not express the therapeutic gene.

Most of the studies investigating the potential of MSCs as gene delivery vehicles have addressed the issue of biodistribution and tumor-specific recruitment of MSCs mainly by *ex vivo* analysis of reporter gene expression. Our data demonstrate the potential of NIS as a dynamic reporter gene offering the possibility of noninvasive *in vivo* tracking of NIS-MSC homing and engraftment at the tumor site by ^{123}I-scintigraphy. This allows a detailed analysis of *in vivo* biodistribution of genetically modified MSCs as well as exact characterization of localization and level of transgene expression, an essential prerequisite for exact planning and monitoring of clinical gene therapy trials.

Our data are consistent with a recently published study by Rad *et al*. (Rad *et al.* 2009), who used superparamagnetic iron oxide-labeled NIS-transduced AC133+ progenitor cells to carry the NIS gene to sites of breast cancer xenografts in a nude mouse model. After i.v. application progenitor cells were successfully tracked by magnetic resonance imaging (MRI), while ^{99m}Tc-SPECT imaging demonstrated NIS gene expression at the tumor site confirming tumor-specific recruitment of stem cells (Rad *et al.* 2009). A similar approach was investigated by Loebinger *et al*., who labeled human MSCs with iron oxide nanoparticles, which allowed tracking of MSCs to lung metastases *in vivo* using MRI (Loebinger *et al.* 2009b). In addition, bioluminescent imaging was used to monitor luciferase-transduced MSC homing and engraftment in a syngeneic breast cancer mouse model (Klopp *et al.* 2007).

In addition to ^{123}I gamma camera imaging, we used small animal whole body positron emission tomography (PET) using ^{124}I as radiotracer. Despite the widespread availability of ^{123}I-scinitgraphy, PET imaging is attractive for tracking the delivery and tumoral engraftment of NIS-MSCs due to its higher sensitivity and enhanced resolution (Dingli *et al.* 2006; Groot-Wassink *et al.* 2004). In addition, fusion of PET with computed tomography (CT) images allows a more robust biodistribution analysis and clearly aids in correlative diagnosis in clinical oncology. With translation from animal to human studies in mind, PET/CT could be the optimal method to study MSC biodistribution, followed by quantification of radioiodine accumulation and exact dosimetric calculations. We have demonstrated the feasibility of monitoring MSC biodistribution by ^{124}I-PET allowing a more detailed three-dimensional analysis of NIS-mediated radioiodine accumulation. In support of our data, MSC engraftment and proliferation in tumor stroma of microscopic tumors has successfully be monitored by ^{18}F-FHBG-PET imaging using herpes simplex virus type 1 thymidine kinase as reporter gene (Hung *et al.* 2005).

The ability to monitor MSC distribution effectively sets the stage for therapeutic application of ^{131}I. As detailed above, and shown in the current therapy study, the application of NIS-transduced MSCs allows noninvasive imaging of their recruitment and engraftment at the tumor site, and also provides a powerful anticancer strategy taking advantage of NIS as a potent therapy gene. NIS expression allows a significant bystander effect based on the crossfire effect of the β-emitters ^{131}I (path length of up to 2.4 mm) or ^{188}Re (path length of 10 mm) that are both transported by the protein. NIS-mediated uptake of ^{131}I or ^{188}Re in NIS-transduced MSCs therefore can kill neighboring tumor cells, but also can target a significant radiation dose to the tumor stroma, which has been recognized as a crucial and vulnerable target for tumor therapy. Due to its function as a reporter gene, and its association with a significant bystander effect, NIS represents an ideal therapy gene in the context of stem cell based gene therapy which was demonstrated in the current study. After three cycles of repetitive MSC injections followed by ^{131}I administration, experimental HCC-xenografts

showed a significant reduction in tumor growth. In addition, immunofluorescence analysis of tumor tissue showed markedly reduced proliferation and decreased blood vessel density in the NIS-MSC/^{131}I treated mice. To date, only relatively few studies have demonstrated the feasibility of MSCs as gene delivery vehicles for the treatment of malignant tumors. Zischek *et al.* demonstrated significant reduction of pancreatic tumor growth and incidence of metastases using HSV-Tk transfected MSCs after treatment with glanciclovir (Zischek *et al.* 2009). In a related study, intratumorally injected TRAIL-secreting umbilical cord blood-derived MSCs significantly reduced tumor growth in a glioma tumor model (Kim *et al.* 2010). However, these studies lack the unique dual function of the NIS gene as detailed here.

MSCs are known to have immunosuppressive functions that may influence therapeutic efficacy. We believe that due the transient nature of the application of the engineered MSCs in concert with the removal of all adoptively applied MSC in the context of therapy in the current study, and based on our previous studies outlined above, this phenomenon is of minor relevance. A negative effect on therapy was not seen in experiments using syngeneic MSC expressing a suicide gene in syngeneic immunocompetent mice (Conrad *et al.* 2011; Zischek *et al.* 2009).

In conclusion, our data demonstrate the high potential of genetically engineered MSCs as tumor-selective delivery vehicles for the human NIS gene after systemic application. NIS as a potent and well characterized reporter gene allowed detailed noninvasive characterization of *in vivo* biodistribution of MSCs by analysis of functional NIS expression by ^{123}I-scintigraphy and ^{124}I-PET imaging, which is an essential prerequisite for exact planning and monitoring of the application of NIS as therapy gene. Moreover, in parallel studies, ^{131}I administration leads to delayed tumor growth. This study therefore opens the exciting prospect of NIS-mediated radionuclide therapy of metastatic cancer taking advantage of the tumor-selective homing of MSCs and the bystander effect of the NIS gene therapy concept.

2.6 Acknowledgements

We are grateful to J. C. Morris, Division of Endocrinology, Mayo Clinic and Medical School, Rochester, MN, USA for providing the NIS-specific antibody, as well as to S. M. Jhiang, Ohio State University, Columbus, OH, USA for supplying the full-length human NIS cDNA. We also thank Wolfgang Münzing, Cornelia Arszol, Sebastian Nowak and Julia Schlichtiger, Department of Nuclear Medicine, Ludwig-Maximilians-University, Munich, Germany, for their assistance with imaging studies and animal work.

This study was supported by grant SFB 824 (Sonderforschungsbereich 824) from the Deutsche Forschungsgemeinschaft, Bonn, Germany, to C. Spitzweg, and by a grant from the Wilhelm-Sander-Stiftung (2008.037.1) to C. Spitzweg and P. Nelson.

The authors declare that there is no financial conflict of interests.

3 Chapter 2

Stromal targeting of sodium iodide symporter using mesenchymal stem cells allows enhanced imaging and therapy of hepatocellular carcinoma

Kerstin Knoop[1], Nathalie Schwenk[1], Patrick Dolp[1], Michael J. Willhauck[1], Christoph Zischek[2], Christian Zach[3], Markus Hacker[3], Burkhard Göke[1], Ernst Wagner[4], Peter J. Nelson[2], Christine Spitzweg[1]

Department of Internal Medicine II[1], Clinical Biochemistry Group, Department of Medical Policlinic IV[2], Department of Nuclear Medicine[3], Department of Pharmacy, Center of Drug Research, Pharmaceutical Biotechnology[4], Ludwig-Maximilians-University, Munich, Germany

3.1 Abstract

The tumor-homing property of mesenchymal stem cells (MSC) has led to their use as delivery vehicles for therapeutic genes. The application of the sodium iodide symporter (NIS) as therapy gene allows non-invasive imaging of functional transgene expression by ^{123}I-scintigraphy or PET-imaging, as well as therapeutic application of ^{131}I or ^{188}Re. Based on the critical role of the chemokine RANTES/CCL5 secreted by MSCs in the course of tumor stroma recruitment, use of the RANTES/CCL5 promoter should allow tumor stroma-targeted expression of NIS after MSC-mediated delivery.

Using a human hepatocellular cancer (HCC) xenograft mouse model (Huh7) we investigated distribution and tumor recruitment of RANTES-NIS-engineered MSCs after systemic injection by gamma camera imaging. ^{123}I-scintigraphy revealed active MSC recruitment and CCL5 promoter activation in the tumor stroma of Huh7 xenografts (6.5% ID/g ^{123}I, biological half-life: 3.7 h, tumor-absorbed dose: 44.3 mGy/MBq). In comparison, 7% ID/g ^{188}Re was accumulated in tumors with a biological half-life of 4.1 h (tumor-absorbed dose: 128.7 mGy/MBq). Administration of a therapeutic dose of ^{131}I or ^{188}Re (55.5 MBq) in RANTES-NIS-MSC treated mice resulted in a significant delay in tumor growth and improved survival without significant differences between ^{131}I and ^{188}Re.

These data demonstrate successful stromal targeting of NIS in HCC tumors by selective recruitment of NIS-expressing MSCs and by use of the RANTES/CCL5 promoter. The resulting tumor-selective radionuclide accumulation was high enough for a therapeutic effect of ^{131}I and ^{188}Re opening the exciting prospect of NIS-mediated radionuclide therapy of metastatic cancer using genetically engineered MSCs as gene delivery vehicles.

3.2 Introduction

Hepatocellular carcinoma (HCC) is the sixth most common malignancy and the third leading cause of cancer-related death worldwide (Parkin *et al.* 2005). The only available, potentially curative treatment options, such as liver transplantation, surgical resection, or radiofrequency ablation are reserved for patients with early-stage HCC. However, more than half of the patients with HCCs are diagnosed at an intermediate or advanced tumor stage with only limited, palliative treatment options, leading to a poor prognosis for these patients (Parkin *et al.* 2005; Pinter *et al.* 2012). Growing HCC require an active tumor stroma with extensive vasculature with high endothelial cell turnover, numerous cancer-associated fibroblasts, inflammatory cells and increased levels of cytokines and chemokines such as TNF-α, TGF-β, IL-6, IL-10, CCL2/MCP-1, CCL3 and RANTES/CCL5 for effective tumor growth (Braunersreuther *et al.* 2012; Niess *et al.* 2011). The tumor stroma is therefore recognized as an important therapeutic target in the treatment of HCCs.

Mesenchymal stem cells (MSC) play a key role in the maintenance and regeneration of diverse tissues. In the course of tissue injury, or during chronic inflammation, MSCs contribute to tissue remodeling by their recruitment to sites of tissue injury (Aquino *et al.* 2010). We and others have shown that MSCs are strongly recruited into the stroma of many malignant tumors. It is thought that growing tumor is seen by the body as a “chronic wound” and MSC act as progenitor cells for components of the tumor stroma (Aquino *et al.* 2010; Conrad *et al.* 2007; Conrad *et al.* 2011; Dwyer *et al.* 2010; Knoop *et al.* 2011; Niess *et al.* 2011; Zischek *et al.* 2009). The tropism of MSCs for tumors represents the basis for the paradigm of the “Trojan horse” approach. Due to their intrinsic tumor homing capacity, MSCs are under development as cellular vehicles for the targeted delivery of therapeutic genes into the stroma of malignant tumors (Klopp *et al.* 2007; Knoop *et al.* 2011; Niess *et al.* 2011; Zischek *et al.* 2009).

Central issues that must be addressed with this therapeutic approach include the development of restricted transgene expression to spare potential damage to non-tumor tissues, enhanced non-invasive *in vivo* imaging techniques that could be applied to patients, and the development of more potent therapy gene strategies.

Karnoub *et al.* recently demonstrated recruitment of MSCs into the tumor stroma of breast cancer, followed by their induced expression of the CC-chemokine RANTES/CCL5 (Regulated on Activation, normal T-cell Expressed and presumably Secreted)/CCL5 (Karnoub *et al.* 2007). CCL5 is a chemoattractant of monocytes, eosinophils and activated CD4 T cells, which signals through the G protein-coupled receptors (GPCR) CCR1, CCR3 and CCR5 (Zlotnik and Yoshie 2000). CCL5 expression is associated with increased tumor neovascularization, as well as enhanced cancer growth and metastasis by autocrine and

paracrine activation of tumor cells and through the recruitment of stromal cell types to sites of primary tumor growth (Karnoub *et al.* 2007).

Due to its expression in follicular cell-derived thyroid cancer cells, the sodium iodide symporter (NIS) provides the molecular basis for diagnostic and therapeutic application of radioiodine for the treatment of thyroid cancer patients. Cloning of NIS has therefore allowed the development of a new therapeutic strategy for the treatment of tumors without endogenous NIS expression based on targeted, tumor-selective NIS gene transfer followed by administration of ^{131}I or other radionuclides that are transported by NIS, such as ^{188}Re or ^{211}At (Hingorani *et al.* ; Spitzweg and Morris 2002; Willhauck *et al.* 2007b; Willhauck *et al.* 2008a). ^{188}Re is characterized by a shorter physical half-life and decay properties that are seen as superior to ^{131}I, and thus may provide a powerful tool to enhance the therapeutic efficacy of NIS-mediated radionuclide therapy, in particular because of its enhanced crossfire effect (max path length of up to 10.4 mm) (Klutz *et al.* 2011b; Willhauck *et al.* 2007b). Importantly, the use of NIS as a theranostic gene offers the possibility of direct non-invasive molecular scintigraphy and PET imaging allowing dosimetric calculations as a crucial prerequisite for the exact planning of therapy studies (Dingli *et al.* 2003b; Groot-Wassink *et al.* 2004; Klutz *et al.* 2011b; Spitzweg and Morris 2002; Willhauck *et al.* 2007b).

In our previous studies, human MSCs were stably transfected with a sodium iodide symporter (NIS)-expressing plasmid, where NIS was driven by the broadly expressed CMV promoter. Using NIS as reporter gene, active MSC recruitment into the tumor stroma of HCC xenografts was demonstrated after systemic injection. In addition, repetitive MSC injections followed by ^{131}I administration showed a significant reduction in tumor growth with an improved survival (Knoop *et al.* 2011). Since MSCs are known to be recruited also in non-tumor tissues such as spleen or skin, the use of the unspecific CMV promoter might be disadvantageous due to transgene expression in these non-target organs with the risk of extratumoral toxicity. Therefore, in the current study, we have made use of the RANTES/CCL5 promoter to biologically target NIS transgene expression in engineered human MSCs to the stroma of HCC xenografts. In parallel, the accumulation and therapeutic efficacy of ^{131}I was examined in direct comparison to ^{188}Re in the context of systemic MSC-mediated NIS gene transfer.

3.3 Methods

Cell culture

Establishment and characterization of MSCs and cultivation of the human HCC cell line Huh7 (JCRB 0403) have been described previously (Knoop *et al.* 2011).

Plasmid construct

The full length NIS cDNA was removed from the pcDNA3 expression vector (kindly provided by Dr S.M. Jhiang, Ohio State University, Columbus, OH, USA) by restriction digestion using XbaI and HindIII, agarose gel purified and ligated into the expression vector pcDNA3-CCL5Pro. CCL5Pro-NIS was removed and ligated in the pCMV/Bsd vector (Invitrogen/Life technologies) using the restriction enzyme HindIII resulting in pCMV/Bsd-RaPro-hNIS. The sequence of the CCL5 promoter used -972 of the upstream region and the complete 5´untranslated region (Nelson *et al.* 1993). The vector included a CMV controlled Bsr2 Blasticidin resistance gene to select transfected cells at a blasticidin concentration of 5µg/ml.

Mesenchymal stem cells

Wild-type MSCs stably transfected with pCMV/Bsd-RaPro-hNIS were established as described previously (Knoop *et al.* 2011). The clone expressing the highest levels of NIS mRNA was subsequently referred to as RANTES-NIS-MSC and used for all further experiments. To prepare cells for injection into mice, cells were detached from culture flasks, washed three times with 1x PBS and resuspended in 1x PBS at a concentration of 500.000 cells per 500µl.

Establishment of Huh7 xenograft tumors

Huh7 xenograft tumors were established in female CD1 nu/nu mice (Charles River, Sulzfeld, Germany) as described previously (Knoop *et al.* 2011). The experimental protocol was approved by the regional governmental commission for animals (Regierung von Oberbayern).

MSC application and radionuclide biodistribution analysis in vivo

Experiments were started when a tumor size of 3 to 5 mm was reached and following a 10-day pretreatment with L-T4 as described previously (Knoop *et al.* 2011). The pretreatment schedule was based on a study by Di Cosmo *et al.* using a dose generally accepted as a supraphysiological LT-4 dose (10 µg L-T4/100 g body weight) (Di Cosmo *et al.* 2009). The mice used in our experiments weighed between 20 – 25 g and therefore a dose of 2 µg L-T4/mice per day was chosen. WT-MSCs or RANTES-NIS-MSCs were injected into the tail

vein at a concentration of 5 x 10^5 cells/500µl PBS. Two groups of mice were established with following treatments: (a) three i.v. applications of RANTES-NIS-MSC in four day intervals (n=48); (b) three i.v. applications of WT-MSC in four day intervals (n=9). As an additional control, in a subset of mice injected with RANTES-NIS-MSC (n=18) the specific NIS-inhibitor sodium-perchlorate ($NaClO_4$, 2 mg per mouse) was injected i.p. 30 min prior to radionuclide administration. 72 h after the last MSC application, 18.5 MBq ^{123}I or 111 MBq ^{188}Re ($^{188}ReO_4^-$ perrenhate) were injected i.p. and radionuclide biodistribution was assessed using a gamma camera equipped with UXHR collimator (Ecam, Siemens, Germany) as described previously (Willhauck *et al.* 2007b; Willhauck *et al.* 2008a); Knoop *et al.*, 2011).

Biodistribution analysis of radionuclides was also performed *ex vivo* after mice were injected with RANTES-NIS-MSCs (n=16) or WT-MSCs (n=6) as described above followed by i.p. injection of 18.5 MBq ^{123}I or 111 MBq ^{188}Re, respectively. As an additional control, a subset of RANTES-NIS-MSC injected mice (n=8) were pretreated with $NaClO_4$. Gamma counter analysis was performed as described previously (Knoop *et al.* 2011).

NIS mRNA analysis by quantitative real-time PCR

Analysis of NIS mRNA expression by quantitative real time PCR (qPCR) was performed as described previously (Knoop *et al.* 2011).

Radionuclide therapy studies in vivo

Following a 10-day L-T4 pretreatment as described above, four groups of mice were established receiving 55.5 MBq ^{131}I (sodium iodide; GE Healthcare Buchler GmbH, Braunschweig, Germany) or ^{188}Re ($^{188}ReO_4^-$ perrhenate; ITG GmbH, Garching, Germany) 48 h after the final of three RANTES-NIS-MSC (RANTES-NIS-MSC + ^{131}I, n=15; RANTES-NIS-MSC + ^{188}Re, n=15) or WT-MSC (WT-MSC + ^{131}I, n=15; WT-MSC + ^{188}Re, n=15) applications in two-day-intervals (each 5 x 10^5 cells/500 µl PBS), respectively. This cycle was repeated once 24 h after the last radionuclide application. 24 h later one additional MSC (5 x 10^5 cells) injection was applied, followed by another radionuclide (55.5 MBq ^{131}I or ^{188}Re, respectively) injection 48 h later (Fig. 5a). As a control group, mice were injected with RANTES-NIS-MSC (n=15) followed by application of saline. Another control group received saline only (n=15). The follow up of mice including tumor measurements were performed as outlined previously (Knoop *et al.*, 2011).

Indirect immunofluorescence assay

Immunofluorescence staining of frozen sections was performed as described previously (Knoop *et al.* 2011) using following primary antibodies: hNIS (mouse monoclonal, provided by J.C. Morris, Division of Endocrinology, Mayo Clinic and Medical School, Rochester, MN),

mouse RANTES/CCL5 (goat polyclonal, AF478, R&D Systems, Minneapolis, USA), SV40 large T-antigen (mouse monoclonal, Calbiochem/Merck, Darmstadt, Germany), CD31 (rat monoclonal, Pharmingen/BD, New York, USA) or Ki67 (rabbit polyclonal, Abcam, Cambrigde, UK). Staining and evaluation of proliferation and vessel density were preformed as described previously (Knoop *et al.* 2011).

Statistical methods

Statistical significance of *in vitro* experiments was tested using Student´s t test. Statistical significance of *in vivo* experiments has been calculated using Man-Whitney U test.

3.4 Results

Radionuclide biodistribution studies after in vivo NIS gene transfer

Significant iodide accumulation was observed in 67% of Huh7 tumors following application of RANTES-NIS-MSCs (Fig. 1a). In contrast, after application of WT-MSCs no tumoral iodide accumulation was measured (Fig. 1c). Serial imaging revealed a tumoral uptake of approximately 6.5% ID/g ^{123}I after application of RANTES-NIS-MSCs with a biological half-life of 3.7 h (Fig. 1g). Considering a tumor mass of 1g, and an effective half-life of 3.5 h for ^{131}I, a tumor absorbed dose of 44.3 ± 8.6 mGy/MBq ^{131}I was calculated. In comparison, approximately 7% ID/g ^{188}Re was concentrated in 67% of Huh7 tumors, with a biological half life of 4.1 h (Fig. 1d, g). With an effective half-life of 3.5 h for ^{188}Re, a tumor absorbed dose of 128.7 ± 28.2 mGy/MBq ^{188}Re was determined. Physiologic accumulation of radionuclides was also observed in thyroid gland and stomach due to endogenous NIS expression as well as in the bladder due to renal excretion of radionuclides (Fig. 1a, c, d, f). In a subset of mice injected with RANTES-NIS-MSCs, pretreatment with perchlorate ($NaClO_4$; 2mg) 30 min prior to injection of the respective radionuclide, completely abolished radionuclide uptake in the tumor as well as in thyroid gland and stomach, confirming that the observed radionuclide accumulation is indeed NIS-mediated (Fig. 1b, e). As expected, physiologic radionuclide accumulation in non-target organs (thyroid gland, stomach, and bladder) was also seen after WT-MSC injection (Fig. 1c, f). As outlined above, in 1/3 of the animals no specific radionuclide accumulation after RANTES-NIS-MSCs injection was observed, however, by immunohistochemistry it was shown, that MSCs were recruited into the tumor stroma to a lower extent (Suppl. Fig. 1), resulting in a radionuclide accumulation which was obviously below the detection limit.

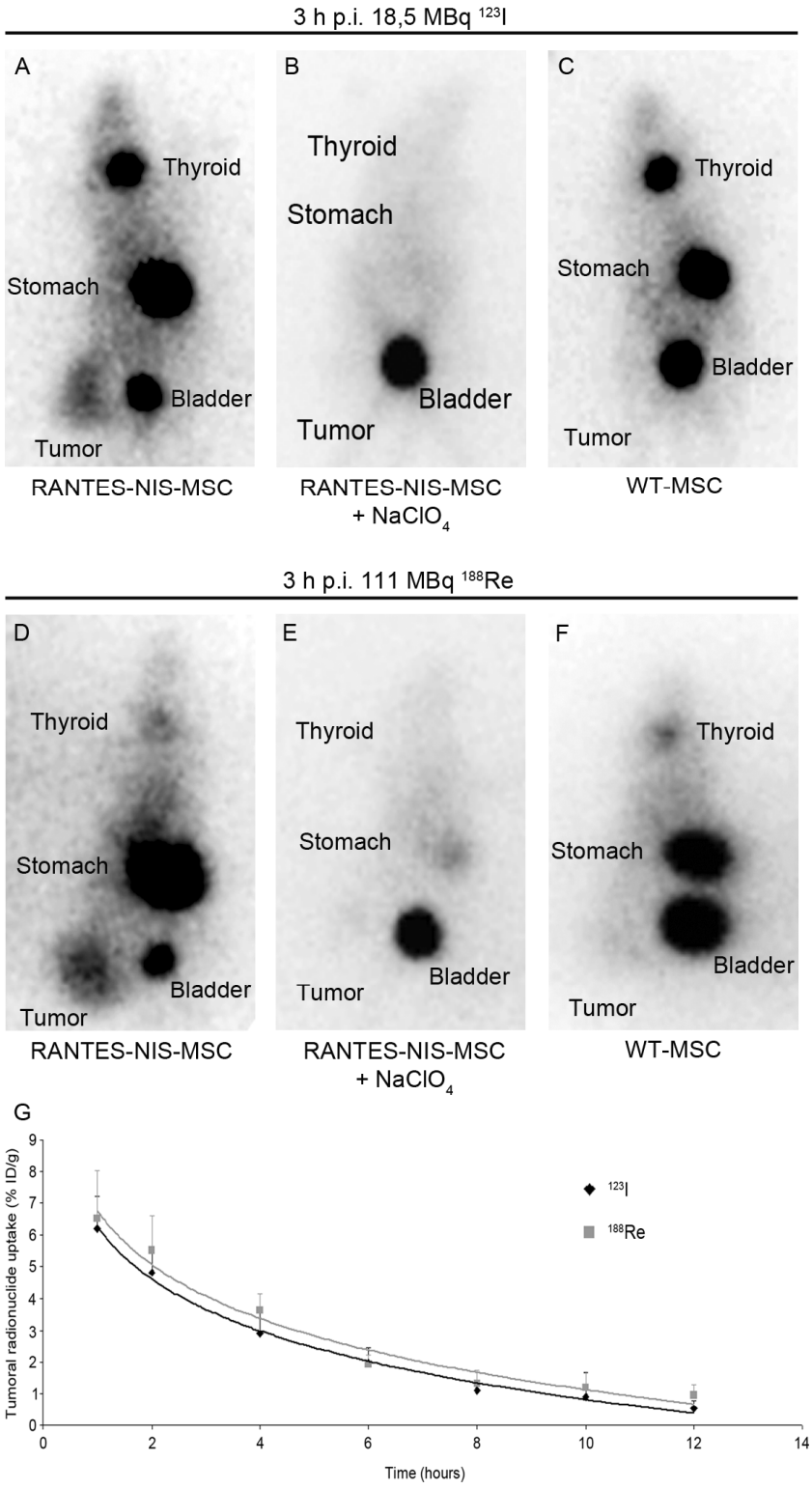

Figure 1 Radionuclide biodistribution studies *in vivo*. Gamma-camera imaging of mice harboring Huh7 tumors after mesenchymal stem cell (MSC)-mediated sodium iodide symporter (NIS) gene delivery 3 hours following ^{123}I or ^{188}Re administration. After three intravenous i.v. applications of RANTES-NIS-MSCs significant tumor-specific iodide (a) and rhenium (d) accumulation was induced, which was completely abolished upon pretreatment with $NaClO_4$ (b) and (e). In contrast, mice injected with WT-MSCs showed no tumoral iodide (c) or rhenium (f) uptake. Radionuclides were also accumulated physiologically in thyroid, stomach and bladder. (g) Time course of ^{123}I and ^{188}Re accumulation in Huh7 tumors after three i.v. RANTES-NIS-MSC applications followed by injection of 18.5 MBq ^{123}I or 111 MBq ^{188}Re, respectively, as determined by serial scanning. Maximum tumoral radioiodine uptake was 6.5% ID/g tumor and 7% ID/g tumor for ^{188}Re, respectively.

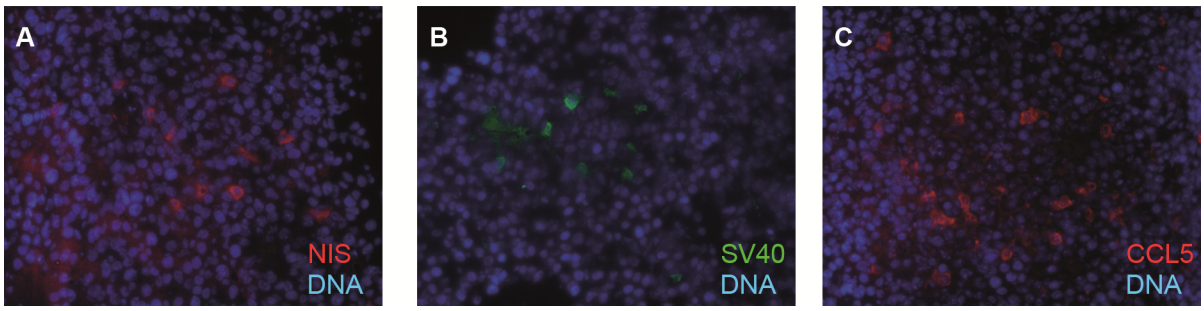

Supplemental Figure 1 Immunohistochemical staining of radionuclide-negative Huh7 tumors after application of RANTES-NIS-MSCs. Radionuclide-negative Huh7 tumors revealed lower levels of NIS-specific immunoreactivity throughout the tumor stroma after application of RANTES-NIS-MSCs (a) with a similar distribution of SV40 large T Ag-positive cells (b) and in the presence of strong RANTES-specific immunoreactivity (c). Magnification: NIS, SV40 large T AG and RANTES/CCL5 staining: x200

Analysis of NIS protein expression by indirect immunofluorescence

The distribution of MSCs in tumors and non-target organs such as liver, kidney and spleen was determined in more detail by immunofluorescence staining using NIS-, SV40 large T Ag- and RANTES/CCL5-specific antibodies. H&E stainings of all organs or tumors are provided (Fig 2 d, h, l, p, t). Immortalization of MSCs via SV40 large T Ag provides a useful marker for the *ex vivo* detection of adoptively transferred MSCs. NIS-specific immunoreactivity based on RANTES/CCL5 promoter activity, was detected throughout the tumor stroma, predominantly in the vicinity of blood vessels, which paralleled the localization of SV40 large T Ag and the distribution of RANTES/CCL5 expression (Fig 2 a-d). Liver and kidneys showed no detectable NIS, SV40 large T Ag or RANTES/CCL5 immunoreactivity (Fig. 2 e-l). In contrast, a high density of SV40 large T Ag-expressing cells was detected in the spleen after RANTES-NIS-MSC application (Fig. 2n), while no NIS- and RANTES/CCL5-specific immunofluorescence staining was observed (Fig. 2 m, o) demonstrating restricted transgene expression. Injection of WT-MSCs resulted in SV40 large T Ag- and RANTES/CCL5-specific immunofluorescene staining in tumors (Fig. 2 r, s) demonstrating active tumoral recruitment of MSCs after i.v. application. In contrast, no NIS-specific immunostaining was observed after WT-MSC gene transfer (Fig. 2 q).

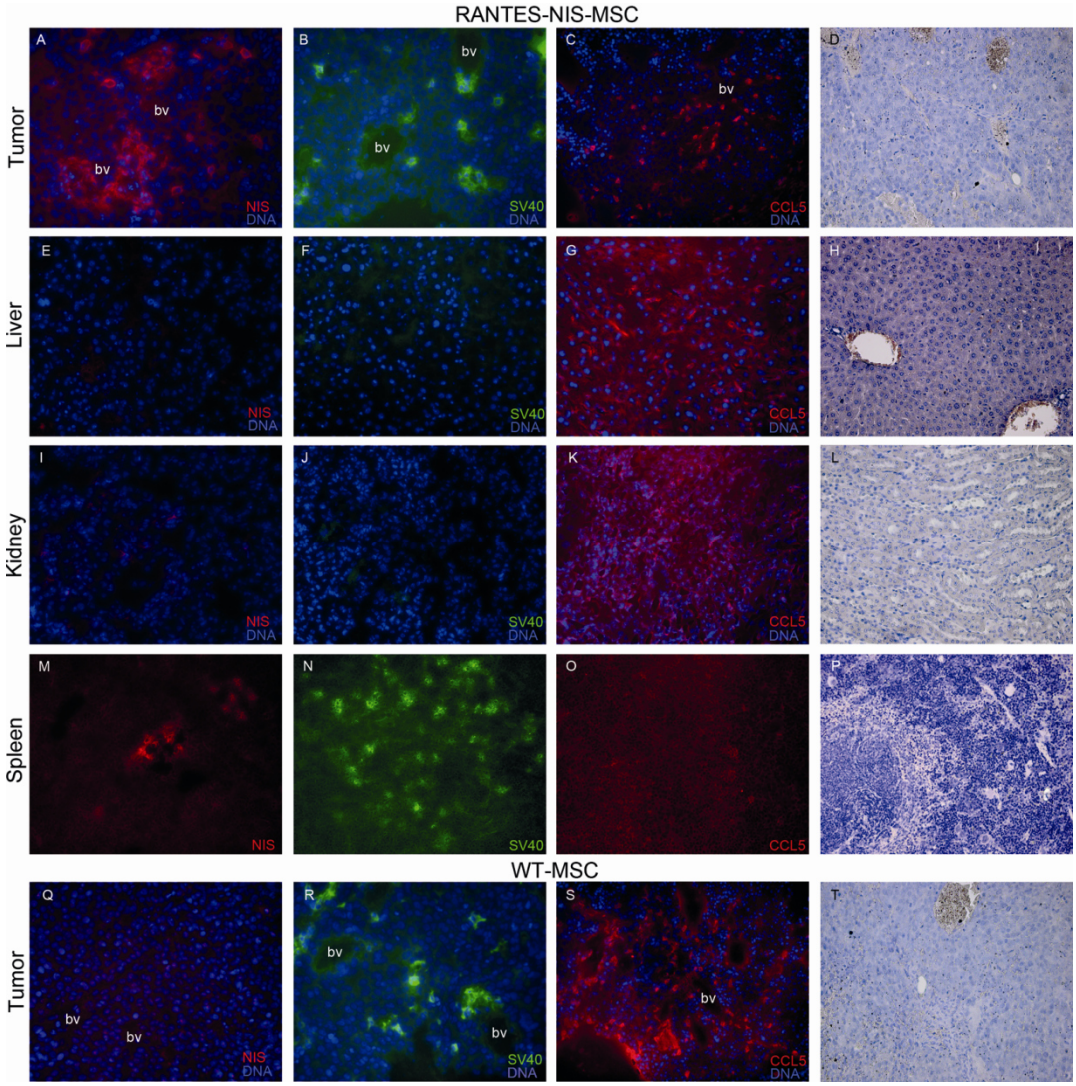

Figure 2 Immunhistochemical staining of Huh7 tumors and non-target organs after application of RANTES-NIS-MSCs or WT-MSCs. After application of RANTES-NIS-MSCs Huh7 tumors revealed NIS-specific immunoreactivity throughout the tumor stroma (a) with a similar distribution of SV40 large T Ag- (b) and RANTES/CCL5-positive cells (c). Other organs, like liver or kidney showed no detectable NIS, SV40 large T Ag or RANTES/CCL5 protein expression (e-g, i-k). In contrast, strong accumulation of SV40 large T Ag-expressing cells was detected in the spleen of mice that where injected with RANTES-NIS-MSCs (n), while no NIS- (m) or RANTES/CCL5-specific immunoreactivity (o) was detected. After application of WT-MSCs no NIS-specific immunoreactivity was detected in Huh7 tumors (q), while strong cytoplasmatic SV40 large T Ag (r) and RANTES/CCL5 (s) staining was detected. Slides were counterstained with Hoechst Nuclear stain. H&E stainings of Huh7 tumors (d), liver (h), kidney (l) and spleen (p) after injection of RANTES-NIS-MSC and tumors of mice injected with WT-MSCs (t) are provided. Magnification (NIS and SV40 large T AG staining: x200; RANTES/CCL5 staining: x100) (bv – blood vessel).

Ex vivo radionuclide biodistribution studies

Significant levels of tumoral iodide and rhenium uptake were confirmed after application of RANTES-NIS-MSCs by *ex vivo* biodistribution studies revealing a radionuclide uptake of 3 – 3.5% ID/organ ^{123}I or ^{188}Re four hours after radionuclide injection. In non-target organs (lung, liver, spleen, kidney) no specific radionuclide accumulation was detected. The competitive NIS inhibitor perchlorate significantly blocked radionuclide uptake in tumors of mice injected

with RANTES-NIS-MSCs (Fig. 3). Significant radionuclide accumulation was also detected in tissues that physiologically express NIS (stomach, thyroid gland) and in the bladder due to renal elimination of radionuclides (Spitzweg *et al.*, 2002; Spitzweg *et al.*, 2001). The thyroid gland and the stomach accumulated approximately 40% and 39% ID/organ, respectively, for ^{123}I and 15% ID/organ and 40% ID/organ, respectively, for ^{188}Re (data not shown). The effective half-life in the thyroid gland was approx. 38 h for ^{131}I and only 6.5 h for ^{188}Re. In this regard it is important to outline that NIS expression is exclusively regulated by thyroid stimulating hormone (TSH) in the thyroid gland, which allows effective downregulation of radionuclide accumulation in the thyroid gland by thyroid hormone pretreatment as shown by Wapnir *et al.* (Wapnir *et al.*, 2004). Moreover, during prolonged anaesthesia for imaging purposes gastric juices are pooled in the stomach which results in significantly higher gastric radionuclide accumulation than routinely observed in humans. In the bladder radionuclide accumulation and retention time can be minimized by stimulation of diuresis thereby lowering the delivered dose and side effects to bladder and adjacent tissues.

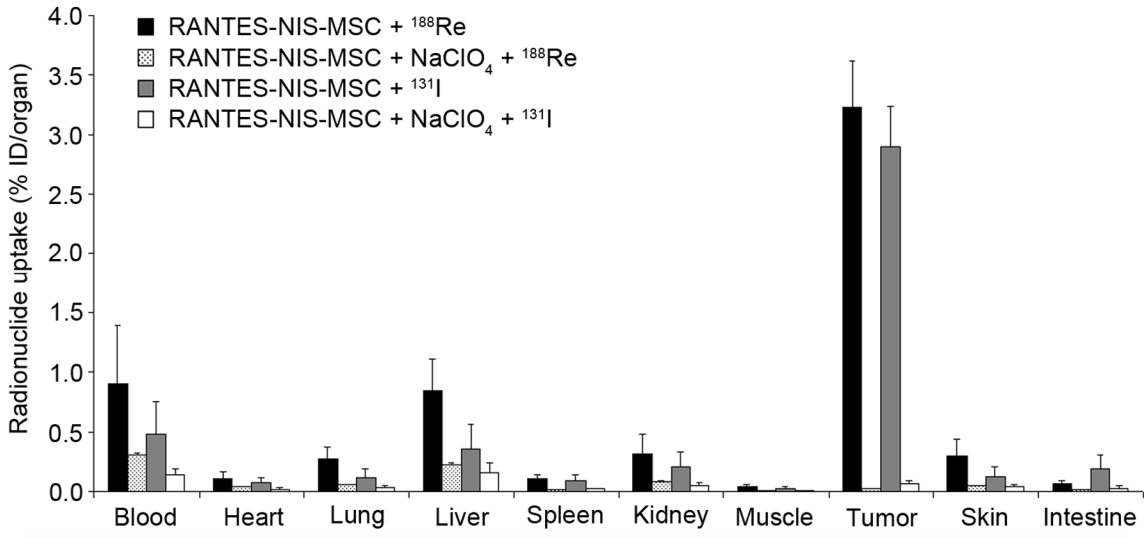

Figure 3 Evaluation of radionuclide biodistribution *ex vivo* 4 hours following injection of 18.5 MBq ^{123}I or 111 MBq ^{188}Re. Tumors in RANTES-NIS-MSC-injected mice showed high perchlorate-sensitive radionuclide uptake activity (~ 3 – 3.5% ID/organ), while no significant radionuclide accumulation was measured in non-target organs. Results are reported as percent of injected dose per organ ± SD.

NIS mRNA analysis by qPCR

mRNA was isolated from tumors and non-target organs (liver, lung, kidney and spleen) after systemic MSC injection and analyzed by qPCR using NIS-specific oligonucleotide primers. Systemic injection of RANTES-NIS-MSCs in tumor-bearing mice resulted in significantly increased levels of NIS mRNA in tumors, whereas no significant NIS mRNA expression was detected in non-target organs (Fig. 4).

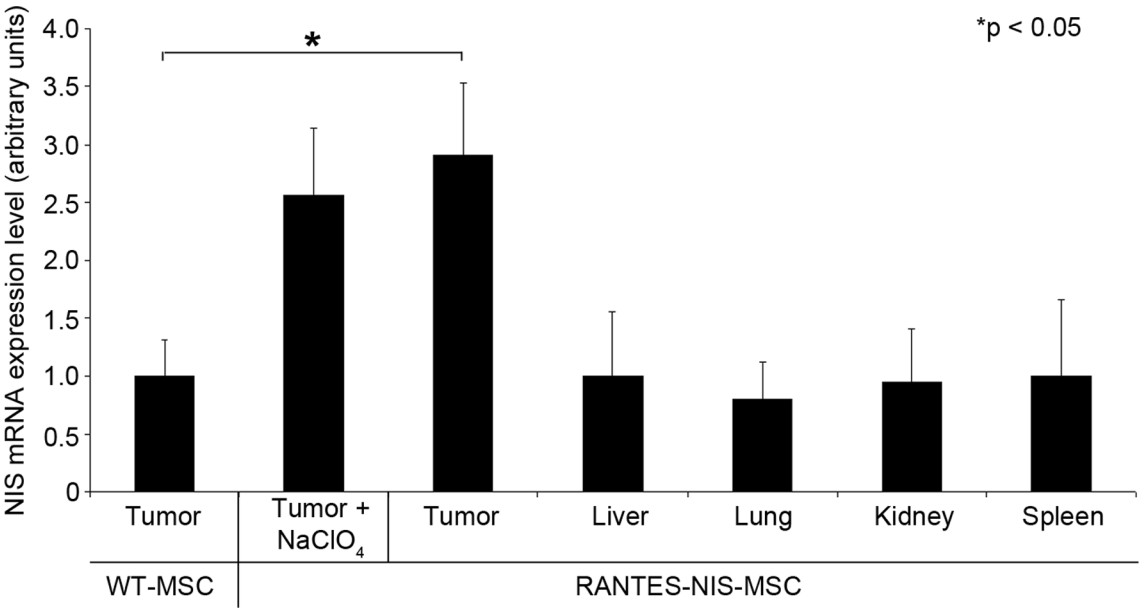

Figure 4 Analysis of NIS mRNA expression in Huh7 tumors and non-target organs by quantitative real-time PCR (qPCR). While only a low background level of NIS mRNA expression was detected in tumors injected with WT-MSCs, significant levels of NIS mRNA expression were induced in Huh7 tumors after three applications of RANTES-NIS-MSCs with or without $NaClO_4$ pretreatment. In non-target organs like liver, lung, kidney or spleen no NIS mRNA expression was detected.

Radionuclide therapy studies in vivo after MSC-mediated systemic NIS gene transfer

The effect of therapeutic radionuclides (^{131}I and ^{188}Re) was then compared and contrasted in the context of RANTES-NIS-MSC treatment. Control mice treated with RANTES-NIS-MSCs followed by saline application, mice treated with WT-MSCs followed by application of ^{131}I or ^{188}Re, or mice treated with saline only showed an exponential tumor growth and had to be killed after 3 – 4 weeks (Fig. 5a). In contrast, RANTES-NIS-MSC and ^{131}I- or ^{188}Re-treated tumors showed a dramatic control of growth (day 24: p=0.02 (NaCl) and p=0.05 (WT-MSC)) that extended through the end of the experiment (nine weeks) (Fig. 5a) and which resulted in an improved survival (Fig. 5b). The application of ^{188}Re did not result in an obvious increase in therapeutic efficacy as compared with ^{131}I, but enhanced therapeutic effects would be difficult due to the dramatic effects of ^{131}I treatment in this experimental setting. No major adverse effects of radionuclide or MSC treatment were observed in terms of lethargy or respiratory failure.

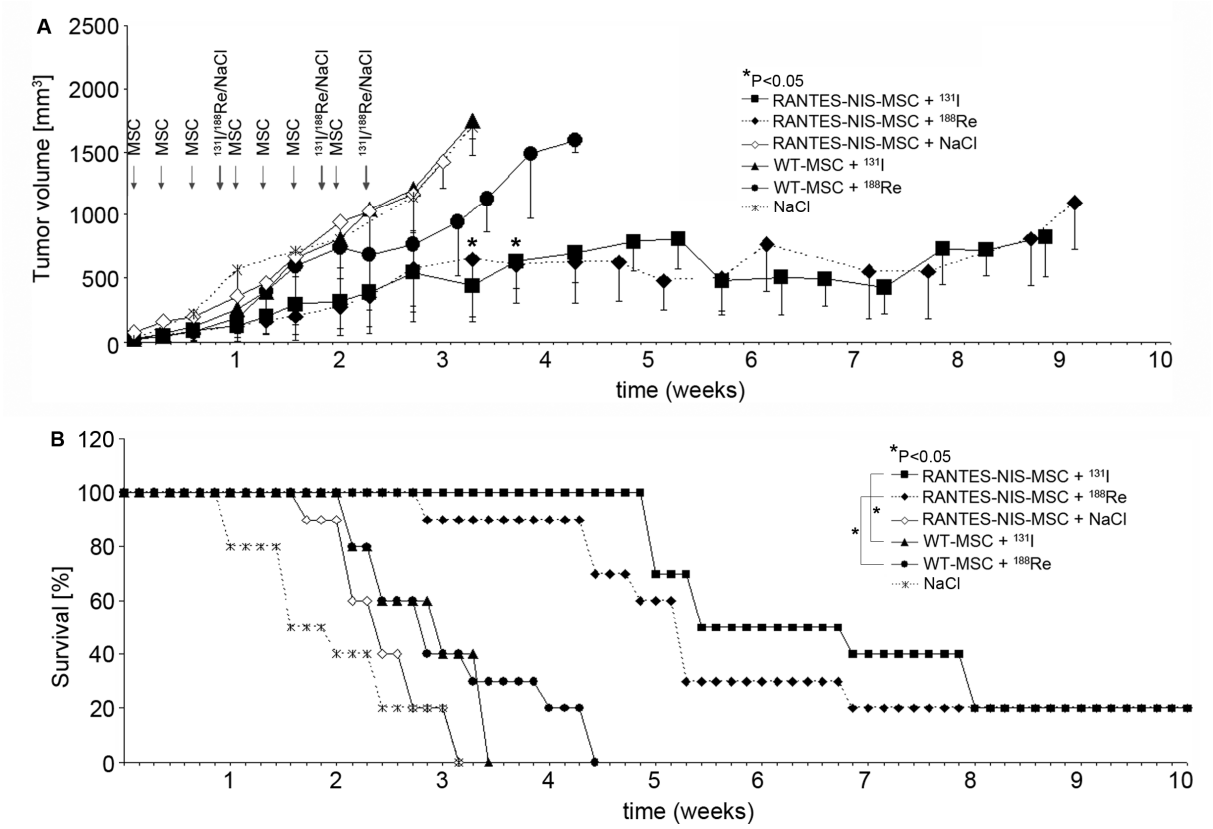

Figure 5 Radionuclide therapy studies in vivo after MSC-mediated systemic NIS gene transfer. Four groups of mice were established receiving 55.5 MBq ^{131}I or ^{188}Re 48 hours after the final of three RANTES-NIS-MSC or WT-MSC applications in 2-day-intervals. This cycle was repeated once 24 hours after the last radionuclide application. Twenty-four hours after these two treatment cycles, one additional MSC injection was administered followed by a third ^{131}I or ^{188}Re (55.5 MBq) injection 48 hours later. ^{131}I and ^{188}Re therapy after RANTES-NIS-MSC application resulted in a significant delay in tumor growth as compared with the control groups, that were injected with WT-MSCs followed by ^{131}I or ^{188}Re or with RANTES-NIS-MSCs followed by saline or with saline only ($p<0.05$) (a). The significantly reduced tumor growth was associated with markedly improved survival (Kaplan-Meier-Plot, $p<0.05$) (b).

At the end of the observation period, mice were sacrificed, tumors dissected followed by H&E staining (Fig. 6f, g) and immunofluorescence staining using a Ki67-specific antibody (green, labelling proliferating cells) and a CD31-specific antibody (red, labelling blood vessels). Striking differences were observed between mice treated with WT-MSC (Fig. 6a, b) or mice treated with saline (Fig. 6c) as compared to mice treated with RANTES-NIS-MSC followed by application of ^{188}Re or ^{131}I (Fig. 6d, e). Tumors of mice injected with RANTES-NIS-MSC followed by NaCl showed a Ki67-index of approx. 62 ± 8% and a mean vessel density of 4.25 ± 0.7% (Fig. 6h, i), whereas tumors treated with RANTES-NIS-MSC and ^{188}Re or ^{131}I showed significantly reduced levels of intratumoral proliferation index (20.3 ± 5%) and blood vessel density (1 ± 0.2%) (Fig. 6h, i).

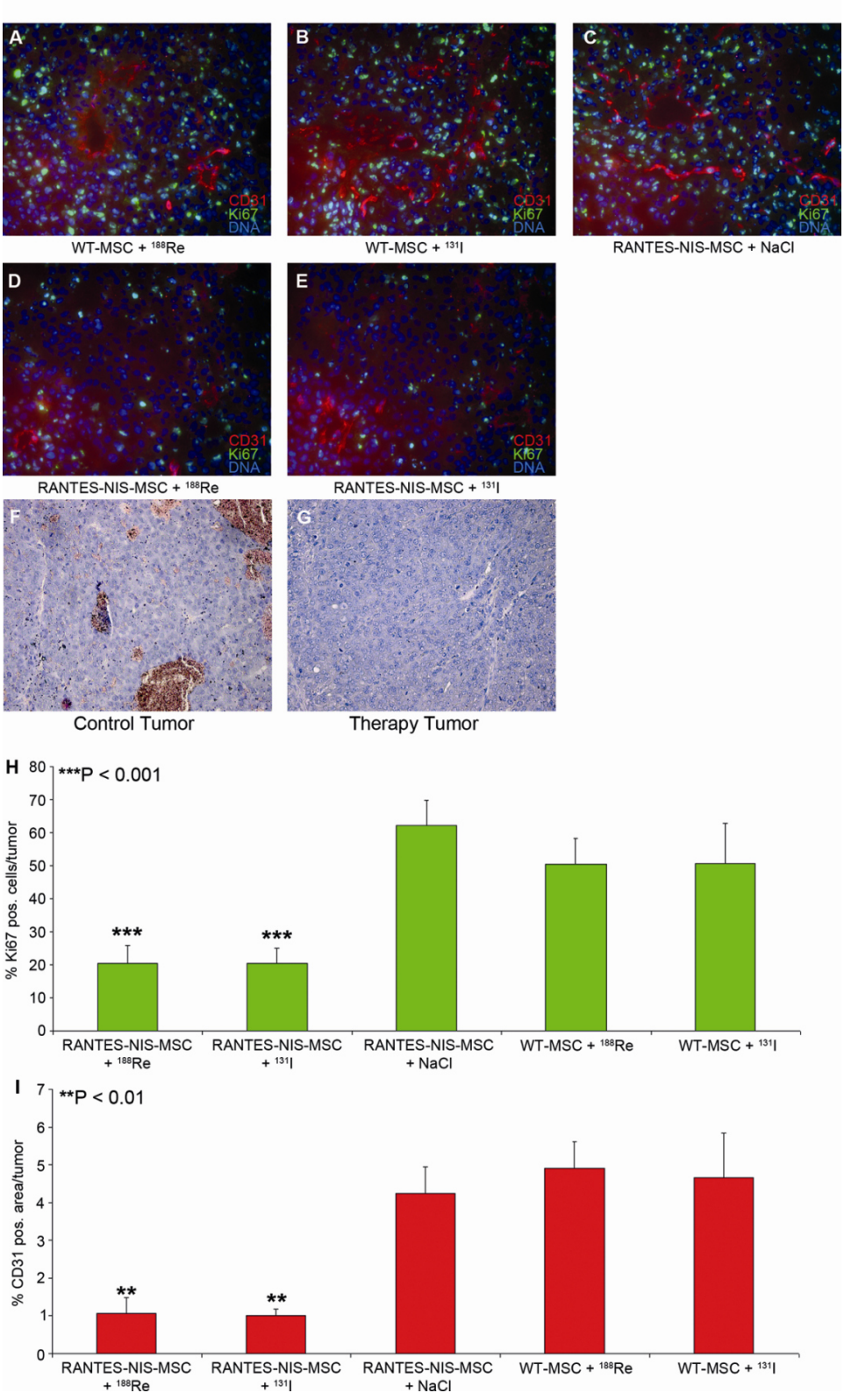

Figure 6 Immunofluorescence analyses of radionuclide therapy studies. Immunofluorescence analysis of tumors using a Ki67-specific antibody (green, labeling proliferating cells) and an antibody against CD31 (red, labeling blood vessels). As compared to control tumors (a – c), RANTES-NIS-MSC and ^{188}Re or ^{131}I treated tumors showed visible differences in tumor cell proliferation and blood vessel density (d, e). Quantification of blood vessel density and tumor cell proliferation showed significantly reduced tumor cell proliferation (20.3 ± 5%)(f) and blood vessel density (1 ± 0.2%)(g) after systemic RANTES-NIS-MSC application in ^{188}Re or ^{131}I treated tumors as compared to control tumors (Ki67: 62 ± 8%, p<0.001; CD31: 4.25 ± 0.7%, p<0.01)(f, g). Slides were counterstained with Hoechst nuclear stain. H&E stainings of control and treated tumors (f, g). Magnification x200.

3.5 Discussion

Several groups including our own have demonstrated that mesenchymal stem cells (MSCs) are actively recruited into growing tumor stroma where they play a major role in forming the tumor's fibrovascular network (Karnoub *et al.* 2007; Knoop *et al.* 2011; Niess *et al.* 2011; Zischek *et al.* 2009). MSC recruitment to tumor stroma is thought to be driven by high local concentrations of inflammatory chemokines and growth factors, such as MCP-1/CCL2, IL-8/CXCL8, RANTES/CCL5, SDF-1α/CXCL12 among others (Karnoub *et al.* 2007; Spaeth *et al.* 2008). Within the tumor stroma, MSCs can differentiate into carcinoma-associated fibroblasts or pericyte-like cells where they contribute to tumor growth through secretion of inflammatory and pro-angiogenic growth factors like VEGF, PDGF, SDF-1α/CXCL12, EGF, IGF, IL-6 and RANTES/CCL5 (Spaeth *et al.* 2009). This tropism of MSCs for tumor environments makes them uniquely suited as tumor stroma-selective gene delivery vehicles. In models of pancreatic, breast and liver cancer we have applied MSCs transduced with herpes simplex virus type 1 thymidine kinase (HSV-Tk) and demonstrated active tumor stroma-selective recruitment of MSCs that significantly reduced tumor growth and metastasizing potential after treatment with ganciclovir (Niess *et al.* 2011; Zischek *et al.* 2009).

MSCs have been used to deliver a diverse array of agents, including interferon-β, cytosine deaminase, tumor-necrosis factor-related apoptosis-inducing ligand, the immunostimulatory chemokine CX3CL1 and oncolytic viruses. These approaches have generally yielded positive antitumor effects (Braunersreuther *et al.* 2012; Spaeth *et al.* 2008). While effective, we sought to evaluate a potentially more flexible and potent therapy gene approach using the sodium iodide symporter (NIS). In a previous study using a liver cancer mouse model MSCs were transfected with NIS under the control of the broadly unspecific CMV promoter. The engineered cells were actively recruited to the tumor and induced a significant antitumor effect after application of ^{131}I (Knoop *et al.* 2011). A similar approach was subsequently confirmed in a breast cancer model by Dwyer *et al.* (Dwyer *et al.* 2011).

With its flexibility with regards to diagnostics, imaging and potent therapeutic actions, the NIS gene represents an important new dimension in MSC-mediated tumor therapy. Because of the potential side effects of MSC recruitment to non-tumor tissues, we examined the potential linkage of restricted tissue expression delivered through the use of the RANTES/CCL5 promoter to NIS-mediated MSC therapy in a model of HCC.

Upregulation of RANTES/CCL5 by MSCs in tumor stroma is associated with their differentiation into cancer-associated fibroblasts. In a murine model of breast cancer, MSCs were shown to increase the number of lung metastases. These effects were mediated in part by the RANTES/CCL5 produced by the MSCs in the presence of breast cancer cells that

acted in a paracrine fashion on cancer cells to enhance their motility, invasion and metastasis (Karnoub *et al.* 2007). Pinilla *et al.* demonstrated that MSCs derived from human adipose tissue (hASCs) produce RANTES/CCL5 in co-culture with breast cancer cells or in breast cancer cell conditioned medium, thereby increasing invasion of cancer cells, and conclude that RANTES/CCL5 plays a crucial role for tumor invasion in the interplay of tissue resident stem cells from fat tissue and breast cancer cells (Pinilla *et al.* 2009).

In our study, human MSCs were engineered to express NIS under control of the RANTES/CCL5 promoter to more specifically target NIS expression to the tumor stroma, and reduce potential side effects linked to MSC recruitment to non-tumor tissues. Initial demonstration of tumor stroma-selective RANTES/CCL5 promoter driven expression of reporter or therapy genes in engineered MSCs was provided by our own work (Zischek *et al.*, 2009), where murine MSCs stably transfected with either reporter genes (red fluorescent protein (RFP), enhanced green fluorescent protein (eGFP)) or a therapy gene (HSV-Tk) driven by the RANTES/CCL5 promoter were used to evaluate the dynamics of expression in mice carrying orthotopic, syngeneic pancreatic tumors (Zischek *et al.* 2009). Application of ganciclovir in these animals resulted in a significant reduction in primary tumor growth, as well as reduced incidence of metastases (Zischek *et al.* 2009). The CCL5-based-transgenic approach was later directly compared to a Tie2-tumor angiogenesis targeting approach in an orthotopic HCC xenograft model (Niess *et al.* 2011). While both methods showed positive results, the results suggested a better outcome when the RANTES/CCL5 promoter was used to drive therapeutic transgenes in engineered MSC (Niess *et al.* 2011; Zischek *et al.* 2009).

In contrast to our experiments, most of the previously published studies analyzed MSC biodistribution and tumor-specific recruitment by *ex vivo* analysis of reporter gene expression. However, using NIS as a reporter gene allows efficient non-invasive imaging of transgene expression by ^{99m}Tc-scintigraphy, ^{123}I-scintigraphy or SPECT, and ^{124}I-PET imaging, as demonstrated in our study, where tumor homing and engraftment of MSCs was non-invasively demonstrated by routine ^{123}I- or ^{188}Re-scintigraphy. This would allow an important new dimension in future patient studies, as exact planning of clinical gene therapy trials requires a thorough understanding of MSC biodistribution as well as level, duration and distribution of transgene expression. Feasibility and efficacy of the NIS gene therapy approach using NIS as a theranostic gene has been shown in several former studies by different groups including our own (Dwyer *et al.* 2005a; Dwyer *et al.* 2005b; Herve *et al.* 2008; Kakinuma *et al.* 2003; Klutz *et al.* 2009; Li *et al.* ; Peerlinck *et al.* 2009; Scholz *et al.* 2005; Spitzweg *et al.* 2007; Spitzweg *et al.* 2001a; Spitzweg *et al.* 2000; Spitzweg *et al.* 1999; Willhauck *et al.* 2007b; Willhauck *et al.* 2008a; Willhauck *et al.* 2008b; Willhauck *et al.* 2008c).

Following systemic application of RANTES-NIS-MSCs, 67% of implanted HCC tumors showed a tumor-specific ^{123}I and ^{188}Re accumulation as shown by gamma camera imaging with a radionuclide accumulation of approx. 6 – 7% ID/g and a biological half-life of 3.7 h, which is comparable to the data we had obtained in our previous study using the CMV promoter to drive NIS expression in MSCs (7 – 9% ID/g, biological half-life 4 h) (Knoop *et al.* 2011). Perchlorate injection prior to radionuclide application and the use of control MSCs confirmed NIS-specific radionuclide accumulation. The *in vivo* imaging data were confirmed by *ex vivo* biodistribution and immunofluorescence analysis, which demonstrated tumor stroma-specific accumulation of MSCs in addition to RANTES/CCL5 promoter activation as shown by immunohistochemical staining. In contrast, non-target organs like liver or kidney showed no NIS, SV40 large T-Ag or RANTES/CCL5 expression. Immunofluorescence analysis did reveal an accumulation of MSCs in the spleen, however, these cells did not show NIS-specific immunoreactivity. The presence of MSCs in the spleen may result either from direct recruitment of the cells (via CCR7) (Von Luttichau *et al.* 2005), or from filtration of the exogenously applied MSCs from the peripheral circulation. Importantly, the lack of RANTES/CCL5 promoter driven transgene expression demonstrates enhanced selectivity of the approach.

After three cycles of repetitive RANTES-NIS-MSC injection followed by the application of ^{131}I or ^{188}Re, an effective control of tumor growth was seen. This was associated with a dramatically improved survival of tumor bearing animals to the end of the nine week experiment. By contrast, control animals showed a maximum survival of four weeks. These results show a significant improvement over those previously reported by us using the CMV promoter to drive NIS expression in the same model system where the mice lived seven weeks after NIS-mediated radioiodine therapy (Knoop *et al.* 2011).

In the current study we also examined the potential use of ^{188}Re as an alternative therapeutic radionuclide to ^{131}I. ^{188}Re is also transported by NIS, but in contrast to ^{131}I, offers the possibility of higher energy deposition in the tumor in a shorter period of time due to its shorter physical half life and higher energy. Another advantage is that ^{188}Re is less harmful to the thyroid, which is primarily caused by the lack of ^{188}Re organification and therefore significantly shorter effective half-life of ^{188}Re in the thyroid gland, thereby not only reducing radiation damage to the thyroid gland but also increasing tumoral ^{188}Re uptake by the elimination or the thyroid “sink” effect (Dadachova *et al.* 2002). In consideration of the scattered MSC biodistribution in the tumor stroma an enhanced therapeutic effect of ^{188}Re based on an increase in crossfire effect, due to the longer path length, was expected. In a breast cancer mouse model Dadachova and colleagues showed a radiation dose 4.5 times higher for ^{188}Re than for ^{131}I resulting in an improved therapeutic efficacy in mice (Dadachova *et al.* 2005). Similarly, in one of our previous studies we have convincingly demonstrated the

superior therapeutic effect of ^{188}Re as compared to ^{131}I in a prostate cancer xenograft mouse model based on a 4.7-fold higher tumor absorbed dose after application of ^{188}Re as compared to ^{131}I (Willhauck *et al.* 2007b). In the current study, however, therapeutic efficacy of ^{188}Re compared to ^{131}I was similar in direct comparison although the tumor absorbed dose for ^{188}Re was calculated to be 3 times higher than for ^{131}I (128.7 mGy/MBq vs. 44.3 mGy/MBq). Based on the survival curve obtained for both radionuclides, it is possible that a maximal therapeutic effect was already achieved with ^{131}I treatment. A more detailed titration of MSC and radionuclide application in future studies may allow a more precise contrasting of the therapeutic consequences of ^{188}Re vs. ^{131}I.

In addition, since dosimetric calculations are optimized for a homogenous tumoral radionuclide uptake and standard dosimetry models not taking into account microdosimetry aspects, calculation of tumor absorbed doses after MSC-mediated NIS gene transfer might be inaccurate due to inhomogeneous NIS expression and therefore inhomogenous radionuclide accumulation in the tumor stroma.

The mechanism underlying RANTES/CCL5 induction by MSC in tumor milieus is not well understood. Osteopontin (OPN), a secreted phosphoprotein that signals through $\alpha_v\beta_3$ integrin and CD44 (Denhardt *et al.* 1995; Mcallister *et al.* 2008; Mi *et al.* 2011) has been shown to induce expression of RANTES/CCL5 in MSCs (Mi *et al.* 2011). EGFR and IGF-1 signalling have also been linked to RANTES/CCL5 upregulation by MSCs (Karar and Maity 2009; Mascia *et al.* 2003). A better understanding of this biology may allow the re-engineering of the RANTES/CCL5 promoter to optimize tumor specificity and reduce potential expression in other tissues (Edelmann *et al.* 2011; Grone *et al.* 1999).

Taken together, our data demonstrate high tumor selectivity of MSC recruitment and improved NIS expression driven by the RANTES/CCL5 promoter after systemic MSC application in a HCC xenograft model. The resulting biologically targeted, tumor-selective radionuclide accumulation was high enough for a therapeutic effect of ^{131}I and ^{188}Re opening the exciting prospect of NIS-mediated radionuclide therapy of metastatic cancer using engineered MSCs as gene delivery vehicles.

3.6 Acknowledgements

We are grateful to J.C. Morris, Division of Endocrinology, Mayo Clinic and Medical School, Rochester, MN, USA for providing the NIS-specific antibody, as well as to S.M. Jhiang, Ohio State University, Columbus, OH, USA for supplying the full-length human NIS cDNA. We also thank W. Münzing, Julia Schlichtiger and Heidrun Zankl, Department of Nuclear Medicine, Ludwig-Maximilians-University, Munich, Germany, for their assistance with the imaging and therapy studies.

This study was supported by grant SFB 824 (Sonderforschungsbereich 824) from the Deutsche Forschungsgemeinschaft, Bonn, Germany, to C. Spitzweg, and by a grant from the Wilhelm-Sander-Stiftung (2008.037.1) to C. Spitzweg and P. J. Nelson.

4 Chapter 3

Effective ^{131}I therapy after mesenchymal stem cell-mediated stromal targeting of the sodium iodide symporter in an orthotopic hepatocellular cancer model

Kerstin Knoop[1], Nathalie Schwenk[1], Kathrin Schmohl[1], Andrea Müller[1], Christian Zach[2], Guido Böning[2], Peter Bartenstein[2], Janette Carlsen[2], Burkhard Göke[1], Ernst Wagner[3], Peter J. Nelson[4], Christine Spitzweg[1]

Department of Internal Medicine II[1], Department of Nuclear Medicine[2], Department of Pharmacy, Center of Drug Research, Pharmaceutical Biotechnology[3], Clinical Biochemistry Group, Department of Medical Policlinic IV[4] Ludwig-Maximilians-University, Munich, Germany

4.1 Abstract

The tumor-homing property of mesenchymal stem cells (MSC) has been used for the delivery of therapeutic genes into tumor environments. The sodium iodide symporter (NIS) is a theranostic gene that allows non-invasive imaging of MSC biodistribution by ^{123}I-scintigraphy or ^{124}I-PET-imaging as well as potent therapeutic application of ^{131}I or ^{188}Re. Expression of the chemokine RANTES/CCL5 is induced by MSCs in the course of tumor stroma recruitment and their differentiation into cancer-associated fibroblasts. We recently demonstrated effective control of an experimental subcutaneous xenograft model of HCC using MSC engineered to express NIS under control of the RANTES promoter (RANTES-NIS-MSC). Here we contrasted these findings with a more clinically relevant experimental orthotopic hepatocellular cancer xenotransplant model established by intrahepatic injection of Huh7 cells in nude mice.

After systemic RANTES-NIS-MSC injection, ^{123}I-scintigraphy and ^{124}I-PET imaging in concert with *ex vivo* biodistribution studies demonstrated MSC recruitment and RANTES/CCL5-promoter activation in the stroma of hepatic tumors. In contrast, limited MSC-mediated NIS expression was detected in healthy liver tissue or non-target organs. The therapeutic effects of NIS-mediated radioiodine therapy (55.5 MBq ^{131}I) showed improved survival of tumor bearing mice. Immunfluorescence studies also demonstrated markedly reduced proliferation and decreased blood vessel density of RANTES-NIS-MSC/^{131}I-treated tumors as compared to controls. We show that the relevant host tumor interactions in an orthotopic HCC tumor model provide a better environment for the facilitated recruitment and activation of RANTES-NIS-engineered MSC. These data convincingly demonstrate the enormous potential of MSC-mediated NIS gene radionuclide therapy in control of hepatocellular carcinoma.

4.2 Introduction

Hepatocellular carcinoma (HCC) is the most common form of liver cancer, and the third most deadly cancer worldwide. The incidence of HCC is increasing due to the expanding prevalence of hepatitis C virus infection. HCC is generally diagnosed at more advanced stages, which limits potential therapeutic options (Parkin *et al.* 2005). If surgical resection of the tumor is possible in limited disease, it offers the best prognosis for long-term patient survival. However, because of extensive disease, or poor liver function, only a small fraction of HCC patients (10-15%) are suitable for surgical resection. This has driven the search for novel therapeutic approaches for advanced HCC.

Solid tumors such as HCC are comprised of tumor cells within a complex stromal matrix that include cells linked to angiogenesis, innate and adaptive immune cells, and cancer-associated fibroblastic (CAF) cells (Yang *et al.* 2011). Mesenchymal stem cells (MSC) can act as progenitors for many of these cell types. In the course of normal tissue repair, MSCs become mobilized from various tissue niches and are recruited to sites of tissue damage to help effect repair. Tumors are seen by the body as something akin to a chronic wound (Aquino *et al.* 2010; Dvorak 1986), which explains the pronounced tropism that adaptively transferred MSCs have for tumor environments, and also provides the biologic basis for use of engineered version of MSCs as vehicles for tumor therapy (Dwyer *et al.* 2011; Knoop *et al.* 2011; Knoop *et al.* 2013; Niess *et al.* 2011; Zischek *et al.* 2009).

However, MSCs can also be recruited to normal tissues as part of tissue homeostasis. Here the expression of “therapy” genes could lead to undesired side effects. We have shown that tumor-specific therapy gene expression can be enhanced through the use of specific gene promoters for driving transgene expression. The promoters derive from genes that are highly induced by MSC in tumor tissues, but show less activity in “normal” tissues. Thus the transgenes become activated when the MSC come in contact with the tumor environment, but are not highly expressed in MSC that may traffic to “non-target” tissues. One such promoter was taken from the chemokine CCL5/RANTES gene (Knoop *et al.* 2013; Niess *et al.* 2011; Zischek *et al.* 2009). Expression of RANTES is induced by MSCs in the course of their recruitment to tumor stroma and subsequent differentiation into CAFs. In addition, RANTES/CCL5 expression is associated with increased tumor neovascularization, as well as enhanced cancer growth and metastases by autocrine and paracrine activation of tumor cells (Karnoub *et al.* 2007). The RANTES promoter was therefore used to help focus MSC-transgene induction within the tumor milieu. Early studies of this approach made use of the suicide gene Herpes simplex virus thymidine kinase (HSV-TK) as a therapy gene in concert with the prodrug ganciclovir. In these studies, murine MSCs were stably transfected with either reporter genes (red fluorescence protein (RFP), enhanced green fluorescence protein

(eGFP)) or a therapy gene (HSV-TK) driven by the RANTES/CCL5 promoter to evaluate the dynamic expression of the transgene in mice carrying orthotopic, syngenic pancreatic tumors. Application of ganciclovir in these animals resulted in a significant reduction of primary tumor growth as well as reduced incidence of metastases (Zischek *et al.* 2009). The CCL5-based transgenic approach was later directly compared to a Tie2-tumor angiogenesis-targeting approach in an orthotopic HCC xenograft model (Niess *et al.* 2011). While the results of these preclinical studies were encouraging, the therapeutic effects delivered by HSV-TK-based suicide gene therapy were limited to bystander killing, and do not allow flexibility of live whole body monitoring. To help address this, these studies were expanded through use of the sodium iodide symporter (NIS) as a theranostic gene. The NIS protein is responsible for the active uptake of iodide by the thyroid, and as such, forms the basis for the diagnostic and therapeutic use of radioiodine in thyroid carcinoma. Use of the NIS gene allows both non-invasive *in vivo* imaging of MSC biodistribution and functional transgene expression by ^{123}I-scintigraphy or ^{124}I-PET-imaging and the delivery of a very potent therapeutic effect by treatment with ^{131}I or ^{188}Re (Hingorani *et al.* 2010; Spitzweg and Morris 2002; Willhauck *et al.* 2007b).

We recently demonstrated the effective control of an experimental subcutaneous xenograft model of HCC using MSC engineered to express NIS under control of the RANTES promoter. Systemic injection of these engineered MSCs led to a significant radioiodine accumulation in subcutaneous HCC xenografts resulting in a delay of tumor growth and improved survival by therapeutic ^{131}I application (Knoop *et al.* 2013). These preliminary results were very encouraging but did not account for the very important additional component of tumor-stromal interaction with the surrounding normal liver tissue environment. We describe here an expanded study using an orthotopic HCC tumor model that better replicates the biology of the tumor in its natural milieu with associated complicating factors.

4.3 Material and methods

Cell culture

The generation of human MSCs has been described previously (Knoop *et al.* 2011). The human hepatocellular cell line Huh7 (JCRB 0403) was cultured in RPMI (Invitrogen/Life technologies, Darmstadt, Germany) supplemented with 10% fetal bovine serum (v/v; PAA) and 1% penicillin/streptomycin. The cell lines were maintained at 37°C and 5% CO_2 in an incubator with 95% humidity.

Plasmid construct and stable transfection of mesenchymal stem cells

The plasmids used, their construction, and the establishment of stably engineered MSC have been described previously (Knoop *et al.* 2011; Knoop *et al.* 2013).

Establishment of hepatic HCC xenografts

The experimental protocol was approved by the regional governmental commission for animals (Regierung von Oberbayern). To establish orthotopic tumor models, nude mice were anesthetized with 2.5% Isofluran in oxygen and placed on a heated mat in the left lateral position. The skin was washed with 70% ethanol and dried using sterile gauze. A 0.5 cm cut was made at the right subcostal region extending through the skin and abdominal wall, and exposing the lower pole of the liver lobe. A 27-gauge needle was then inserted at the upper liver lobe and 50 µl of tumor cell suspension ($1x10^6$ cells) in PBS was injected over 15sec. The needle was removed and the injection site was gently pressed with a Q-tip to prevent bleeding and the reflux of tumor cells into the abdomen or abdominal wall. The abdominal wall and the skin were then sutured separately using a Monosyn® 5/0 fiber.

The mice were pre- and post-treated with Carprofen (5 mg/kg) to minimize wound pain. The animals were maintained under specific pathogen-free conditions with access to mouse chow and water ad libitum.

MSC application and radionuclide biodistribution studies in vivo

The eMSC experiments were initiated two weeks after intrahepatic tumor cell injection. Pretreatment with the thyroid hormone L-T4 (levothyroxine, (10 µg L-T4/100 g body weight) was used to reduce thyroidal NIS expression (Di Cosmo *et al.* 2009). WT-MSCs or RANTES-NIS-MSCs were applied via the tail vein at a concentration of 5×10^5 cells/500µl PBS. Two groups of mice were established and treated as follows: (a) three i.v. applications of RANTES-NIS-MSC in four day intervals (n=20); (b) three i.v. applications of WT-MSC in four day intervals (n=7). As an additional control, in a subset of mice injected with RANTES-NIS-MSC (n=8) the specific NIS-inhibitor sodium-perchlorate ($NaClO_4$, 2 mg per mouse) was

injected i.p. 30 min prior to radionuclide administration. 48 h after the last MSC application, 18.5 MBq ^{123}I was injected i.p. and radionuclide biodistribution was assessed using a gamma camera equipped with UXHR collimator (Ecam, Siemens, Germany) as previously described (Willhauck *et al.* 2007b; Willhauck *et al.* 2008a). Small-animal PET imaging was performed in a subgroup of mice treated with RANTES-NIS-MSC (n=7) receiving a dose of 12 MBq ^{124}I. PET-Imaging procedure was described previously (Knoop *et al.* 2011).

Analysis of radionuclide biodistribution ex vivo

For *ex vivo* biodistribution studies, mice were injected with RANTES-NIS-MSCs (n=15) or WT-MSCs (n=5) as described above followed by i.p. injection of 18.5 MBq ^{123}I. A subset of RANTES-NIS-MSC injected mice (n=5) were treated with $NaClO_4$ prior to radionuclide administration as an additional control. Four hours after radioiodine injection, mice were sacrificed and organs of interest were dissected, weighed and ^{123}I accumulation was measured in a gamma counter. Results were reported as percentage of injected dose per organ (% ID/organ).

Analysis of NIS mRNA expression using quantitative real-time PCR

Total RNA was isolated from the liver or other tissues using the RNeasy Mini Kit (Qiagen, Hilden, Germany) according to the manufacturer's recommendations and quantitative real-time PCR (qPCR) was performed as described previously (Klutz *et al.* 2009).

Radionuclide therapy studies in vivo

Therapeutic applications of MSCs followed by ^{131}I or saline were performed as described previously by Knoop *et al*. (Knoop *et al.* 2013). The following groups were established: RANTES-NIS-MSC + ^{131}I (n=20), RANTES-NIS-MSC + NaCl (n=20) and WT-MSC + ^{131}I (n=20).

By protocol, mice were sacrificed when healthy liver tissue reached less than 20%, or in case of weight loss representing more than 10% of starting weight, or when impairment of breathing, drinking or eating behavior was observed.

Immunohistochemical analysis

Immunohistochemical and immunofluorescence staining procedures for the expression of NIS and SV40 large T Ag, as well as indirect immunofluorescence analysis, and quantification of cellular proliferation (Ki67) and blood vessel density (CD31), were performed as described previously (Knoop *et al.* 2013).

Statistical methods

Statistical significance of *in vitro* experiments was tested using Student´s t test. Statistical significance of the *in vivo* experiments has been calculated using the Man-Whitney U test.

4.4 Results

Radioiodine biodistribution in a hepatic HCC xenograft model after MSC-mediated NIS gene transfer

To assess the potential effect of eMSC-NIS-based therapy in a clinically more relevant model, an orthotopic tumor model of hepatic HCC xenograft was used. In these experiments the human hepatocellular carcinoma cell line Huh7 was injected into the right liver lobe of immune-compromised mice, leading to the establishment of solid intrahepatic xenografts after five weeks. MSC treatment was initiated three weeks after intrahepatic tumor cell injection. RANTES-NIS-MSCs or WT-MSCs were injected via the tail vein 3-times in 4-day-intervalls. 48 hours after the last MSC injection, 18.5 MBq ^{123}I were applied to determine the iodide accumulation in the hepatic xenografts by gamma camera imaging. Three hours after ^{123}I injection, enhanced iodide uptake activity was detected in the right liver lobe, which resulted in a maximum uptake of 16.5 ± 1 % ID/g with a biological half-life of 3.4 hours, and a tumor absorbed dose of 96 mGy/MBq (Fig. 1a, d). In contrast, control mice with intrahepatic Huh7 xenografts treated with WT-MSCs showed no iodide uptake after radioiodine application (Fig. 1c). Treatment of a subgroup of the RANTES-NIS-MSC-injected mice with the competitive NIS inhibitor perchlorate 30min prior to radioiodine injection showed a complete blockade of radionuclide accumulation in intrahepatic Huh7 xenografts as well as in physiologically NIS-expressing organs including the thyroid gland and stomach. The high iodide accumulation in the bladder results from renal excretion of the radionuclides (Fig. 1b). To improve the resolution of radioiodine uptake in the liver area, and to more clearly differentiate between hepatic and gastric iodide accumulation, additional PET imaging studies were performed using ^{124}I. Three-dimensional data were subsequently generated using iterative reconstructions of list mode data (0-40min), which provided better anatomical definition. 48 hours after the last RANTES-NIS-MSC administration, 12 MBq ^{124}I were applied and selective iodide accumulation was detected in intrahepatic Huh7 xenografts three hours after ^{124}I application (Fig. 1 e – g). In 70% of RANTES-NIS-MSC-treated mice a maximum uptake of 13.6 ± 1.9 % ID/g was measured in intrahepatic Huh7 xenografts.

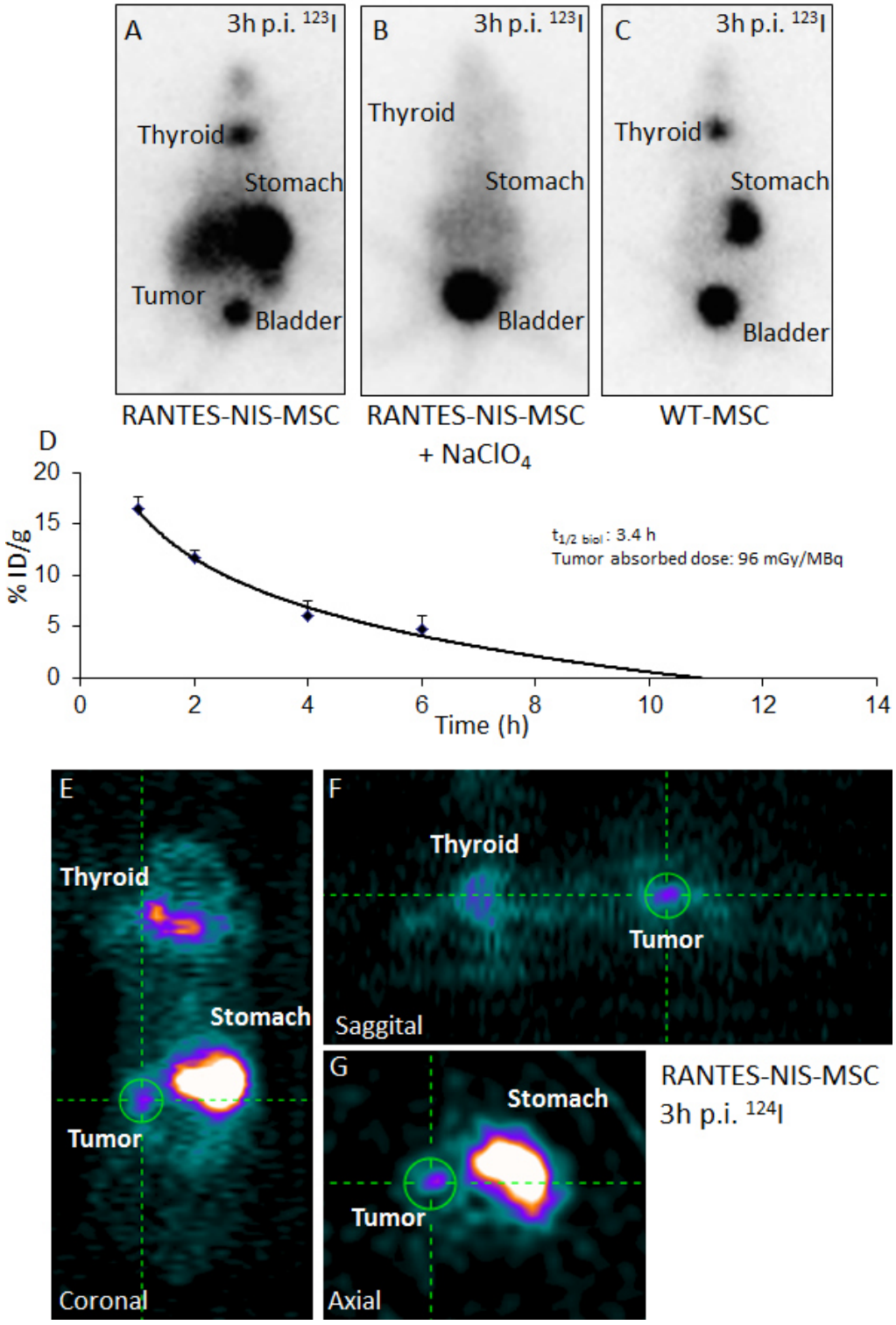

Figure 1 Radioiodine accumulation in an hepatic Huh7 xenograft mouse model following systemic RANTES-NIS-MSC administration. Systemic injection with RANTES-NIS-MSCs resulted in enhanced iodide accumulation in livers of mice harbouring intrahepatic HCC tumors three hours after radionuclide administration as shown by ^{123}I-gamma-camer imaging (a) and small animal ^{124}I-PET imaging (e – f), which was completely blocked upon treatment with the NIS-specific inhibitor ($NaClO_4$) (b). Mice systemically injected with WT-MSC showed no tumoral iodide uptake (c). Iodide uptake activity resulted in a maximum uptake of 16.5 ± 1 % ID/g with a biological half-life of 3.4 hours and a tumor absorbed dose of 96 mGy/MBq (d).

Ex vivo radioiodine biodistribution studies

In addition to the imaging studies, quantitative *ex vivo* biodistribution studies were performed four hours after injection of 18.5 MBq ^{123}I. In hepatic Huh7 xenograft-bearing mice, an iodide uptake of 6.9 ± 1.8 % ID/g tumor tissue was found, supporting the results of the imaging studies. In addition, no iodide uptake activity was measured in non-target organs, or tumors from mice injected with WT-MSCs. Mice injected with RANTES-NIS-MSCs and treated with the competitive NIS inhibitor perchlorate showed no iodide uptake activity in tumors (Fig. 2) as well as thyroid gland and stomach (data not shown).

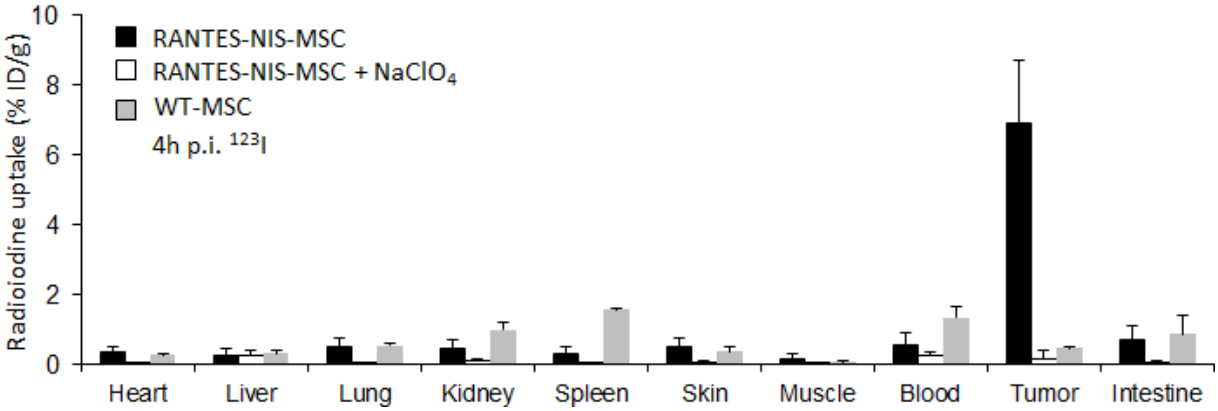

Figure 2 *Ex vivo* radioiodine biodistribution studies. *Ex vivo* biodistribution studies four hours after 18.5 MBq ^{123}I injection revealed an iodide uptake of 6.9 ± 1.8 % ID/g in intrahepatic HCC tumors of mice treated with RANTES-NIS-MSC, whereas no significant radioiodine uptake was measured in non-target organs, after pretreatment with perchlorate or after systemic injection of WT-MSC. Results are reported as percent of injected dose per g ± SD.

Analysis of NIS protein expression by indirect immunofluorescence

The distribution of MSCs in tumors was determined in more detail by immunofluorescence staining using NIS- and SV40 large T Ag- specific antibodies. SV40 large T Ag was used to immortalize the MSCs and could thus can be used as a target to assess biodistribution of engineered MSCs, while human NIS-specific antibodies allowed the determination of RANTES promote-induced NIS transgene expression. Paraffin-embedded tissues from liver were processed for immunofluorescence staining using both sets of antibodies. In intrahepatic HCC tumors of mice treated with RANTES-NIS-MSCs, NIS-specific immunoreactivity was detected and was confined to the tumor (Fig. 3a), while no NIS-specific staining was seen in the surrounding normal liver tissue. This biodistribution pattern was confirmed by SV40 large T Ag-specific staining demonstrating the presence of eMSCs in intrahepatic tumor tissue (Fig. 3b) and not into normal liver tissue. Systemic injection of WT-MSCs showed no NIS-specific immunoreactivity in intrahepatic HCC tumors (Fig. 3c) or in normal liver tissue; however, SV40 large T Ag staining still demonstrated active MSC

recruitment into intrahepatic tumors, thus supporting tumor-selective eMSC recruitment (Fig. 3d).

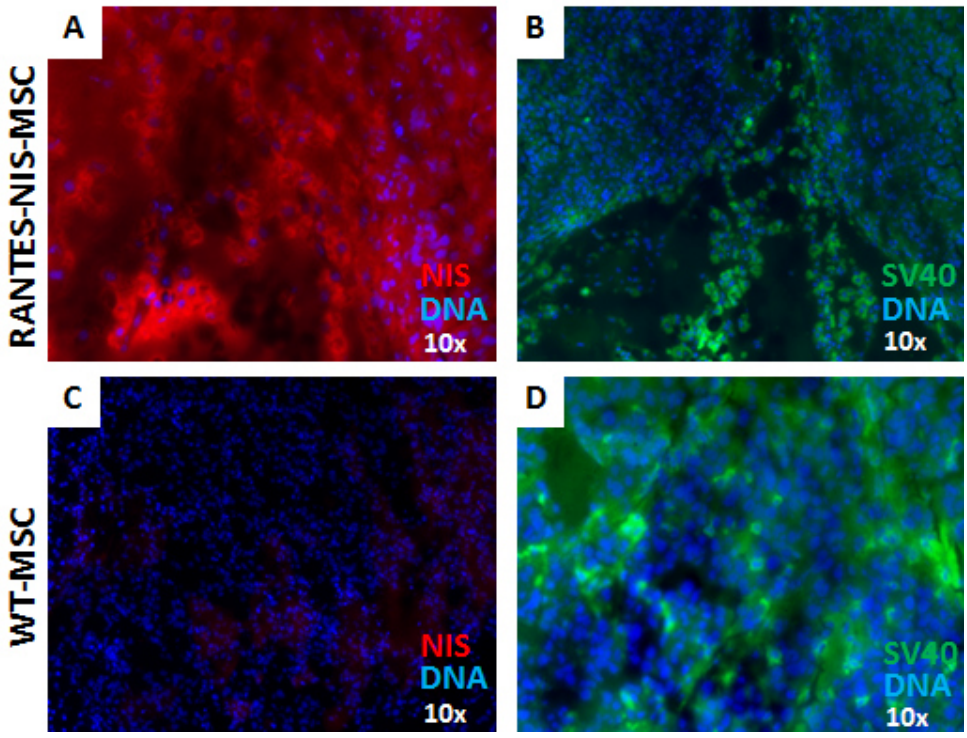

Figure 3 Analysis of NIS protein expression after systemic RANTES-NIS-MSC injection by indirect immunofluorescence. Hepatic Huh7 xenografts in RANTES-NIS-MSC-treated mice showed NIS-specific immune-reactivity (a), which was similar to the localization of the MSC-specific SV40 large T Ag staining (b). Systemic injection of WT-MSC resulted in no NIS-specific immuno reactivity (c), despite a strong SV40 large T Ag staining (d), confirming specific MSC recruitment in to the tumor.

Therapeutic application of ^{131}I resulted in improved survival of mice harboring hepatic Huh7 xenografts

The therapeutic effect of ^{131}I was assessed in mice carrying intrahepatic HCC tumors using the therapy regime optimized in previous studies (Knoop *et al.* 2013). The protocol is based on three cycles of systemic eMSC injecetions followed by ^{131}I (Fig. 4a). After systemic injection of RANTES-NIS-MSCs followed by ^{131}I injection a significantly improved survival of up to four weeks was observed as compared to control groups of mice injected with RANTES-NIS-MSC followed by saline application, or mice treated with WT-MSC followed by the application of ^{131}I (Fig. 4a).

One week after the last radioiodine injection, a subset of mice was sacrificed, livers were removed and characterized by immunofluorescence analysis for cellular proliferation (Ki67, green) and blood vessel density (CD31, red) markers. Striking differences were observed between therapy and control groups (Fig. 4 b – d). Mice treated with RANTES-NIS-MSCs followed by ^{131}I showed decreased proliferation (Ki67: 37.38 ± 5.85 %) (Fig. 4f) and blood

vessel density (CD31: 3.43 ± 0.61 %) (Fig. 4e), whereas control mice treated with RANTES-NIS-MSC followed by saline or mice treated with WT-MSC followed by ^{131}I application revealed high blood vessel density (CD31) (RANTES-NIS-MSC + NaCl: 6.23 ± 0.69 %; WT-MSC + ^{131}I: 7.15 ± 1.2 %) (Fig. 4e, f) and high levels of proliferation (Ki67) (RANTES-NIS-MSC + NaCl: 66.9 ± 10.65 %; WT-MSC + ^{131}I: 61.18 ± 10.22 %) (Fig. 4e, f). At the end of the observation period, the remaining animals were sacrificed and analyzed, still showing reduced proliferation and blood vessel density in the therapy group albeit to a lower extent (RANTES-NIS-MSC + ^{131}I: Ki67: 54.9 ± 12.1 %, CD31: 4.3 + 1.1 %), as compared to control groups (RANTES-NIS-MSC + NaCl: Ki67: 76.5 ± 11.2 %, CD31: 6.2 ±1.4 %; WT-MSC + ^{131}I: Ki67: 72.42 ± 10.8 %, CD31: 6.3 ± 1.3 %) (data not shown).

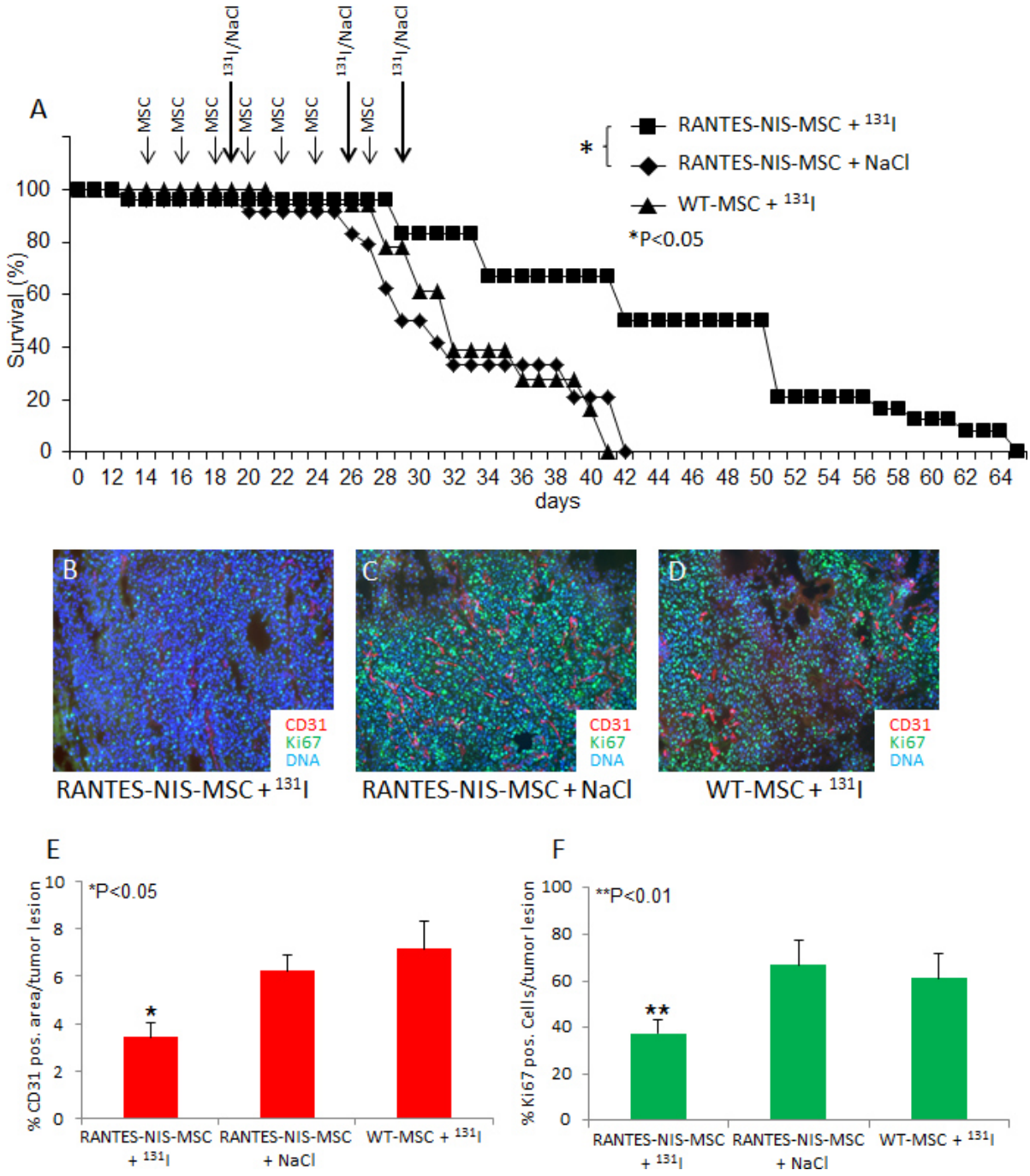

Figure 4 Therapeutic application of ^{131}I resulted in an improved survival of mice harbouring intrahepatic Huh7 xenografts. Two groups of mice were established receiving 55.5 MBq ^{131}I after the final of three RANTES-NIS-MSC or WT-MSC applications in two-day-intervals. This cycle was repeated once 24 hours after the last radioiodine application. 24 hours after these two treatment cycles, one additional MSC injection was administered followed by a third ^{131}I injection 48 hours later. A further control group received RANTES-NIS-MSCs and saline. Therapeutic application of ^{131}I after i.v. injection of RANTES-NIS-MSCs resulted in significantly improved survival as compared to the control groups (a). Immunofluorescence analyses of intrahepatic HCC tumors using a Ki67-specific antibody (green, labelling proliferating cells) and an antibody against CD31 (red, labelling blood vessels) showed striking differences in tumor cell proliferation and blood vessel density in hepatic HCC tumors of mice treated with RANTES-NIS-MSCs and ^{131}I (b), which was significantly reduced (Ki67: 37.38 ± 5.85 %; CD31: 3.43 ± 0.61 % (e, f)) as compared to the control groups of mice treated with RANTES-NIS-MSC and saline (c) (CD31: 6.23 ± 0.69 %; Ki67: 66.9 ± 10.65 % (e, f)) or WT-MSC and ^{131}I (d) (CD31: 7.15 ± 1.2 %; Ki67: 61.18 ± 10,22 % (e, f)). Slides were counterstained with Hoechst nuclear stain. Magnification x200.

4.5 Discussion

Gene therapy represents a promising and active field of cancer therapy. Although previous studies have yielded some exciting results in animals models, clinical trials have shown limited antitumor efficacy, at least in part due to insufficient gene delivery to tumor sites (Komarova *et al.* 2006). Introducing a therapeutic transgene into mesenchymal stem cells (MSC) represents an emerging cell-based delivery strategy (Studeny *et al.* 2002). The rationale for using bone marrow-derived MSCs as delivery vehicles to tumors is based on the concept that MSCs are actively recruited from the blood into tissues in response to injury (Aquino *et al.* 2010). As the microenvironment of a solid tumor is similar to that of an injured tissue, solid tumors provide a permissive environment for the efficient engraftment of exogenously applied MSCs (Kidd *et al.* 2009; Nakamizo *et al.* 2005).

We and others have previously shown the clinical potential of engineered MSC as therapy vehicles for the treatment of various tumor models. In models of pancreatic, breast and liver cancer, we have applied MSCs transduced with HSV-TK and demonstrated active tumor stroma-selective recruitment of MSCs that significantly reduced tumor growth and metastasizing potential after treatment with ganciclovir (Conrad *et al.* 2011; Niess *et al.* 2011; Zischek *et al.* 2009).

Hepatocellular carcinoma (HCC) is one of the most common types of malignant tumors worldwide. Because of their easy establishment, most interventional studies published to date have relied on subcutaneous HCC xenograft models. By contrast, orthotopic implantation of liver tumors allows the important inclusion of relevant host tumor-interactions leading to a clinically more relevant microenvironment and thus allows more insight into the potential effect of therapeutic approaches.

An important step in translational medicine is the fusion of diagnosis and therapy, which allows for the refinement of diagnostic and therapeutic procedures for disease evaluation. The use of such a “theranostic” approach has become increasingly important in pre-clinical and clinical research, in particular in gene therapy approaches with the development of a series of new viral and non-viral vectors and an increasing repertoire of therapy genes.

A series of studies by different research groups including our own have shown the feasibility and efficacy of the use of NIS as a theranostic gene (Dwyer *et al.* 2011; Grunwald *et al.* 2013c; Klutz *et al.* 2009; Knoop *et al.* 2013; Spitzweg *et al.* 2000). NIS serves as a reporter gene allowing efficient non-invasive imaging of vector biodistribution and transgene expression by ^{123}I-scintigraphy or SPECT and ^{124}I-PET imaging and therefore provides a novel method for repetitive *in vivo* monitoring of tumor homing and engraftment of MSCs (Dwyer *et al.* 2011; Knoop *et al.* 2011; Knoop *et al.* 2013), which represents an essential prerequisite for the exact planning of clinical gene therapy trails.

After proof-of-principle of the MSC-mediated NIS gene transfer approach in subcutaneous xenografts in our earlier studies (Knoop *et al.* 2011; Knoop *et al.* 2013), the next crucial step was to study the potential of this approach in a clinically more relevant tumor model. Subcutaneous xenografts are simple to perform; they show low intra-procedure mortality and allow easy visualization and monitoring of tumor growth. However, it does not allow for the inclusion of specific effects that derive from the host-tissue environment. A capsule is often formed around subcutaneous tumors and metastases rarely occur (Fidler 1990; Nakajima *et al.* 1990; Yang *et al.* 2011). The biochemical milieu and blood supply are also different in the skin than in the source organ. This is especially true in the case of liver tumors, where a portal vein system and drug-detoxifying enzymes exist. In this context, the response to chemotherapeutic agents has been shown to vary depending on whether the tumor is ectopic or orthotopic (Wilmanns *et al.* 1992; Yao *et al.* 2003). In one of our earlier studies, Niess *et al*. generated an intrahepatic HCC xenograft model in mice by intrahepatic injection of Huh7 HCC cells (Niess *et al.* 2011). After systemic injection of MSCs either transfected with a red fluorescence protein (RFP) gene or a HSV-TK gene under the control of the RANTES promoter, tumor-specific recruitment was monitored *ex vivo* by detection of RFP. Therapeutic potential was demonstrated by the use of RANTES/HSV-TK transfected MSCs and additional treatment with ganciclovir which resulted in an significantly reduced tumor growth (Niess *et al.* 2011).

In the present study we also used the orthotopic HCC xenograft model for evaluation of the MSC-mediated NIS gene delivery concept using the RANTES promoter to drive tumor stroma-selective NIS expression. After systemic injection of RANTES-NIS-MSCs, ^{123}I-gamma-camera and ^{124}I-PET imaging demonstrated tumor stroma-targeted MSC recruitment and transgene activation by significant iodide uptake activity in the intrahepatic HCC xengrafts. The tumor-specific iodide uptake activity was further confirmed by *ex vivo* biodistribution studies. Interestingly, the iodide uptake activity observed in the intrahepatic xenografts (max. uptake 16.5 % ID/g ^{123}I) was even higher than we had reported previously in subcutaneous tumors (max. uptake 6.5 % ID/g ^{123}I) (Knoop *et al.* 2013), which could be the result of the more representative tumor stroma milieu in the liver with enhanced stromal growth as compared to the subcutaneous milieu leading to a more active MSC recruitment and engraftment. This also resulted in doubling of the tumor-absorbed dose that was achieved in the intrahepatic HCC model (96 mGy/MBq) as compared to the subcutaneous tumor model (44.3 mGy/MBq) (Knoop *et al.* 2013). Three cycles of repetitive RANTES-NIS-MSC injection followed by the application of ^{131}I resulted in a dramatically improved survival of tumor-bearing mice up to 9 weeks as compared to 5 weeks in the control groups.

Taken together, in the current study we were able to translate our previous findings of MSC-mediated systemic NIS gene delivery in subcutaneous liver cancer xenografts into a clinically

more relevant mouse model of intrahepatic liver cancer xenografts. Non-invasive ^{123}I-scintigraphy and ^{124}I-PET imaging demonstrated remarkable tumor-selectivity of MSC recruitment and NIS expression driven by the tumor stroma-specific RANTES/CCL5 promoter after systemic MSC application. The resulting biologically targeted, tumor-selective radionuclide accumulation was high enough for a significant therapeutic effect of ^{131}I. These data convincingly demonstrate the enormous potential of MSC-mediated NIS gene radionuclide therapy of advanced and /or metastatic cancer.

4.6 Acknowledgements

We are grateful to J.C. Morris, Division of Endocrinology, Mayo Clinic and Medical School, Rochester, MN, USA for providing the NIS-specific antibody, as well as to S.M. Jhiang, Ohio State University, Columbus, OH, USA for supplying the full-length human NIS cDNA. We also thank Roswitha Beck and Rosel Oos, Department of Nuclear Medicine, Ludwig-Maximilians-University, Munich, Germany, for their assistance with the imaging and therapy studies.

5 Chapter 4

Mesenchymal stem cell (MSC)-mediated, tumor stroma-targeted radioiodine therapy of metastatic colon cancer using the sodium iodide symporter (NIS) as theranostic gene

Kerstin Knoop[1], Nathalie Schwenk[1], Kathrin Schmohl[1], Andrea Müller[1], Christian Zach[3], Clemens Cyran[4], Janette Carlsen[3], Guido Böning[3], Peter Bartenstein[3], Burkhard Göke[1], Ernst Wagner[4], Peter J. Nelson[2], Christine Spitzweg[1]

Department of Internal Medicine II[1], Clinical Biochemistry Group, Department of Internal Medicine and Policlinic IV[2], Department of Nuclear Medicine[3], Department of Clinical Radiology, Laboratory for Experimental Radiology[4], Department of Pharmacy, Center of Drug Research, Pharmaceutical Biotechnology[5], Ludwig-Maximilians-University, Munich, Germany

5.1 Translational Relevance

Engineered mesenchymal stem cells are currently being tested clinically as therapy vehicles for solid tumors. Most preclinical data generated to date has focused on primary tumors. The sodium iodide symporter (NIS) represents one of the oldest and most successful targets for molecular imaging and targeted radionuclide therapy by the application of radioiodine for the management of thyroid cancer. Cloning of the NIS gene allowed investigation of its expression and regulation in thyroidal and non-thyroidal tissues paving the way for a novel cytoreductive gene therapy. In previous studies we demonstrated the potential of mesenchymal stem cells (MSC) as tumor-selective gene delivery vehicles based on their homing to the tumor stroma. This translational study is the first preclinical trial to demonstrate the potential of MSC-mediated NIS gene delivery in a hepatic colon cancer metastases model, as shown by NIS-targeted radionuclide imaging and a therapeutic effect of radioiodine, resulting in an improved survival.

5.2 Abstract

The tumor-homing property of mesenchymal stem cells (MSCs) allows targeted delivery of therapeutic genes into the tumor microenvironment. The application of the sodium iodide symporter (NIS) as a theranostic gene allows non-invasive imaging of MSC biodistribution and transgene expression before therapeutic radioiodine application. We have previously shown that linking therapeutic transgene expression to induction of the chemokine CCL5/RANTES allows a more focused expression within primary tumors as the adoptively transferred MSC develop CAF-like characteristics. While RANTES/CCL5-NIS-targeting has shown efficacy in the treatment of primary tumors, it was not clear if it would also be effective in controlling the growth of metastatic disease.

In the present study, we investigated the biodistribution and tumor recruitment of MSCs engineered to express the NIS gene under control of the RANTES/CCL5 promoter (RANTES-NIS-MSC) in a colon cancer liver metastasis mouse model established by intrasplenic injection of the human colon cancer cell line LS174t.

Five days after intrasplenic tumor cell injection RANTES-NIS-MSCs were injected intravenously three times followed by ^{123}I-scintigraphy and ^{124}I-PET imaging. Results show selective MSC recruitment and RANTES/CCL5-promoter activation in the stroma of liver metastases as evidenced by tumor-selective iodide accumulation, immunohistochemistry and real-time PCR. Therapeutic application of ^{131}I in RANTES-NIS-MSC-treated mice resulted in a significant delay in tumor growth and improved overall survival.

These results convincingly demonstrate selective recruitment and activation of RANTES-NIS-MSC into liver metastases of colon cancer allowing tumor-specific iodide accumulation. This novel gene therapy approach opens the prospect of NIS-mediated radionuclide therapy of metastatic cancer after MSC-mediated gene delivery.

5.3 Introduction

Effective control of metastatic disease represents a central challenge in the treatment of solid tumors. Colorectal cancer is the third most common cancer world-wide, with the liver being the most common site of metastases. While the prognosis of resectable colorectal liver metastases was improved in the recent years, 5-year survival rates after resection are still not higher than 25% to 40%, and survival rates have remained poor for unresectable disease (Siegel *et al.* 2013).

An emerging tumor therapy approach is based on the use of adoptively transferred mesenchymal stem cells (MSCs) as vehicles engineered to express specific reporter and/or therapy genes (eMSC). This approach makes use of the innate ability of MSCs to migrate to damaged tissue in the course of tissue repair (Aquino *et al.* 2010). Tumors are seen by the body as chronic, never healing wounds that drive continuous tissue remodeling thus providing the basis for the marked tumor tropism of MSCs (Dvorak 1986). We and others have harnessed this biology by using eMSC to deliver anti-cancer gene products deep into tumor stromal environments (Conrad *et al.* 2007; Conrad *et al.* 2011; Conrad *et al.* 2009; Knoop *et al.* 2011; Knoop *et al.* 2013; Niess *et al.* 2011; Zischek *et al.* 2009). Adoptively transferred MSCs are actively recruited to growing tumors where they contribute to the formation of the “benign” stromal compartment containing a variety of distinct cell types, including endothelial cells, smooth muscle cells, and pericytes/carcinoma-associated fibroblasts that provide important support for the growth of solid tumors. However, MSCs also contribute to normal tissue homeostasis and therefore also migrate to non-tumor environments under these conditions. In order to reduce potential side effects of transgene expression in non-tumor-associated tissues, the therapeutic utility of eMSCs has been enhanced by the use of tumor stroma-specific gene promoters linked to unique differentiation pathways activated as MSC respond to tumor microenvironments. For example, the Tie2 promoter/enhancer is activated as MSC respond to angiogenic signals within tumor environments, but is not strongly activated in normal tissue settings (Niess *et al.* 2011; Zacharek *et al.* 2007). MSC engineered to express the suicide gene herpes simplex virus thymidine kinase (HSV-TK) under control of the Tie2 promoter/enhancer showed selective expression of transgenes following systemic injection of the eMSC into mice with growing breast, pancreatic or liver tumors. Further, the TK gene product generated in the tumor environment, in combination with application of the prodrug ganciclovir resulted in a significant reduction in primary tumor growth, as well as prolongation of life (Conrad *et al.* 2011; Niess *et al.* 2011). While this approach was effective in targeting large primary tumors, the Tie2-based strategy showed low efficacy in the treatment of tumor metastases. To address this, an alternative targeting approach was developed with the use of the

RANTES/CCL5 promoter to drive transgene expression in MSCs. In the course of differentiation into carcinoma-associated fibroblasts (CAFs), a key cell type in the establishment and progression of solid tumors, MSCs induce expression of the chemokine RANTES (Karnoub *et al.* 2007; Zlotnik and Yoshie 2000). eMSC engineered to express HSV-TK under control of the RANTES promoter in concert with GCV treatment led not only to a significant reduction in the growth of primary pancreatic carcinoma, but also dramatically reduced incidence of metastases in a pancreatic cancer model (Zischek *et al.* 2009).

In order to enhance potential therapeutic benefit of MSC-mediated gene therapy, a more aggressive therapy gene was developed. The sodium iodide symporter (NIS) protein is responsible for the active uptake of iodide from the blood into the thyroid gland, and as such, forms the molecular basis for the diagnostic and therapeutic use of radioiodine, that has been used for almost 70 years in the management of differentiated thyroid cancer (Spitzweg and Morris 2002). One of the major advantages of NIS as a therapy gene is not only the extensive experience that clinicians already have with NIS-mediated radioiodine therapy, but also its dual function as therapy as well reporter gene (Spitzweg and Morris 2002);(Spitzweg 2009);(Baril *et al.* ; Hingorani *et al.* 2010; Penheiter *et al.* 2012a; Penheiter *et al.* 2012b). MSCs engineered to express NIS can be monitored by whole body imaging using ^{123}I-scintigraphy/SPECT or ^{124}I- and ^{18}F-TFB-PET allowing direct, non-invasive *in vivo* imaging of MSC biodistribution and functional transgene expression (Dingli *et al.* 2003a; Groot-Wassink *et al.* 2004; Jauregui-Osoro *et al.* 2010). Importantly, a robust therapeutic effect can be delivered through ^{131}I or ^{188}Re application resulting in a potentially stronger therapeutic effect than that seen with standard suicide genes (Knoop *et al.* 2011; Knoop *et al.* 2013). In the present study, the efficacy of RANTES-based eMSC targeting of NIS expression was evaluated in an experimental mouse model of colon cancer liver metastases.

5.4 Material and methods

Cell culture

The establishment and characterization of MSCs has been described previously (Knoop *et al.* 2011). The human colon carcinoma cell line LS174t (ATCC CCL188) was cultured in RPMI (Invitrogen/Life technologies, Darmstadt, Germany) supplemented with 10% fetal bovine serum (v/v; PAA) and 1% penicillin/streptomycin. The cell lines were maintained at 37°C and 5% CO_2 in an incubator with 95% humidity.

Plasmid construct and stable transfection of mesenchymal stem cells

Plasmids and their synthesis as well as the establishment of stably transfected cell lines have been described previously (Knoop *et al.* 2011; Knoop *et al.* 2013).

Establishment of a hepatic colon cancer metastases mouse model

The experimental protocol was approved by the regional governmental commission for animals (Regierung von Oberbayern). Fully anesthetized female CD-1 nu/nu mice (Charles River, Sulzfeld, Germany) were placed in the right lateral position. After the skin was washed (70% ethanol), a 0.5 cm cut was made at the left subcostal region exposing the lower pole of the spleen. A 27-gauge needle was then inserted at the upper splenic pole and 50 µl of tumor cell suspension ($1x10^6$ cells in 1xPBS) was injected. The abdominal wall and the skin were then sutured separately using a Monosyn® 5/0 fiber. 48 h later the abdominal wall was re-opened at the same site and a splenectomy was performed, followed by suturing of the abdominal wall and the skin. Mice were pre- and post-treated with Carprofen (5 mg/kg) to minimize wound pain. The induction of liver metastases with this technique was highly reproducible; histological liver studies showed that 90% of injected mice developed disseminated liver metastases. Animals were maintained under specific pathogen-free conditions with access to mouse chow and water ad libitum.

MSC application and radionuclide biodistribution studies in vivo

The eMSC applications were initiated five days after intrasplenic tumor cell injection, before metastatic disease was visible. Pretreatment with thyroid hormone L-T4 (levothyroxine) effectively downregulates thyroidal NIS expression, the treatment schedule used was based in part on the study by Di Cosmo *et al*. using a supraphysiological LT-4 dose (10 µg L-T4/100 g body weight) (Di Cosmo *et al.* 2009). Mice weighed between 20 – 25 g, and therefore a dose of 2 µg L-T4/mouse/d was applied. WT-MSCs or RANTES-NIS-MSCs were applied via the tail vein at 5 x 10^5 cells/500µl PBS. Two groups of mice were established and treated as follows: (a) three intravenous (i.v.) applications of RANTES-NIS-MSC in three day intervals

(n=22); (b) three i.v. applications of WT-MSC in three day intervals (n=7). As an additional control, in a subset of mice injected with RANTES-NIS-MSC (n=7) the specific NIS-inhibitor sodium-perchlorate ($NaClO_4$, 2 mg per mouse) was injected intraperitoneally (i.p.) 30 min prior to radionuclide administration. 48 h after the last MSC application, 18.5 MBq ^{123}I was injected i.p. and radionuclide biodistribution was assessed using a gamma camera equipped with UXHR collimator (Ecam, Siemens, Germany) as described previously (Willhauck *et al.* 2007b; Willhauck *et al.* 2008a). Small-animal PET imaging was performed in a subgroup of mice treated with RANTES-NIS-MSC (n=8) receiving a dose of 12 MBq ^{124}I 48 h after the last MSC application. The PET-imaging procedure was described previously (Knoop *et al.* 2011).

Analysis of radioiodine biodistribution ex vivo

For *ex vivo* biodistribution studies, mice were injected with RANTES-NIS-MSCs (n=15) or WT-MSCs (n=5) as described above followed by i.p. injection of 18.5 MBq ^{123}I. A subset of RANTES-NIS-MSC injected mice (n=5) were treated with $NaClO_4$ prior to radionuclide administration as an additional control. Three hours after radioiodine injection, mice were sacrificed and organs of interest were dissected, weighed and ^{123}I accumulation was measured in a gamma counter. Results were reported as percentage of injected dose per organ (% ID/organ).

Analysis of NIS mRNA expression using quantitative real-time PCR

Total RNA was isolated from the liver and other tissues using the RNeasy Mini Kit (Qiagen, Hilden, Germany) according to the manufacturer's recommendations and quantitative real-time PCR (qPCR) was performed as described previously (Klutz *et al.* 2009).

Radioiodine (^{131}I) therapy studies in vivo

Following a 10-day L-T4 pretreatment as outlined above, two groups of mice were established that each received 55.5 MBq ^{131}I (sodium iodide; GE Healthcare Buchler GmbH, Braunschweig, Germany) 48 h after three RANTES-NIS-MSC (RANTES-NIS-MSC + ^{131}I, n=15) or WT-MSC (WT-MSC + ^{131}I, n=15) applications given in two-day-intervals (each 5 x 10^5 cells/500 µl PBS). 24 h later we applied two more rounds of two MSC (5 x 10^5 cells) injections (in two-day-intervals) followed by 55.5 MBq ^{131}I 48 h later (Fig. 5A). As control, one further group of mice was treated with saline instead of radionuclides after injection of RANTES-NIS-MSC (n=15). By protocol, mice were sacrificed when healthy liver tissue reached less than 20%, or in case of weight loss of more than 10% of initial weight, or when impairment of breathing, drinking or eating behavior was observed.

Magnetic Resonance Imaging (MRI)

For MRI examinations, animals were anaesthetized by i.p. injections of ketamine (Inresa Arzneimittel, Freiburg, Germany) 100mg/kg body weight) and xylazine (Bayer, Leverkusen, Germany) 10mg/kg body weight) and a 27-gauge tail vein catheter was placed for subsequent contrast media administration. MRI was performed on a clinical 3 Tesla system (Magnetom Skyra, Siemens Healthcare, Erlangen, Germany) with animals in prone position, using a clinical wrist coil (Siemens Healthcare, Erlangen, Germany). MRI acquisition was performed using a brief imaging protocol with T1 sequences in axial and coronal view for optimal delineation of intrahepatic tumor manifestations. T1-weighted FLASH3D sequences were acquired pre-contrast and after a standardized i.v. manual bolus injection of 100 µl of Gadolinium-based contrast medium (Primovist®, Bayer Healthcare AG, Berlin, Germany). Sequence details were TR=5.74 ms; TE=2.26 ms; ST=1 mm; α=10°; matrix size 416×416; reconstructed matrix 832×832; field of view 150×150 mm^2; spatial resolution 0.18×0.18×1 mm^3; 80 slices; acquisition time 142 sec.

Immunohistochemical analysis

Immunohistochemical and immunofluorescence staining procedures for the expression of NIS and SV40 large T Ag as well as quantification of cellular proliferation (Ki67) and blood vessel density (CD31) were performed as described previously (Knoop *et al.* 2013).

Statistical methods

Statistical significance of *in vitro* experiments was tested using Student´s t test. Statistical significance of the *in vivo* experiments has been calculated using the Man-Whitney U test.

5.5 Results

Radioiodine* in vivo *imaging studies

To study the potential utility of RANTES driven NIS-based eMSC treatment of colon cancer liver metastases, human colon cancer cells LS174t were injected into the spleen of nude mice followed by splenectomy 48 hours later. In 90% of mice, 14 days thereafter multifocal colon cancer metastases were routinely detected in the liver. To evaluate the ability of eMSC to target early stages of liver metastases, five days after intrasplenic tumor cell injection - before visible metastases developed - eMSCs were injected via the tail (see Materials and Methods). The biodistribution of eMSC expressing NIS under control of the RANTES promoter was then determined by ^{123}I-scintigraphy after injection of 18.5 MBq ^{123}I. Enhanced iodide uptake activity was detected in the liver area by gamma camera imaging two hours after 18.5 MBq ^{123}I injection (Fig. 1a), which resulted in a maximum uptake of 12.1 ± 2.6 % ID/g with a biological half-life of 2.9 h, and a tumor absorbed dose of 63.2 mGy/MBq (Fig. 1g). In contrast, after injection of WT-MSC no liver-specific iodide accumulation was detected (Fig. 1c). To further demonstrate NIS-specificity of iodide uptake in the liver region, a subset of RANTES-NIS-MSC-treated mice received $NaClO_4$ 30 min prior to radioiodine injection, which resulted in a complete blockade of iodide accumulation in liver metastases, in addition to thyroid gland and stomach (Fig. 1b), which represent physiologically NIS-expressing organs. The high iodide accumulation seen in the bladder is a result of renal iodide excretion. To improve the resolution of radioiodine uptake in the liver area, and to more clearly differentiate between hepatic and gastric iodide accumulation, additional PET imaging studies were performed using ^{124}I. Three-dimensional data were subsequently generated using iterative reconstructions of list mode data (0-40min), which provided better anatomical definition. 48 hours after the last RANTES-NIS-MSC administration, 12 MBq ^{124}I were applied and selective iodide accumulation was detected in single metastases three hours after ^{124}I application (Fig. 1d – f). In 70% of RANTES-NIS-MSC-treated mice a maximum uptake of 16.2 ± 3.5 % ID/g was measured in single nodules.

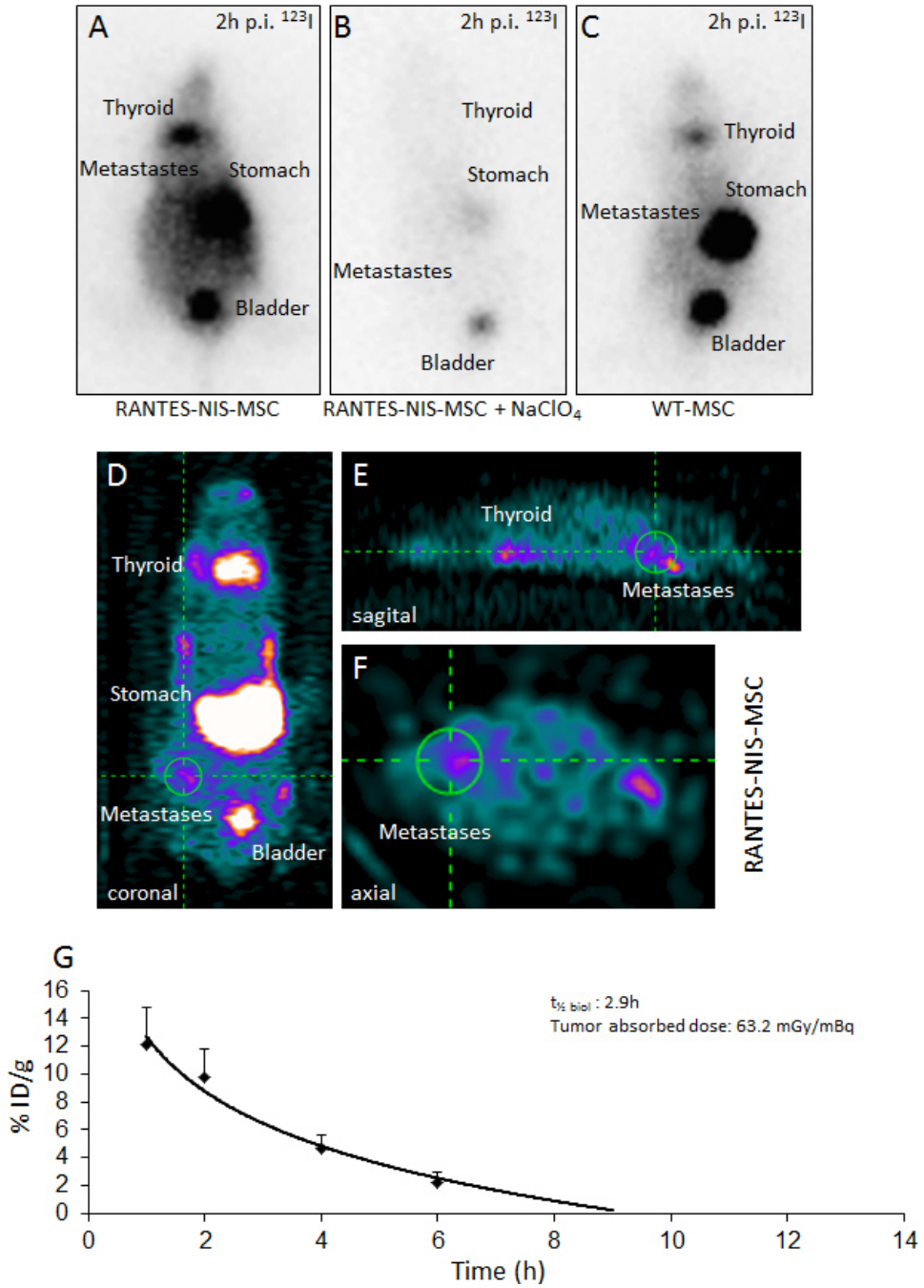

Figure 1 Radioiodine accumulation in liver metastases following systemic RANTES-NIS-MSC administration. Systemic injection with RANTES-NIS-MSCs resulted in enhanced iodide accumulation in livers of mice harbouring colon cancer metastases two hours after radionuclide administration as shown by ^{123}I-gamma-camera imaging (**a**) and small animal ^{124}I-PET imaging (**d – f**), which was completely blocked upon treatment with the NIS-specific inhibitor $NaClO_4$ (**b**). I.v. injection of WT-MSCs did not result in enhanced radioiodine accumulation in the liver region (**c**). Iodide uptake activity resulted in a maximum uptake of 12.1 ± 2.6 % ID/g with a biological half-live of 2.9 hours and a tumor absorbed dose of 63.2 mGy/MBq (**g**).

Ex vivo *radioiodine biodistribution study*

To complement the imaging studies, *ex vivo* gamma counter analysis of radioiodine biodistribution was performed which confirmed increased iodide uptake (approximately 6.1 ±

1.1 % ID/g) in the liver of RANTES-NIS-MSC-treated mice 3 hours after ^{123}I injection (Fig. 2). In non-target organs, or in organs of WT-MSC-injected mice, only background levels of iodide uptake were detected (Fig. 2). In additional control mice injected with RANTES-NIS-MSC, administration of the competitive inhibitor perchlorate resulted in a blockade of iodide uptake in liver (Fig. 2) as well as thyroid gland and stomach (data not shown).

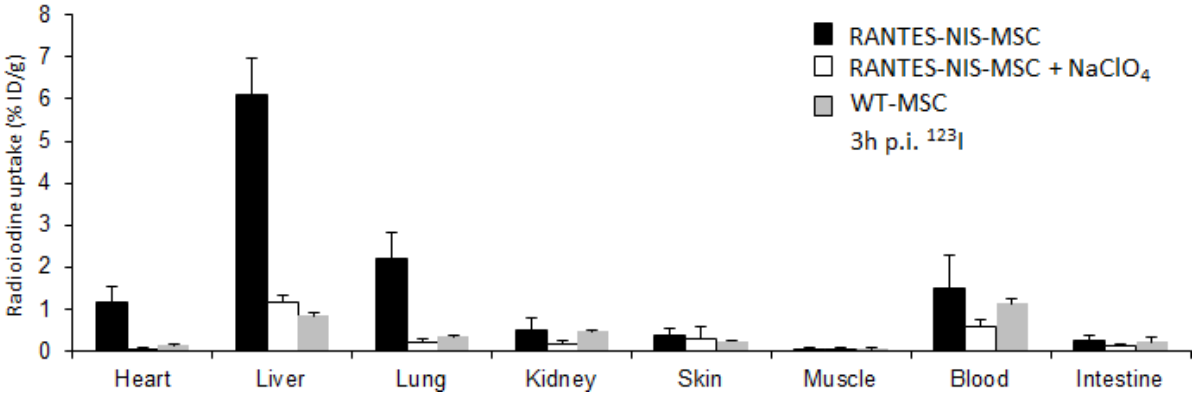

Figure 2 Ex vivo biodistribution studies. *Ex vivo* biodistribution studies 3 hours after injection of 18.5 MBq ^{123}I revealed a hepatic iodide uptake of approx. 6.1 ± 1.1% ID/g, while no significant radioiodine uptake was measured in non-target organs, after pretreatment with perchlorate, or after systemic injection of WT-MSCs. Results are reported as percent of injected dose per g ±SD.

Immunohistochemical analysis of eMSC / transgene biodistribution

eMSC biodistribution was further analyzed *ex vivo* using immunohistochemistry. SV40 large T Ag was used to immortalize the MSCs and could thus be used as target to assess the biodistribution of eMSCs, while human NIS-specific antibodies allowed the determination of RANTES promoter-induced NIS transgene expression. Paraffin-embedded tissues from liver and additional “non-target” organs (lung, kidneys) were processed for immunohistochemical staining using both sets of antibodies. In liver metastases of mice treated with RANTES-NIS-MSCs, NIS-specific immunoreactivity was confined to metastatic nodules, and no NIS-specific staining was seen in the surrounding normal liver tissue (Fig. 3a). This biodistribution pattern was confirmed by SV40 large T Ag-specific staining which confirmed the presence of eMSCs in the metastases and not into the normal liver tissue (Fig. 3c). Systemic injection of WT-MSCs in mice harboring colon cancer liver metastases showed no NIS-specific immunoreactivity in metastases or in normal liver tissue (Fig. 3b); However, SV40 large T Ag staining still demonstrated active WT-MSC recruitment into the metastatic nodules (Fig. 3d), thus supporting tumor-selective eMSC recruitment. Immunofluorescence analysis confirmed co-localization of NIS- and SV40 large T Ag staining in the stroma of liver metastases of tumor-bearing mice after injection of RANTES-NIS-MSC (Fig. 3e – g).

In non-target organs such as lung or kidney, no NIS-specific or SV40 large T Ag-specific staining was detected in mice treated with RANTES-NIS-MSCs (Fig. 3h – k).

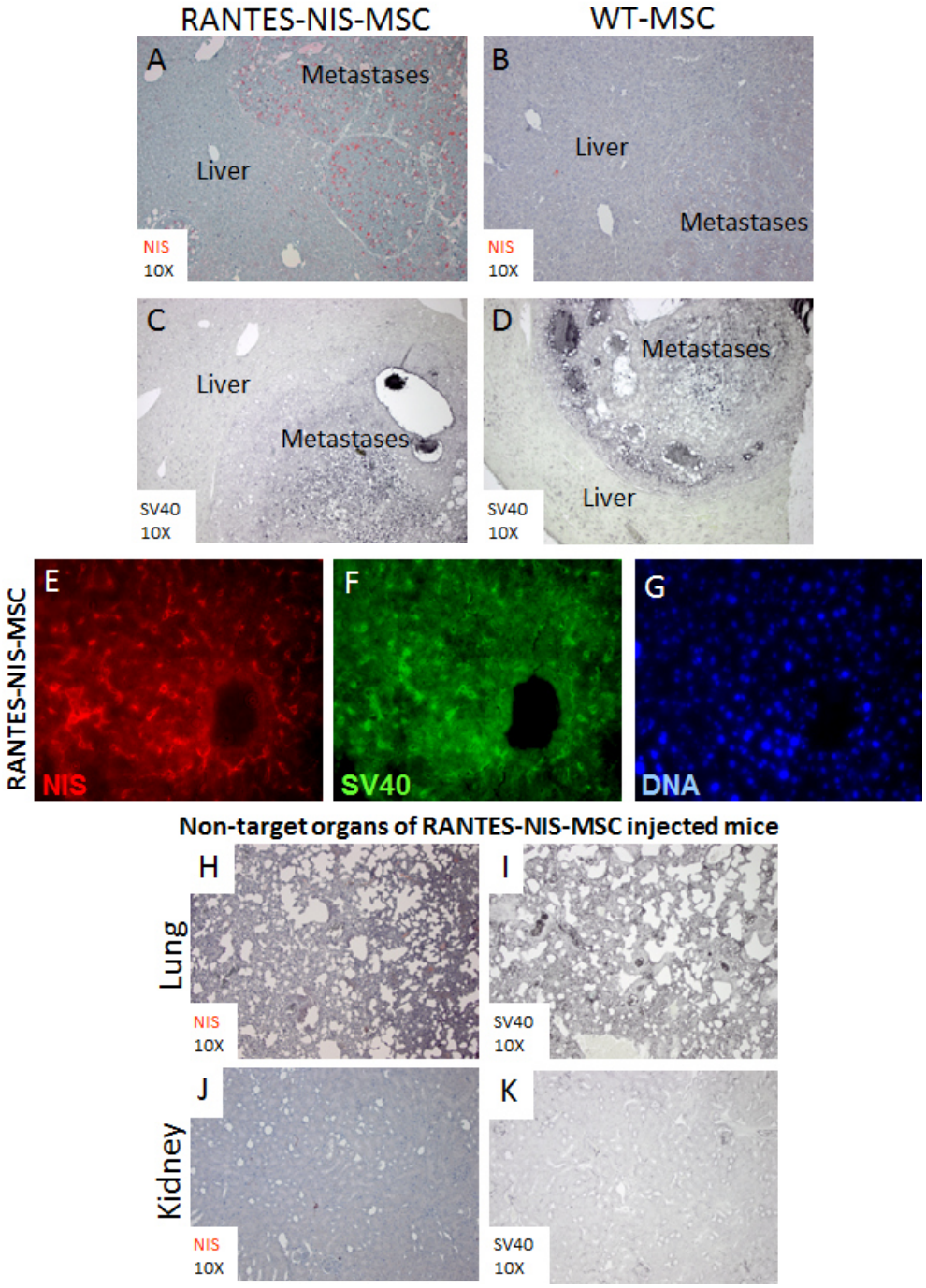

Figure 3 Immunohistological analysis of eMSC distribution in colon cancer liver metastases. Following systemic RANTES-NIS-MSC injection, strong NIS-specific immunreactivity was detected confined to metastatic tissue (**a**), whereas normal liver tissue did not show NIS-specific immunostaining. No NIS-specific immunreactivity was detected following systemic injection of WT-MSCs (**b**). SV40 large T Ag staining demonstrated the presence of RANTES-NIS-MSC (**c**) and WT-MSC (**d**) in hepatic colon cancer metastases. Immunofluorescence analyses confirmed the co-localisation of RANTES promoter-mediated NIS expression with MSC-specific SV40 large T Ag-specific staining (**e–g**). Non-target organs including lung and kidney were negative for NIS-specific immunostaining (**h, j**) as well as MSC-specific SV40 large T Ag-specific staining (**i, k**) in colon cancer liver metastases-bearing mice following treatment with RANTES-NIS-MSC.

Analysis of NIS mRNA expression

As a final validation of RANTES-induced transgene expression, NIS mRNA expression levels from whole metastatic liver tissue and non-target organs were analyzed by quantitative real-time PCR using NIS-specific oligonucleotide primers. Metastatic livers from mice treated with RANTES-NIS-MSCs revealed a 7.6-fold increased level of NIS mRNA expression as compared to metastatic livers from mice treated with WT-MSCs. As expected, additional treatment with the competitive NIS inhibitor perchlorate ($NaClO_4$) had no influence on NIS mRNA expression in metastases-bearing mice injected with RANTES-NIS-MSC (7.4-fold increase). In contrast, non-target organs like lung or kidney showed no NIS mRNA expression in RANTES-NIS-MSC- or WT-MSC-treated mice (Fig. 4).

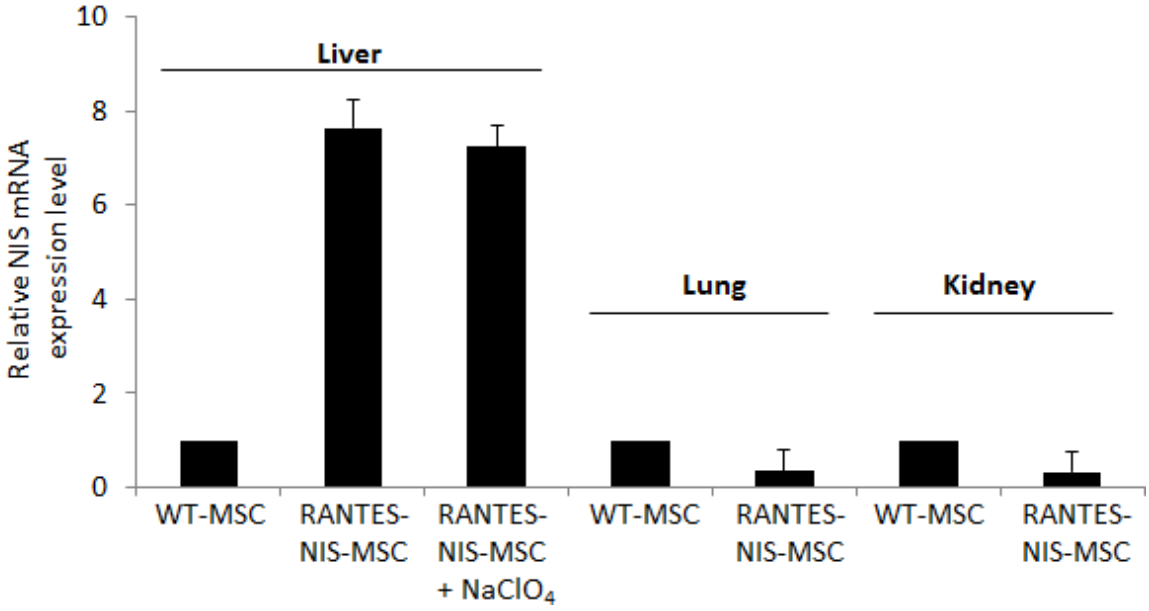

Figure 4 Analysis of NIS mRNA expression levels. Quantitative real time PCR revealed only background levels of NIS mRNA expression in liver metastases of mice injected with WT-MSC, whereas significant levels of NIS mRNA expression were detected in the livers of mice harbouring colon cancer liver metastases after application of RANTES-NIS-MSC injections (7.6-fold) and in mice additionally treated with the competitive NIS inhibitor perchlorate ($NaClO_4$) (7.4-fold). In non-target organs including lung and kidney no NIS mRNA expression was seen after injection of RANTES-NIS-MSC or WT-MSC.

^{131}I therapy study

The therapeutic effect of ^{131}I was assessed in mice carrying colon cancer liver metastases using the therapy regime optimized in previous studies. The protocol is based on three cycles of eMSC injections followed by ^{131}I as outlined in Materials and Methods. After systemic injection of RANTES-NIS-MSC followed by ^{131}I injection a significantly improved survival of up to 14 days was observed as compared to control groups (Fig. 5a).

Growth of metastases was monitored by MRI starting before the first ^{131}I application after three injections of eMSCs (10 Days after intrasplenic tumor cell injection) when the tumor load in the liver was moderate (approximately 40%) (Fig. 5b). Over time, an exponential tumor growth was seen in the control groups (RANTES-NIS-MSC + NaCl or WT-MSC + ^{131}I) (Fig. 5d) as compared to the therapy group (RANTES-NIS-MSC + ^{131}I) that showed a significantly reduced tumor growth (Fig. 5c). MRI images at day 19 showed a reduced hepatic tumor load of approximately 63% in the therapy group (RANTES-NIS-MSC + ^{131}I) as compared to a tumor load of at least 80-90% in the control group (RANTES-NIS-MSC + NaCl), while mice of the control groups not even survived the last ^{131}I or saline application, respectively.

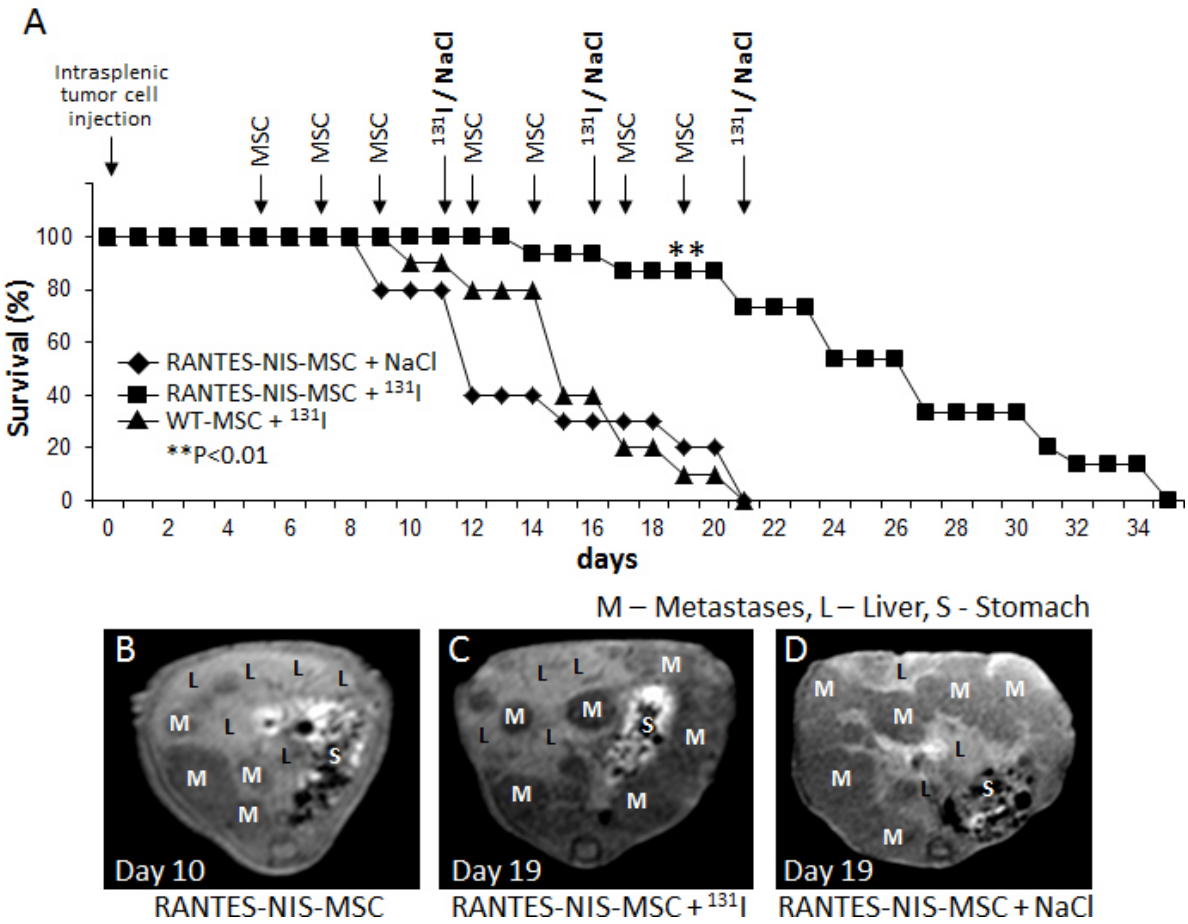

Figure 5 Therapeutic efficacy of ^{131}I in hepatic colon cancer metastases-bearing mice after systemic application of RANTES-NIS-MSC. Mice harbouring hepatic colon cancer metastases received two rounds of repetitive RANTES-NIS-MSC or WT-MSC applications followed by ^{131}I (55.5 MBq) administration. 24 h thereafter two additional MSC injections were applied followed by a third injection of ^{131}I. A further control group received saline instead of ^{131}I. Therapeutic application of ^{131}I after injection of RANTES-NIS-MSCs resulted in significantly improved survival as compared to the control groups (**a**). Monitoring of metastases growth showed 10 days after intrasplenic LS174t cell injection small metastases in the liver with a hepatic tumor load of approx. 40% (**b**). Within one week exponential tumor growth was observed in the control group (RANTES-NIS-MSC + NaCl, tumor load approx. 80-90%) (**d**) as compared to the therapy group (RANTES-NIS-MSC + ^{131}I) (**c**), which revealed delayed metastases growth (tumor load approx. 63%) at day 19 after intrasplenic tumor cell injection.

At the end of experiments, animals were sacrificed, and their organs removed and characterized by immunofluorescence analysis for cellular proliferation (Ki67, green) and blood vessel density (CD31, red) markers. The results showed striking differences between therapy and control groups (Fig. 6a – c). Mice treated with RANTES-NIS-MSCs followed by ^{131}I showed decreased proliferation (Ki76: 23.3 % ± 2.5%) and blood vessel density (CD31: 3.1% ± 0.2%), whereas control mice treated with RANTES-NIS-MSC followed by NaCl or treated with WT-MSCs followed by ^{131}I revealed high blood vessel density (RANTES-NIS-MSC + NaCl: CD31: 6.6% ± 0.7%; WT-MSC + ^{131}I: CD31: 7.8% ± 0.8%) and high levels of proliferation (RANTES-NIS-MSC + NaCl: Ki67: 73.8% ± 6.9%; WT-MSC + ^{131}I: Ki67: 76.5% ± 6,7%) (Fig.6d, e).

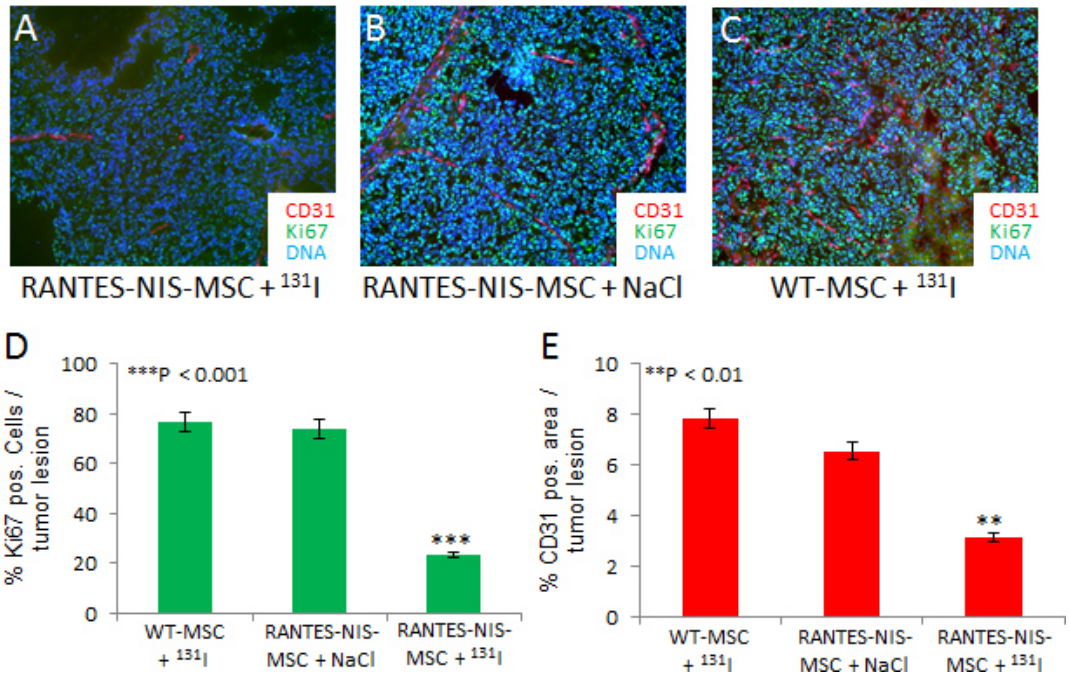

Figure 6 Ex vivo analyses of therapeutic effect. Immunofluorescence analyses of liver metastases using a Ki67-specific antibody (green, labelling proliferating cells) and an antibody against CD31 (red, labelling blood vessels) showed striking difference in tumor cell proliferation and blood vessel density in metastases of mice treated with RANTES-NIS-MSCs and ^{131}I, (**a**), which was significantly reduced (Ki67: 23.3 % ± 2.5%; CD31: 3.1% ± 0.2% (**d, e**)) as compared to the control groups of mice treated with RANTES-NIS-MSC and saline (**b**) (Ki67: 73.8% ± 6.9%, CD31: 6.6% ± 0.7% (**d, e**)) or WT-MSC and ^{131}I (**c**) (Ki67: 76.5% ± 6,7%, CD31: 7.8% ± 0.8% (**d, e**). Slides were counterstained with Hoechst nuclear stain. Magnification x200.

5.6 Discussion

Colorectal cancer with advanced hepatic metastatic disease represents a major clinical problem. Despite advances in chemotherapy regimens, the only potential cure for patients presenting with colon cancer liver metastases remains surgical resection. At present, five-year survival rates following liver resection still range between 25% - 40% compared to 0% - 5% for non-operated patients, demonstrating the need for expanded therapeutic protocols (Siegel *et al.* 2013).

Gene therapy represents an emerging therapy modality in the general treatment of cancer. It is based on the selective introduction of a diverse array of potential therapy genes within different tumor environments using various vehicles (Tang *et al.* 2010). In the present study, an emerging gene therapy approach was used in which the therapy gene was expressed in the context of eMSC-based protocols. eMSCs are excellent gene delivery vehicles based in part on their relative ease of engineering and expansion *in vitro*, while retaining their multilineage potential. Importantly, they also show a remarkable natural tropism for solid tumors (Dwyer and Kerin 2010; Dwyer *et al.* 2010; Tang *et al.* 2010). An array of therapy proteins have already been demonstrated to be successfully delivered to tumor environments using eMSC, including interferon-gamma, TRAIL ligands, IL-12, the chemokine CX3CL1, as well as various suicide genes (Deng *et al.* 2014; Gao *et al.* 2010; Kim *et al.* 2008). Recent studies have also shown that adoptively applied MSC can also efficiently home to tumor metastases opening the door to the potential use of eMSC for treatment of metastatic disease (Chen *et al.* 2008; Shinagawa *et al.* 2013; Su *et al.* 2013; Zhao *et al.* 2012).

In one recent study, the authors used an IL-12-based eMSC approach that showed, in experimental models of melanoma, breast and hepatoma tumors, reduced progression of metastases at midstage of development, and even regression at later stages following an extended course of i.v. immunotherapy using IL-12 gene-engineered MSCs (Chen *et al.* 2008).

In addition to MSCs, related progenitor cells have also shown efficacy as therapy vehicles. In a model of metastatic breast cancer, Aboody *et al*. showed that human neural stem cells (NSC) can also target tumor metastases in multiple organs including liver, lymph nodes, and lung. The NSCs were engineered to constitutively secrete the suicide gene carboxylesterase (eNSC-rCE). This suicide gene encodes an enzyme that alters the CPT-11 prodrug into SN-38, a potential topoisomerase I inhibitor. The final result is that high doses of the therapy drug are generated only where carboxylesterase is expressed. Systemic administration of tumor-bearing mice with eNSC-rCE cells, in concert with CPT-11 treatment, resulted in reduced metastastic tumor burden in lung and lymph nodes (Zhao *et al.* 2012).

The down side of gene therapy using traditional suicide genes is that even though they act through bystander killing, their effects are limited to the cells most proximal to the cells expressing the gene. In contrast, NIS-targeted radioiodine therapy is associated with a higher degree of bystander killing effect that results from 1) the crossfire effect of the β-emitter ^{131}I and 2) the radiation-induced biological bystander effect (Hingorani *et al.* 2007). This therapy concept has been effectively used for the treatment of differentiated thyroid cancer for almost 70 years and still represents one of the most effective systemic anticancer radiotherapies available to the clinician today.

The application of the NIS gene as a combined imaging/therapy gene has been an area of expanded research in various tumor settings over the past few years. The ability to non-invasively monitor the biodistribution of NIS expression after local and - even more important - systemic gene delivery provides an essential extension to the clinical setting. NIS itself is nontoxic; it is seen as “self” by the immune system, thus limiting potential immunogenicity; and a large numbers of NIS-compatible radioactive tracers are available including ^{123}I for scintigraphy/SPECT, and ^{124}I- and ^{18}F-TFB for PET imaging (Jauregui-Osoro *et al.* 2010). Finally, NIS transgene expression allows the delivery of a robust therapeutic effect through ^{131}I or ^{188}Re application application (Dwyer *et al.* 2005a; Dwyer *et al.* 2006; Dwyer *et al.* 2011; Herve *et al.* 2008; Kakinuma *et al.* 2003; Knoop *et al.* 2013; Peerlinck *et al.* 2009; Willhauck *et al.* 2007b; Willhauck *et al.* 2008c). The flexibility of this approach has been demonstrated more recently, in studies using oncolytic viruses and non-viral nanoparticles equipped with the NIS gene in order to facilitate non-invasive *in vivo* vector imaging as well as ^{131}I-based radiotherapy after systemic application. We recently demonstrated tumor-selective radioiodine uptake and therapeutic efficacy of radiovirotherapy after systemic delivery of the NIS gene using a dendrimer-coated replication-selective adenovirus (Grunwald *et al.* 2013b; 2013c). To optimize adenovirus shielding and targeting, we physically coated replication-selective adenoviruses carrying the human NIS gene with a conjugate consisting of cationic poly(amidoamine) (PAMAM) dendrimer with or without an attached targeting ligand, the peptidic, epidermal growth factor receptor (EGFR)-specific ligand GE11. Systemic injection resulted in reduction of adenovirus liver pooling and decreased hepatotoxicity as well as increased transduction efficiency in peripheral hepatocellular xenograft tumors. Gamma camera imaging showed significantly higher levels of tumor-specific iodide accumulation resulting in a significantly enhanced oncolytic effect, which was further increased by therapeutic radioiodine treatment. (Grunwald *et al.* 2013b; 2013c). In an additional study by our group, nanoparticles based on linear polyethylenimine (LPEI) shielded by polyethylene glycol (PEG) and coupled with the EGFR-specific ligand GE11 was used to target a NIS-expressing plasmid to hepatocellular Huh7 xenograft model in nude mice resulting in a

significant tumoral iodide uptake after systemic injection and a significant delay in tumor growth after therapeutic application of ^{131}I (Klutz *et al.* 2011a).

In previous studies we demonstrated proof of concept of systemic NIS gene delivery using MSCs as delivery vehicles using subcutaneous xenograft mouse models (Knoop *et al.* 2011; Knoop *et al.* 2013). Systemic application of eMSCs expressing NIS under the control of the tumor stroma-specific RANTES promoter (RANTES-NIS-MSC) led to a significant radioiodide accumulation in a subcutaneous hepatocellular Huh7 xenograft model in nude mice resulting in a delay of tumor growth and improved survival by therapeutic ^{131}I application (Knoop *et al.* 2013). However, while therapeutic efficacy has been demonstrated in subcutaneous solid tumor models using MSCs engineered to express NIS using the RANTES promoter, its potential efficacy in the treatment of tumor metastases represents a clinically important open issue. In the current study a liver metastasis model of colon cancer was used to analyze the biodistribution of MSC recruitment and NIS-mediated radioiodine accumulation.

By ^{123}I gamma-camera or ^{124}I PET imaging NIS-eMSCs were shown to specifically home to liver metastases, and by extrapolation, induce RANTES promoter-driven NIS transgene expression, resulting in a tumor-selective radioiodine accumulation of up to 12% ID/g and a biological half-life of approx. 3 h. While ^{123}I scintigraphic imaging showed a diffusely elevated radioiodine uptake in the hepatic area of mice carrying disseminated liver metastases, ^{124}I small animal whole body PET imaging allowed a more detailed three-dimensional analysis of NIS-mediated radioiodine accumulation with higher resolution showing iodide uptake confined to metastatic nodules. *Ex vivo* analysis showed enhanced and NIS-specific iodine uptake in the liver of colon cancer metastases-bearing mice after treatment with NIS-eMSCs. This was further validated by immunohistological and quantitative PCR analyses. Immunohistology demonstrated strong immunoreactivity strictly confined to metastatic tissue without NIS and SV40 large T Ag expression in normal liver tissue or non-target organs. No metastatic spread was seen outside the liver, which was also reflected in negative tissue radioiodine uptake studies.

In the therapy studies a significant reduction of tumor growth was observed associated with a significantly extended life span which is highly significant considering the aggressive growth of tumor metastases in this model. Hepatic tumor load as monitored *in vivo* by MRI showed a tumor load of approx. 40% prior to the first ^{131}I application. Tumor growth increased dramatically to at least 80% in the control groups as compared to only 63% in the therapy group. These findings correlate with markedly reduced proliferation and blood vessel density in the tumors of the therapy group as measured by immunofluorescence analysis.

In contrast to our study, many of previously published studies on gene therapy of metastatic disease analyzed therapeutic efficacy by *ex vivo* analyses. Zischek *et al*. showed reduced level of metastases in a pancreatic carcinoma mouse model a by *ex vivo* analyses after

treatment with MSCs expressing the HSV-TK suicide gene However, the authors could not determine if this was due to direct effects on the primary tumor (leading to reduced production of metastases) or direct targeting of metastatic disease (Zischek *et al.* 2009). This study relied on *ex vivo* analysis of tumor growth. With the translation from animal to human studies in mind, in our current study we used contrast enhanced MRI to monitor the growth of hepatic colon cancer metastases over time *in vivo*. The contrast between tumor and normal tissue was enhanced by a liver-specific contrast agent (Primovist®), which allowed an optimal evaluation of treatment effects in hepatic metastases. MRI is emerging as a powerful method to investigate the potential effects of treatment approaches in mice. A study of Lavilla-Alonso *et al*. describes an optimized MRI protocol for analyzing the antitumor effects of an intrasplenically administered oncolytic adenovirus therapy, which resulted in reducing visceral tumor load and development of liver metastases (Lavilla-Alonso *et al.* 2011).

In conclusion, in the current study we were able to translate our previous promising findings of MSC-mediated systemic NIS gene delivery in subcutaneous liver cancer xenografts into a clinically more relevant mouse model of show in a hepatic colon cancer metastases. Non-invasive ^{123}I gamma camera and ^{124}I PET imaging demonstrated remarkable tumor selectivity of MSC recruitment and NIS expression driven by the tumor stroma-specific RANTES/CCL5 promoter after systemic MSC application. The tumor stroma-targeted iodide uptake confined to liver metastases was strong enough for a significant reduction of metastases growth monitored in vivo by MRI resulting in in significantly improved survival. These data therefore convincingly demonstrate the enormous potential of MSC-mediated NIS gene radionuclide therapy in metastatic cancer.

5.7 Acknowledgements

We are grateful to J.C. Morris, Division of Endocrinology, Mayo Clinic and Medical School, Rochester, MN, USA for providing the NIS-specific antibody, as well as to S.M. Jhiang, Ohio State University, Columbus, OH, USA for supplying the full-length human NIS cDNA. We also thank Roswitha Beck, Rosel Oos and Andreas Delker (Department of Nuclear Medicine, Ludwig-Maximilians-University, Munich, Germany) and Matthias Moser (Department of Clinical Radiology, Laboratory for Experimental Radiology, University Hospitals Munich, Munich, Germany) for their assistance with the imaging and therapy studies.

6 Summary

The tumor homing property of mesenchymal stem cells (MSC) has led to their use as delivery vehicles for reporter and therapeutic genes. The sodium iodide symporter (NIS) represents one of the oldest and most successful targets for molecular imaging and radionuclide therapy, as it provides the molecular basis for the diagnostic and therapeutic application of radioiodine that has been successfully used for more than 70 years in the treatment of thyroid cancer patients, and represents the most effective form of systemic anticancer radiotherapy available to the clinicians today. Its theranostic properties allow non-invasive imaging of functional NIS expression by ^{123}I-scintigraphy or ^{124}I-PET imaging, as well as robust therapeutic effects by treatment with ^{131}I or ^{188}Re. The application of NIS as reporter gene represents a novel mechanism for the evaluation of tumor selectivity, and general efficacy of the use of MSCs as gene delivery vehicles.

In the first part of this thesis, human bone marrow derived CD34$^-$ MSCs were stably transfected with a NIS-expressing plasmid in which NIS was driven by the unspecific cytomegalovirus (CMV) promoter (NIS-MSC). After *in vitro* characterization of NIS-MSCs, MSC-mediated NIS expression was analysed *in vivo* via ^{123}I-scintigraphy and ^{124}I-PET imaging. The therapeutic potential of ^{131}I-based therapy was then evaluated. After establishment of a subcutaneous hepatocellular carcinoma (HCC) (Huh7) xenograft model in nude mice, NIS-MSCs were systemically injected and radioiodine biodistribution as well as tumor selectivity analysed using non-invasive imaging procedures. ^{123}I-scintigraphy, ^{124}I-PET imaging and *ex vivo* biodistribution analyses revealed active MSC recruitment into HCC xenografts as shown by tumor-selective iodide accumulation (9.5 % ID/g ^{123}I, biological half-life: 4 h) that was confirmed by *ex vivo* biodistribution studies, immunostaining and quantitative real-time PCR analyses. Finally, the use of NIS as therapeutic gene in HCC xenografts led to a pronounced delay in tumor growth after application of ^{131}I which was associated with improved survival. These results convincingly show tumor-selective recruitment of MSCs in HCC xenografts that can be used for targeted delivery of NIS as reporter and therapy gene.

The next goal of this study, we attempted to refine the tumor stroma selectivity of MSC-mediated NIS expression. Upregulation of the chemokine CCL5 (RANTES) by MSCs within the tumor stroma in the process of tumor stroma recruitment of MSCs, and their differentiation into cancer associated fibroblasts, is thought to play an important role in cancer growth and metastases. Therefore, use of the RANTES/CCL5 promoter to drive NIS expression in genetically engineered MSCs should allow tumor stroma selectivity of NIS expression after MSC-mediated delivery. MSCs were stably transfected with a plasmid in

which NIS was driven by the RANTES/CCL5 promoter (RANTES-NIS-MSC). After systemic injection of RANTES-NIS-MSC in the same HCC xenograft mouse model that was used in the previous studies, ^{123}I-scintigraphy revealed active MSC recruitment into the tumor stroma as well as CCL5 promoter activation as shown by tumor-selective NIS-mediated iodide accumulation (6.5% ID/g ^{123}I, biological half-life: 3.7 h). The iodide uptake activity in the tumor was sufficient for a therapeutic effect with ^{131}I demonstrating a significant delay of tumor growth and improved overall survival. In addition, the potential of ^{188}Re, which is also transported by NIS, as an alternative diagnostic and therapeutic radionuclide was examined. In contrast to ^{131}I, it offers the possibility of higher energy deposition in the tumor in a shorter period of time due to its shorter physical half-life and higher energy of beta particles. Due to the longer path length of beta particles of 10.4 mm as compared to 2.4 mm for ^{131}I, also an enhanced crossfire effect is expected which could serve as an advantage in the context of MSC-mediated NIS gene delivery due to the scattered MSC distribution in the tumor stroma. Systemic application of RANTES-NIS-MSC in subcutaneous HCC tumor-bearing mice resulted in ^{188}Re accumulation specifically in the tumor (7 % ID/g, biological half-life: 4.1 h). However, in direct comparison to ^{131}I, the therapeutic effect of ^{188}Re was similar after RANTES-NIS-MSC-mediated NIS gene delivery resulting in a marked delay in tumor growth and significantly improved survival over ten weeks after NIS-mediated radionuclide therapy, although the tumor-absorbed dose for ^{188}Re was calculated to be three-times higher than for ^{131}I. Based on the survival data obtained for both radionuclides, it is possible that a maximal therapeutic effect was already achieved with ^{131}I treatment. Therapeutic results showed a significant improvement over those we previously reported using the CMV promoter to drive NIS expression in the same model system where the mice lived only seven weeks after NIS mediated radioiodine therapy. In comparison to the first part of the thesis, these results demonstrate high tumor selectivity of MSC recruitment and NIS expression driven by the RANTES/CCL5 promoter after systemic MSC application. The resulting biologically targeted, tumor-selective radionuclide accumulation was high enough for a significant enhanced therapeutic effect of ^{131}I and ^{188}Re in a HCC xenograft model.

In the next stage we established an orthotopic HCC xenograft model to study MSC recruitment and therapy in the context of normal tissue-tumor interplay. Human HCC cells were injected in the right liver lobe which resulted in a single orthotopic liver tumor. RANTES-NIS-MSCs were systemically injected and MSC biodistribution and NIS expression analysed by *in vivo* imaging studies, followed by *ex vivo* radioiodine biodistribution studies as well as NIS expression analysis. ^{123}I-scintigraphy, ^{124}I-PET imaging and *ex vivo* studies demonstrated active MSC recruitment and RANTES promoter-driven NIS expression in the intrahepatic HCC xenograft model, while no NIS expression was seen in healthy liver tissue or in non-target organs. The iodide uptake activity in intrahepatic xenografts was higher than

in subcutaneous flank tumors, which may be due to an enhanced tumor stroma growth within the hepatic environment. The tumoral radioiodine uptake was also high enough for a therapeutic effect of ^{131}I therapy resulting in an improved survival after systemic injection of RANTES-NIS-MSCs. The tumor homing capacity of the NIS expressing MSCs under the control of a tumor stroma specific promoter highlights their potential use for future clinical investigation and justifies investigation in more advanced tumor models.

While therapeutic effects have been demonstrated in xenograft solid tumor models using RATNES-NIS-MSCs, its potential efficacy in treatment of tumor metastases represents a clinically important issue. Therefore, in the last part of the thesis a hepatic colon cancer metastases model was established. Colon cancer cells were injected into the spleen resulting in induction of multifocal liver metastases. After systemic injection of RANTES-NIS-MSCs, imaging studies (^{123}I-scintigraphy and ^{124}I-PET) demonstrated specific MSC-homing to liver metastases as shown by enhanced iodide uptake activity in the liver, whereas healthy liver tissue and non-target organs did not reveal NIS-specific iodide uptake. Successful therapeutic radioiodine treatment resulted in an improved survival in hepatic colon cancer metastases-bearing mice after systemic injection of RANTES-NIS-MSCs. Growth of metastases was observed by magnetic resonance imaging (MRI) showing a significantly delay in tumor mass after therapeutic treatment (63 %) as compared to the control group revealing a tumor mass of 80% after the last of three ^{131}I or NaCl application, respectively.

In conclusion, the data of this thesis convincingly demonstrate the potential of genetically engineered MSCs as tumor-selective gene transfer vehicles for the theranostic NIS gene based on their tumor-specific homing after systemic injection in various tumor models including liver metastases models, which opens the exciting prospect of clinical application of targeted NIS-mediated radionuclide therapy of non-thyroidal cancers, even in metastatic disease.

7 Publications

7.1 Original papers

Stromal targeting of sodium iodide symporter using mesenchymal stem cells allows enhanced imaging and therapy of hepatocellular carcinoma.
Knoop K, Schwenk N, Dolp P, Willhauck MJ, Zischek C, Zach C, Hacker M, Göke B, Wagner E, Nelson PJ, Spitzweg C.
Hum Gene Ther. 2013 Mar;24(3):306-16

Image-guided tumor-selective radioiodine therapy of liver cancer after systemic nonviral delivery of the sodium iodide symporter gene.
Klutz K, Willhauck MJ, Dohmen C, Wunderlich N, **Knoop K**, Zach C, Senekowitsch-Schmidtke R, Gildehaus FJ, Ziegler S, Fürst S, Göke B, Wagner E, Ogris M, Spitzweg C.
Hum Gene Ther. 2011 Dec;22(12):1563-7

Image-guided, tumor stroma-targeted ^{131}I therapy of hepatocellular cancer after systemic mesenchymal stem cell-mediated NIS gene delivery.
Knoop K, Kolokythas M, Klutz K, Willhauck MJ, Wunderlich N, Draganovici D, Zach C, Gildehaus FJ, Böning G, Göke B, Wagner E, Nelson PJ, Spitzweg C.
Mol Ther. 2011 Sep;19(9):1704-13

7.2 Manuscripts in preparation

Mesenchymal stem cell (MSC)-mediated, tumor stroma-targeted radioiodine therapy of metastatic colon cancer using the sodium iodide symporter (NIS) as theranostic gene
Knoop K, Schwenk N, Schmohl K, Müller A, Zach C, Cyran C, Carlsen J, Böning G, Bartenstein P, Göke B, Wagner E, Nelson PJ, Spitzweg C, *submitted*

Effective ^{131}I therapy after mesenchymal stem cell-mediated stromal targeting of the sodium iodide symporter in an orthotopic hepatocellular cancer model
Knoop K, Schwenk N, Schmohl K, Müller A, Zach C, Cyran C, Carlsen J, Böning G, Bartenstein P, Göke B, Wagner E, Nelson PJ, Spitzweg C, *in preparation*

7.3 Oral Presentations

57th Annual Meeting of the German Society of Endocrinology, Berlin, March 2014
In vivo imaging of mesenchymal stem cell recruitment into the tumor stroma of hepatocellular carcinoma (HCC) using a HIF-specific sodium iodide symporter gene system
Kerstin Knoop, Nathalie Schwenk, Patrick Dolp, Michael J Willhauck, Christoph Zischek, Guido Böning, Heidrun Zankl, Marcus Hacker, Burkhard Göke, Ernst Wagner, Peter J Nelson, Christine Spitzweg

Collaborative Congress of the European Society of Gene and Cell Therapy and the Spanish Society of Gene and Cell Therapy, Madrid, Spain, October 2013
In vivo imaging of mesenchymal stem cell recruitment into the tumor stroma of hepatocellular carcinoma (HCC) using a HIF-1α-specific sodium iodide symporter gene system
Kerstin Knoop, Andrea M Müller, Kathrin A Schmohl, Nathalie Schwenk, Janette Carlsen, Marcus Hacker, Burkhard Göke, Ernst Wagner, Peter J Nelson, Christine Spitzweg

95th Annual Meeting of the Endocrine Society, San Francisco, CA, USA, June 2013
Stromal targeting of sodium iodide symporter using mesenchymal stem cells allows radioiodine imaging and therapy of hepatic colon cancer metastases
Kerstin Knoop, Nathalie Schwenk, Patrick Dolp, Michael J Willhauck, Christoph Zischek, Guido Böning, Heidrun Zankl, Marcus Hacker, Burkhard Göke, Ernst Wagner, Peter J Nelson, Christine Spitzweg

Collaborative Congress of the European Society of Gene and Cell Therapy and the French Society of Gene and Cell Therapy, Versailles, France, October 2012
Imaging of mesenchymal stem cell recruitment into the stroma of hepatic colon cancer metastases using the sodium iodide symporter (NIS)
Kerstin Knoop, Nathalie Schwenk, Patrick Dolp, Michael J Willhauck, Christoph Zischek, Guido Böning, Heidrun Zankl, Marcus Hacker, Burkhard Göke, Ernst Wagner, Peter J Nelson, Christine Spitzweg

Collaborative Congress of the European Society of Gene and Cell Therapy and the British Society of Gene Therapy, Brighton, UK, October 2011
Visualization of active homing of mesenchymal stem cells into the tumor stroma of hepatocellular carcinoma (HCC) using the sodium iodide symporter as reporter gene
Kerstin Knoop, Nathalie Schwenk, Patrick Dolp, Michael J Willhauck, Christoph Zischek, Christian Zach, Dan Draganovici, Julia Schlichtiger, Burkhard Göke, Ernst Wagner, Peter J Nelson, Christine Spitzweg

17th Annual Meeting of the German Society for Gene Therapy, Munich, October 2010
Tumor stroma-specific NIS gene delivery using mesenchymal stem cells
Kerstin Knoop, Marie Kolokythas, Kathrin Klutz, Michael J Willhauck, Nathalie Wunderlich, Dan Draganovici, Christian Zach, Franz Josef Gildehaus, Burkhard Göke, Ernst Wagner, Peter Nelson, Christine Spitzweg

92nd Annual Meeting of the Endocrine Society, San Diego, CA, USA, June 2010
In vivo imaging of mesenchymal stem cell recruitment into the tumor stroma of hepatocellular carcinoma (HCC) using the sodium iodide symporter as reporter gene
Kerstin Knoop, Marie Kolokythas, Christoph Zischek, Kathrin Klutz, Michael J Willhauck, Nathalie Wunderlich, Dan Draganovici, Christian Zach, Franz Josef Gildehaus, Burkhard Göke, Ernst Wagner, Peter Nelson, Christine Spitzweg

7.4 Poster Presentations

56th Annual Meeting of the German Society of Endocrinology, Hamburg, March 2013
Imaging of mesenchymal stem cell recruitment into the stroma of hepatic colon cancer metastases using the sodium iodide symporter (NIS)
Kerstin Knoop, Nathalie Schwenk, Patrick Dolp, Michael J Willhauck, Christoph Zischek, Guido Böning, Heidrun Zankl, Marcus Hacker, Burkhard Göke, Ernst Wagner, Peter J Nelson, Christine Spitzweg

82nd Annual Meeting of the American Thyroid Association, Quebec, Canada, September 2012

Stromal targeting of sodium iodide symporter using mesenchymal stem cells allows enhanced imaging and therapy of hepatocellular carcinoma

Kerstin Knoop, Nathalie Schwenk, Patrick Dolp, Michael J Willhauck, Christoph Zischek, Christian Zach, Markus Hacker, Burkhard Göke, Ernst Wagner, Peter J Nelson, Christine Spitzweg

82nd Annual Meeting of the American Thyroid Association, Quebec, Canada, September 2012

Visualization of Active Homing of Mesenchymal Stem Cells into Hepatic Colon Cancer Metastases Using the Sodium Iodide Symporter as Reporter Gene

Kerstin Knoop, Nathalie Schwenk, Patrick Dolp, Michael J Willhauck, Christoph Zischek, Guido Böning, Heidrun Zankl, Marcus Hacker, Burkhard Göke, Ernst Wagner, Peter J Nelson, Christine Spitzweg

Joint Conference of the Germany Society for Gene Therapy and the LOEWE Center for Cell and Gene Therapy Frankfurt, Frankfurt, March 2012

Visualization of Active Homing of Mesenchymal Stem Cells into Hepatic Colon Cancer Metastases Using the Sodium Iodide Symporter as Reporter Gene

Kerstin Knoop, Nathalie Schwenk, Patrick Dolp, Michael J Willhauck, Christoph Zischek, Guido Böning, Heidrun Zankl, Marcus Hacker, Burkhard Göke, Ernst Wagner, Peter J Nelson, Christine Spitzweg

93rd Annual Meeting of the Endocrine Society, Boston, MA, USA, June 2011

Therapeutic potential of stem cell-mediated sodium iodide symporter (NIS) gene delivery in liver cancer

Kerstin Knoop, Marie Kolokythas, Christoph Zischek, Kathrin Klutz, Michael J Willhauck, Nathalie Wunderlich, Dan Draganovici, Christian Zach, Franz Josef Gildehaus, Burkhard Göke, Ernst Wagner, Peter J Nelson, Christine Spitzweg

7.5 Awards

Travel grant, European European Society of Gene and Cell Therapy, Madrid, Spain, October 2013

In vivo imaging of mesenchymal stem cell recruitment into the tumor stroma of hepatocellular carcinoma (HCC) using a HIF-1α-specific sodium iodide symporter gene system

Kerstin Knoop, Andrea M Müller, Kathrin A Schmohl, Nathalie Schwenk, Janette Carlsen, Marcus Hacker, Burkhard Göke, Ernst Wagner, Peter J Nelson, Christine Spitzweg

Travel grant, Glaxo Smith Kline, 95th Annual Meeting of the Endocrine Society, San Francisco, CA, USA, June 2013

Stromal targeting of sodium iodide symporter using mesenchymal stem cells allows radioiodine imaging and therapy of hepatic colon cancer metastases

Kerstin Knoop, Nathalie Schwenk, Patrick Dolp, Michael J Willhauck, Christoph Zischek, Guido Böning, Heidrun Zankl, Marcus Hacker, Burkhard Göke, Ernst Wagner, Peter J Nelson, Christine Spitzweg

Travel grant, German Society for Gene Therapy, Frankfurt, March 2012

Visualization of Active Homing of Mesenchymal Stem Cells into Hepatic Colon Cancer Metastases Using the Sodium Iodide Symporter as Reporter Gene

Kerstin Knoop, Nathalie Schwenk, Patrick Dolp, Michael J Willhauck, Christoph Zischek, Guido Böning, Heidrun Zankl, Marcus Hacker, Burkhard Göke, Ernst Wagner, Peter J Nelson, Christine Spitzweg

8 References

Anderberg C, Li H, Fredriksson L, Andrae J*, et al.* (2009). Paracrine signaling by platelet-derived growth factor-CC promotes tumor growth by recruitment of cancer-associated fibroblasts. Cancer Res 69, 369-78.

Aquino JB, Bolontrade MF, Garcia MG, Podhajcer OL*, et al.* (2010). Mesenchymal stem cells as therapeutic tools and gene carriers in liver fibrosis and hepatocellular carcinoma. Gene Ther 17, 692-708.

Balkwill F. (2004). The significance of cancer cell expression of the chemokine receptor CXCR4. Semin Cancer Biol 14, 171-9.

Baril P, Martin-Duque P, Vassaux G. Visualization of gene expression in the live subject using the Na/I symporter as a reporter gene: applications in biotherapy. Br J Pharmacol 159, 761-71.

Barton KN, Stricker H, Brown SL, Elshaikh M*, et al.* (2008). Phase I study of noninvasive imaging of adenovirus-mediated gene expression in the human prostate. Mol Ther 16, 1761-9.

Bhowmick NA, Moses HL. (2005). Tumor-stroma interactions. Curr Opin Genet Dev 15, 97-101.

Bhowmick NA, Neilson EG, Moses HL. (2004). Stromal fibroblasts in cancer initiation and progression. Nature 432, 332-7.

Blechacz B, Splinter PL, Greiner S, Myers R*, et al.* (2006). Engineered measles virus as a novel oncolytic viral therapy system for hepatocellular carcinoma. Hepatology 44, 1465-77.

Braunersreuther V, Viviani GL, Mach F, Montecucco F. (2012). Role of cytokines and chemokines in non-alcoholic fatty liver disease. World J Gastroenterol 18, 727-35.

Burke RS, Pun SH. (2008). Extracellular Barriers to in Vivo PEI and PEGylated PEI Polyplex-Mediated Gene Delivery to the Liver. Bioconjug Chem 19, 693-704.

Carlson SK, Classic KL, Hadac EM, Dingli D*, et al.* (2009). Quantitative molecular imaging of viral therapy for pancreatic cancer using an engineered measles virus expressing the sodium-iodide symporter reporter gene. AJR Am J Roentgenol 192, 279-87.

Cattaneo R, Miest T, Shashkova EV, Barry MA. (2008). Reprogrammed viruses as cancer therapeutics: targeted, armed and shielded. Nat Rev Microbiol 6, 529-40.

Cengic N, Baker CH, Schutz M, Goke B*, et al.* (2005). A novel therapeutic strategy for medullary thyroid cancer based on radioiodine therapy following tissue-specific sodium iodide symporter gene expression. J Clin Endocrinol Metab 90, 4457-64.

Chen X, Lin X, Zhao J, Shi W*, et al.* (2008). A tumor-selective biotherapy with prolonged impact on established metastases based on cytokine gene-engineered MSCs. Mol Ther 16, 749-56.

Conrad C, Gottgens B, Kinston S, Ellwart J*, et al.* (2002). GATA transcription in a small rhodamine 123(low)CD34(+) subpopulation of a peripheral blood-derived CD34(-)CD105(+) mesenchymal cell line. Exp Hematol 30, 887-95.

Conrad C, Gupta R, Mohan H, Niess H*, et al.* (2007). Genetically engineered stem cells for therapeutic gene delivery. Curr Gene Ther 7, 249-60.

Conrad C, Huesemann Y, Niess H, Von Luettichau I*, et al.* (2011). Linking Transgene Expression of Engineerd Mesenchymal Stem Cells and Angiopoietin-1-induced Differentiation to Target Cancer Angiogenesis. Ann Surg 253, 566-71.

Conrad C, Niess H, Huss R, Huber S*, et al.* (2009). Multipotent mesenchymal stem cells acquire a lymphendothelial phenotype and enhance lymphatic regeneration in vivo. Circulation 119, 281-9.

Dadachova E, Bouzahzah B, Zuckier LS, Pestell RG. (2002). Rhenium-188 as an alternative to iodine-131 for treatment of breast tumors expressing the sodium/iodide symporter (NIS). Nucl Med Biol 29, 13-18.

Dadachova E, Nguyen A, Lin EY, Gnatovskiy L*, et al.* (2005). Treatment with rhenium-188-perrhenate and iodine-131 of NIS-expressing mammary cancer in a mouse model remarkably inhibited tumor growth. Nucl Med Biol 32, 695-700.

Dai GH, Xiu JG, Zhou ZJ, Chen ZC*, et al.* (2007). [Effect of superparamagnetic iron oxide labeling on neural stem cell survival and proliferation]. Nan Fang Yi Ke Da Xue Xue Bao 27, 49-51, 55.

Deng Q, Zhang Z, Feng X, Li T*, et al.* (2014). TRAIL-secreting mesenchymal stem cells promote apoptosis in heat-shock-treated liver cancer cells and inhibit tumor growth in nude mice. Gene Ther.

Denhardt DT, Lopez CA, Rollo EE, Hwang SM*, et al.* (1995). Osteopontin-induced modifications of cellular functions. Ann N Y Acad Sci 760, 127-42.

Di Cosmo C, Liao XH, Dumitrescu AM, Weiss RE*, et al.* (2009). A thyroid hormone analog with reduced dependence on the monocarboxylate transporter 8 for tissue transport. Endocrinology 150, 4450-8.

Dingli D, Diaz RM, Bergert ER, O'connor MK*, et al.* (2003a). Genetically targeted radiotherapy for multiple myeloma. Blood 102, 489-496.

Dingli D, Kemp BJ, O'connor MK, Morris JC*, et al.* (2006). Combined I-124 positron emission tomography/computed tomography imaging of NIS gene expression in animal models of stably transfected and intravenously transfected tumor. Mol Imaging Biol 8, 16-23.

Dingli D, Peng K-W, Harvey ME, Greipp PR*, et al.* (2004). Image-guided radiovirotherapy for multiple myeloma using a recombinant measles virus expressing the thyroidal sodium iodide symporter. In *Blood*. pp 1641-1646.

Dingli D, Russell SJ, Morris JC. (2003b). In vivo imaging and tumor therapy with the sodium iodide symporter. J Cell Biochem 90, 1079-1086.

Direkze NC, Hodivala-Dilke K, Jeffery R, Hunt T*, et al.* (2004). Bone marrow contribution to tumor-associated myofibroblasts and fibroblasts. Cancer Res 64, 8492-5.

Duffy MR, Parker AL, Bradshaw AC, Baker AH. (2012). Manipulation of adenovirus interactions with host factors for gene therapy applications. Nanomedicine (Lond) 7, 271-88.

Dvorak HF. (1986). Tumors: wounds that do not heal. Similarities between tumor stroma generation and wound healing. N Engl J Med 315, 1650-9.

Dwyer RM, Bergert ER, O'connor M K, Gendler SJ*, et al.* (2005a). In vivo radioiodide imaging and treatment of breast cancer xenografts after MUC1-driven expression of the sodium iodide symporter. Clin Cancer Res 11, 1483-9.

Dwyer RM, Bergert ER, O'connor MK, Gendler SJ*, et al.* (2006). Adenovirus-mediated and targeted expression of the sodium-iodide symporter permits in vivo radioiodide imaging and therapy of pancreatic tumors. Hum Gene Ther 17, 661-8.

Dwyer RM, Kerin MJ. (2010). Mesenchymal stem cells and cancer: tumor-specific delivery vehicles or therapeutic targets? Hum Gene Ther 21, 1506-12.

Dwyer RM, Khan S, Barry FP, O'brien T*, et al.* (2010). Advances in mesenchymal stem cell-mediated gene therapy for cancer. Stem Cell Res Ther 1, 25.

Dwyer RM, Potter-Beirne SM, Harrington KA, Lowery AJ*, et al.* (2007). Monocyte chemotactic protein-1 secreted by primary breast tumors stimulates migration of mesenchymal stem cells. Clin Cancer Res 13, 5020-7.

Dwyer RM, Ryan J, Havelin RJ, Morris JC*, et al.* (2011). Mesenchymal Stem Cell-mediated delivery of the sodium iodide symporter supports radionuclide imaging and treatment of breast cancer. Stem Cells 29, 1149-57.

Dwyer RM, Schatz SM, Bergert ER, Myers RM*, et al.* (2005b). A preclinical large animal model of adenovirus-mediated expression of the sodium-iodide symporter for radioiodide imaging and therapy of locally recurrent prostate cancer. Mol Ther 12, 835-41.

Edelmann SL, Nelson PJ, Brocker T. (2011). Comparative promoter analysis in vivo: identification of a dendritic cell-specific promoter module. Blood 118, e40-9.

Engels B, Rowley DA, Schreiber H. (2012). Targeting stroma to treat cancers. Semin Cancer Biol 22, 41-9.

Fidler IJ. (1990). Critical factors in the biology of human cancer metastasis: twenty-eighth G.H.A. Clowes memorial award lecture. Cancer Res 50, 6130-8.

Fischer M, Juremalm M, Olsson N, Backlin C*, et al.* (2003). Expression of CCL5/RANTES by Hodgkin and Reed-Sternberg cells and its possible role in the recruitment of mast cells into lymphomatous tissue. Int J Cancer 107, 197-201.

Forte G, Minieri M, Cossa P, Antenucci D*, et al.* (2006). Hepatocyte growth factor effects on mesenchymal stem cells: proliferation, migration, and differentiation. Stem Cells 24, 23-33.

Fritz V, Jorgensen C. (2008). Mesenchymal stem cells: an emerging tool for cancer targeting and therapy. Curr Stem Cell Res Ther 3, 32-42.

Gao D, Mittal V. (2009). The role of bone-marrow-derived cells in tumor growth, metastasis initiation and progression. Trends Mol Med 15, 333-43.

Gao P, Ding Q, Wu Z, Jiang H*, et al.* (2010). Therapeutic potential of human mesenchymal stem cells producing IL-12 in a mouse xenograft model of renal cell carcinoma. Cancer Lett 290, 157-66.

Gnecchi M, Zhang Z, Ni A, Dzau VJ. (2008). Paracrine mechanisms in adult stem cell signaling and therapy. Circ Res 103, 1204-19.

Goel A, Carlson SK, Classic KL, Greiner S*, et al.* (2007). Radioiodide imaging and radiovirotherapy of multiple myeloma using VSV({Delta}51)-NIS, an attenuated vesicular stomatitis virus encoding the sodium iodide symporter gene. In *Blood*. pp 2342-2350.

Grone HJ, Weber C, Weber KS, Grone EF*, et al.* (1999). Met-RANTES reduces vascular and tubular damage during acute renal transplant rejection: blocking monocyte arrest and recruitment. FASEB J 13, 1371-83.

Groot-Wassink T, Aboagye EO, Wang Y, Lemoine NR*, et al.* (2004). Quantitative imaging of Na/I symporter transgene expression using positron emission tomography in the living animal. Mol Therapy 9, 436-442.

Grunwald GK, Klutz K, Willhauck MJ, Schwenk N*, et al.* (2013a). Sodium iodide symporter (NIS)-mediated radiovirotherapy of hepatocellular cancer using a conditionally replicating adenovirus. Gene Ther 20, 625-33.

Grunwald GK, Vetter A, Klutz K, Willhauck MJ*, et al.* (2013b). EGFR-Targeted Adenovirus Dendrimer Coating for Improved Systemic Delivery of the Theranostic NIS Gene. Mol Ther Nucleic Acids 2, e131.

Grunwald GK, Vetter A, Klutz K, Willhauck MJ*, et al.* (2013c). Systemic image-guided liver cancer radiovirotherapy using dendrimer-coated adenovirus encoding the sodium iodide symporter as theranostic gene. J Nucl Med 54, 1450-7.

Hall B, Dembinski J, Sasser AK, Studeny M*, et al.* (2007). Mesenchymal stem cells in cancer: tumor-associated fibroblasts and cell-based delivery vehicles. Int J Hematol 86, 8-16.

Hanahan D, Weinberg RA. (2000). The hallmarks of cancer. Cell 100, 57-70.

Hanahan D, Weinberg RA. (2011). Hallmarks of cancer: the next generation. Cell 144, 646-74.

Herve J, Cunha AS, Liu B, Valogne Y*, et al.* (2008). Internal radiotherapy of liver cancer with rat hepatocarcinoma-intestine-pancreas gene as a liver tumor-specific promoter. Hum Gene Ther 19, 915-26.

Hingorani M, Spitzweg C, Vassaux G, Newbold K*, et al.* (2010). The biology of the sodium iodide symporter and its potential for targeted gene delivery. Curr Cancer Drug Targets 10, 242-67.

Hingorani M, White CL, Agrawal VK, Vidal L*, et al.* (2007). Combining radiation and cancer gene therapy: a potential marriage of physical and biological targeting? Curr Cancer Drug Targets 7, 389-409.

Hocking AM, Gibran NS. (2010). Mesenchymal stem cells: paracrine signaling and differentiation during cutaneous wound repair. Exp Cell Res 316, 2213-9.

Hung SC, Deng WP, Yang WK, Liu RS*, et al.* (2005). Mesenchymal stem cell targeting of microscopic tumors and tumor stroma development monitored by noninvasive in vivo positron emission tomography imaging. Clin Cancer Res 11, 7749-56.

Jauregui-Osoro M, Sunassee K, Weeks AJ, Berry DJ*, et al.* (2010). Synthesis and biological evaluation of [(18)F]tetrafluoroborate: a PET imaging agent for thyroid disease and reporter gene imaging of the sodium/iodide symporter. Eur J Nucl Med Mol Imaging 37, 2108-16.

Kakinuma H, Bergert ER, Spitzweg C, Cheville JC*, et al.* (2003). Probasin promoter (ARR(2)PB)-driven, prostate-specific expression of the human sodium iodide symporter (h-NIS) for targeted radioiodine therapy of prostate cancer. Cancer Res 63, 7840-4.

Karar J, Maity A. (2009). Modulating the tumor microenvironment to increase radiation responsiveness. Cancer Biol Ther 8, 1994-2001.

Karnoub AE, Dash AB, Vo AP, Sullivan A*, et al.* (2007). Mesenchymal stem cells within tumour stroma promote breast cancer metastasis. Nature 449, 557-63.

Kidd S, Spaeth E, Dembinski JL, Dietrich M*, et al.* (2009). Direct evidence of mesenchymal stem cell tropism for tumor and wounding microenvironments using in vivo bioluminescent imaging. Stem Cells 27, 2614-23.

Kim SM, Lim JY, Park SI, Jeong CH*, et al.* (2008). Gene therapy using TRAIL-secreting human umbilical cord blood-derived mesenchymal stem cells against intracranial glioma. Cancer Res 68, 9614-23.

Kim SM, Oh JH, Park SA, Ryu CH*, et al.* (2010). Irradiation Enhances the Tumor Tropism and Therapeutic Potential of TRAIL-Secreting Human Umbilical Cord Blood-Derived Mesenchymal Stem Cells in Glioma Therapy. Stem Cells.

Klopp AH, Spaeth EL, Dembinski JL, Woodward WA*, et al.* (2007). Tumor irradiation increases the recruitment of circulating mesenchymal stem cells into the tumor microenvironment. Cancer Res 67, 11687-95.

Klutz K, Russ V, Willhauck MJ, Wunderlich N*, et al.* (2009). Targeted radioiodine therapy of neuroblastoma tumors following systemic nonviral delivery of the sodium iodide symporter gene. Clin Cancer Res 15, 6079-86.

Klutz K, Schaffert D, Willhauck MJ, Grunwald GK*, et al.* (2011a). Epidermal growth factor receptor-targeted (131)I-therapy of liver cancer following systemic delivery of the sodium iodide symporter gene. Mol Ther 19, 676-85.

Klutz K, Willhauck MJ, Wunderlich N, Zach C*, et al.* (2011b). Sodium iodide symporter (NIS)-mediated radionuclide ((131)I, (188)Re) therapy of liver cancer after transcriptionally targeted intratumoral in vivo NIS gene delivery. Hum Gene Ther 22, 1403-12.

Knoop K, Kolokythas M, Klutz K, Willhauck MJ*, et al.* (2011). Image-guided, tumor stroma-targeted 131I therapy of hepatocellular cancer after systemic mesenchymal stem cell-mediated NIS gene delivery. Mol Ther 19, 1704-13.

Knoop K, Schwenk N, Dolp P, Willhauck MJ*, et al.* (2013). Stromal targeting of sodium iodide symporter using mesenchymal stem cells allows enhanced imaging and therapy of hepatocellular carcinoma. Hum Gene Ther 24, 306-16.

Komarova S, Kawakami Y, Stoff-Khalili MA, Curiel DT*, et al.* (2006). Mesenchymal progenitor cells as cellular vehicles for delivery of oncolytic adenoviruses. Mol Cancer Ther 5, 755-66.

Konig JE, Senge T, Allhoff EP, Konig W. (2004). Analysis of the inflammatory network in benign prostate hyperplasia and prostate cancer. Prostate 58, 121-9.

Korbling M, Estrov Z. (2003). Adult stem cells for tissue repair - a new therapeutic concept? N Engl J Med 349, 570-82.

Kumar S, Chanda D, Ponnazhagan S. (2008). Therapeutic potential of genetically modified mesenchymal stem cells. Gene Ther 15, 711-5.

Lavilla-Alonso S, Abo-Ramadan U, Halavaara J, Escutenaire S*, et al.* (2011). Optimized mouse model for the imaging of tumor metastasis upon experimental therapy. PLoS One 6, e26810.

Li H, Fan X, Houghton J. (2007). Tumor microenvironment: the role of the tumor stroma in cancer. J Cell Biochem 101, 805-15.

Li H, Peng KW, Dingli D, Kratzke RA*, et al.* (2010). Oncolytic measles viruses encoding interferon beta and the thyroidal sodium iodide symporter gene for mesothelioma virotherapy. Cancer Gene Ther 17, 550-8.

Loebinger MR, Eddaoudi A, Davies D, Janes SM. (2009a). Mesenchymal stem cell delivery of TRAIL can eliminate metastatic cancer. Cancer Res 69, 4134-42.

Loebinger MR, Kyrtatos PG, Turmaine M, Price AN*, et al.* (2009b). Magnetic resonance imaging of mesenchymal stem cells homing to pulmonary metastases using biocompatible magnetic nanoparticles. Cancer Res 69, 8862-7.

Luboshits G, Shina S, Kaplan O, Engelberg S*, et al.* (1999). Elevated expression of the CC chemokine regulated on activation, normal T cell expressed and secreted (RANTES) in advanced breast carcinoma. Cancer Res 59, 4681-7.

Mascia F, Mariani V, Girolomoni G, Pastore S. (2003). Blockade of the EGF receptor induces a deranged chemokine expression in keratinocytes leading to enhanced skin inflammation. Am J Pathol 163, 303-12.

Mcallister SS, Gifford AM, Greiner AL, Kelleher SP*, et al.* (2008). Systemic endocrine instigation of indolent tumor growth requires osteopontin. Cell 133, 994-1005.

Menon LG, Picinich S, Koneru R, Gao H*, et al.* (2007). Differential gene expression associated with migration of mesenchymal stem cells to conditioned medium from tumor cells or bone marrow cells. Stem Cells 25, 520-8.

Merron A, Peerlinck I, Martin-Duque P, Burnet J*, et al.* (2007). SPECT/CT imaging of oncolytic adenovirus propagation in tumours in vivo using the Na/I symporter as a reporter gene. Gene Ther 14, 1731-8.

Meyer M, Wagner E. (2006). Recent developments in the application of plasmid DNA-based vectors and small interfering RNA therapeutics for cancer. Hum.Gene Ther. 17, 1062-1076.

Mi Z, Bhattacharya SD, Kim VM, Guo H*, et al.* (2011). Osteopontin promotes CCL5-mesenchymal stromal cell-mediated breast cancer metastasis. Carcinogenesis 32, 477-87.

Mohr A, Lyons M, Deedigan L, Harte T*, et al.* (2008). Mesenchymal stem cells expressing TRAIL lead to tumour growth inhibition in an experimental lung cancer model. J Cell Mol Med 12, 2628-43.

Mrowietz U, Schwenk U, Maune S, Bartels J*, et al.* (1999). The chemokine RANTES is secreted by human melanoma cells and is associated with enhanced tumour formation in nude mice. Br J Cancer 79, 1025-31.

Mueller MM, Fusenig NE. (2004). Friends or foes - bipolar effects of the tumour stroma in cancer. Nat Rev Cancer 4, 839-49.

Nakajima M, Morikawa K, Fabra A, Bucana CD*, et al.* (1990). Influence of organ environment on extracellular matrix degradative activity and metastasis of human colon carcinoma cells. J Natl Cancer Inst 82, 1890-8.

Nakamizo A, Marini F, Amano T, Khan A*, et al.* (2005). Human bone marrow-derived mesenchymal stem cells in the treatment of gliomas. Cancer Res 65, 3307-18.

Nelson PJ, Kim HT, Manning WC, Goralski TJ*, et al.* (1993). Genomic organization and transcriptional regulation of the RANTES chemokine gene. J Immunol 151, 2601-12.

Niess H, Bao Q, Conrad C, Zischek C*, et al.* (2011). Selective targeting of genetically engineered mesenchymal stem cells to tumor stroma microenvironments using tissue-specific suicide gene expression suppresses growth of hepatocellular carcinoma. Ann Surg 254, 767-74; discussion 774-5.

Olumi AF, Grossfeld GD, Hayward SW, Carroll PR*, et al.* (1999). Carcinoma-associated fibroblasts direct tumor progression of initiated human prostatic epithelium. Cancer Res 59, 5002-11.

Orimo A, Gupta PB, Sgroi DC, Arenzana-Seisdedos F*, et al.* (2005). Stromal fibroblasts present in invasive human breast carcinomas promote tumor growth and angiogenesis through elevated SDF-1/CXCL12 secretion. Cell 121, 335-48.

Orimo A, Weinberg RA. (2006). Stromal fibroblasts in cancer: a novel tumor-promoting cell type. Cell Cycle 5, 1597-601.

Parkin DM, Bray F, Ferlay J, Pisani P. (2005). Global cancer statistics, 2002. CA Cancer J Clin 55, 74-108.

Peerlinck I, Merron A, Baril P, Conchon S*, et al.* (2009). Targeted radionuclide therapy using a Wnt-targeted replicating adenovirus encoding the Na/I symporter. Clin Cancer Res 15, 6595-601.

Penheiter AR, Griesmann GE, Federspiel MJ, Dingli D*, et al.* (2012a). Pinhole micro-SPECT/CT for noninvasive monitoring and quantitation of oncolytic virus dispersion and percent infection in solid tumors. Gene Ther 19, 279-87.

Penheiter AR, Russell SJ, Carlson SK. (2012b). The sodium iodide symporter (NIS) as an imaging reporter for gene, viral, and cell-based therapies. Curr Gene Ther 12, 33-47.

Pereira RF, O'hara MD, Laptev AV, Halford KW*, et al.* (1998). Marrow stromal cells as a source of progenitor cells for nonhematopoietic tissues in transgenic mice with a phenotype of osteogenesis imperfecta. Proc Natl Acad Sci U S A 95, 1142-7.

Pinilla S, Alt E, Abdul Khalek FJ, Jotzu C*, et al.* (2009). Tissue resident stem cells produce CCL5 under the influence of cancer cells and thereby promote breast cancer cell invasion. Cancer Lett 284, 80-5.

Pinter M, Hucke F, Graziadei I, Vogel W*, et al.* (2012). Advanced-Stage Hepatocellular Carcinoma: Transarterial Chemoembolization versus Sorafenib. Radiology 263, 590-9.

Pittenger MF. (2008). Mesenchymal stem cells from adult bone marrow. Methods Mol Biol 449, 27-44.

Pittenger MF, Mackay AM, Beck SC, Jaiswal RK*, et al.* (1999). Multilineage potential of adult human mesenchymal stem cells. Science 284, 143-7.

Rad AM, Iskander AS, Janic B, Knight RA*, et al.* (2009). AC133+ progenitor cells as gene delivery vehicle and cellular probe in subcutaneous tumor models: a preliminary study. BMC Biotechnol 9, 28.

Ren C, Kumar S, Chanda D, Chen J*, et al.* (2008). Therapeutic potential of mesenchymal stem cells producing interferon-alpha in a mouse melanoma lung metastasis model. Stem Cells 26, 2332-8.

Richard-Fiardo P, Franken PR, Lamit A, Marsault R*, et al.* (2012). Normalisation to blood activity is required for the accurate quantification of Na/I symporter ectopic expression by SPECT/CT in individual subjects. PLoS One 7, e34086.

Riedel C, Dohan O, De La Vieja A, Ginter CS*, et al.* (2001). Journey of the iodide transporter NIS: from its molecular identification to its clinical role in cancer. Trends Biochem Sci 26, 490-6.

Rominger A, Wagner E, Mille E, Boning G*, et al.* Endogenous competition against binding of [(18)F]DMFP and [(18)F]fallypride to dopamine D(2/3) receptors in brain of living mouse. Synapse 64, 313-22.

Schichor C, Birnbaum T, Etminan N, Schnell O*, et al.* (2006). Vascular endothelial growth factor A contributes to glioma-induced migration of human marrow stromal cells (hMSC). Exp Neurol 199, 301-10.

Scholz IV, Cengic N, Baker CH, Harrington KJ*, et al.* (2005). Radioiodine therapy of colon cancer following tissue-specific sodium iodide symporter gene transfer. Gene Ther 12, 272-80.

Shinagawa K, Kitadai Y, Tanaka M, Sumida T*, et al.* (2013). Stroma-directed imatinib therapy impairs the tumor-promoting effect of bone marrow-derived mesenchymal stem cells in an orthotopic transplantation model of colon cancer. Int J Cancer 132, 813-23.

Siegel R, Naishadham D, Jemal A. (2013). Cancer statistics, 2013. CA Cancer J Clin 63, 11-30.

Son BR, Marquez-Curtis LA, Kucia M, Wysoczynski M*, et al.* (2006). Migration of bone marrow and cord blood mesenchymal stem cells in vitro is regulated by stromal-derived factor-1-CXCR4 and hepatocyte growth factor-c-met axes and involves matrix metalloproteinases. Stem Cells 24, 1254-64.

Soria G, Lebel-Haziv Y, Ehrlich M, Meshel T*, et al.* (2012). Mechanisms regulating the secretion of the promalignancy chemokine CCL5 by breast tumor cells: CCL5's 40s loop and intracellular glycosaminoglycans. Neoplasia 14, 1-19.

Spaeth E, Klopp A, Dembinski J, Andreeff M*, et al.* (2008). Inflammation and tumor microenvironments: defining the migratory itinerary of mesenchymal stem cells. Gene Ther 15, 730-8.

Spaeth EL, Dembinski JL, Sasser AK, Watson K*, et al.* (2009). Mesenchymal stem cell transition to tumor-associated fibroblasts contributes to fibrovascular network expansion and tumor progression. PLoS One 4, e4992.

Spitzweg C. (2009). Gene therapy in thyroid cancer. Horm Metab Res 41, 500-9.

Spitzweg C, Baker CH, Bergert ER, O'connor MK*, et al.* (2007). Image-guided radioiodide therapy of medullary thyroid cancer after carcinoembryonic antigen promoter-targeted sodium iodide symporter gene expression. Hum Gene Ther 18, 916-24.

Spitzweg C, Dietz AB, O'connor MK, Bergert ER*, et al.* (2001a). In vivo sodium iodide symporter gene therapy of prostate cancer. Gene Ther 8, 1524-31.

Spitzweg C, Harrington KJ, Pinke LA, Vile RG*, et al.* (2001b). Clinical review 132: The sodium iodide symporter and its potential role in cancer therapy. J Clin Endocrinol Metab 86, 3327-35.

Spitzweg C, Morris JC. (2002). The sodium iodide symporter: its pathophysiological and therapeutic implications. Clin Endocrinol (Oxf) 57, 559-74.

Spitzweg C, O'connor MK, Bergert ER, Tindall DJ*, et al.* (2000). Treatment of prostate cancer by radioiodine therapy after tissue-specific expression of the sodium iodide symporter. Cancer Res 60, 6526-30.

Spitzweg C, Zhang S, Bergert ER, Castro MR*, et al.* (1999). Prostate-specific antigen (PSA) promoter-driven androgen-inducible expression of sodium iodide symporter in prostate cancer cell lines. Cancer Res 59, 2136-41.

Stormes KA, Lemken CA, Lepre JV, Marinucci MN*, et al.* (2005). Inhibition of metastasis by inhibition of tumor-derived CCL5. Breast Cancer Res Treat 89, 209-12.

Studeny M, Marini FC, Champlin RE, Zompetta C*, et al.* (2002). Bone marrow-derived mesenchymal stem cells as vehicles for interferon-beta delivery into tumors. Cancer Res 62, 3603-8.

Studeny M, Marini FC, Dembinski JL, Zompetta C*, et al.* (2004). Mesenchymal stem cells: potential precursors for tumor stroma and targeted-delivery vehicles for anticancer agents. J Natl Cancer Inst 96, 1593-603.

Su B, Cengizeroglu A, Farkasova K, Viola JR*, et al.* (2013). Systemic TNFalpha gene therapy synergizes with liposomal doxorubicine in the treatment of metastatic cancer. Mol Ther 21, 300-8.

Sugimoto H, Mundel TM, Kieran MW, Kalluri R. (2006). Identification of fibroblast heterogeneity in the tumor microenvironment. Cancer Biol Ther 5, 1640-6.

Tan MC, Goedegebuure PS, Belt BA, Flaherty B*, et al.* (2009). Disruption of CCR5-dependent homing of regulatory T cells inhibits tumor growth in a murine model of pancreatic cancer. J Immunol 182, 1746-55.

Tanaka T, Bai Z, Srinoulprasert Y, Yang BG*, et al.* (2005). Chemokines in tumor progression and metastasis. Cancer Sci 96, 317-22.

Tang C, Russell PJ, Martiniello-Wilks R, Rasko JE*, et al.* (2010). Concise review: Nanoparticles and cellular carriers-allies in cancer imaging and cellular gene therapy? Stem Cells 28, 1686-702.

Teo GS, Ankrum JA, Martinelli R, Boetto SE*, et al.* (2012). Mesenchymal stem cells transmigrate between and directly through tumor necrosis factor-alpha-activated endothelial cells via both leukocyte-like and novel mechanisms. Stem Cells 30, 2472-86.

Thalmeier K, Huss R. (2001). Highly efficient retroviral gene transfer into immortalized CD34(-) cells and organ distribution after transplantation into NOD/SCID mice. Cytotherapy 3, 245-51.

Touchefeu Y, Harrington KJ, Galmiche JP, Vassaux G. (2010). Review article: gene therapy, recent developments and future prospects in gastrointestinal oncology. Aliment Pharmacol Ther 32, 953-68.

Trujillo MA, Oneal MJ, Mcdonough S, Qin R*, et al.* A probasin promoter, conditionally replicating adenovirus that expresses the sodium iodide symporter (NIS) for radiovirotherapy of prostate cancer. Gene Ther.

Uchibori R, Tsukahara T, Mizuguchi H, Saga Y*, et al.* (2013). NF-kappaB activity regulates mesenchymal stem cell accumulation at tumor sites. Cancer Res 73, 364-72.

Viola A, Sarukhan A, Bronte V, Molon B. (2012). The pros and cons of chemokines in tumor immunology. Trends Immunol 33, 496-504.

Von Luettichau I, Nelson PJ, Pattison JM, Van De Rijn M*, et al.* (1996). RANTES chemokine expression in diseased and normal human tissues. Cytokine 8, 89-98.

Von Luttichau I, Notohamiprodjo M, Wechselberger A, Peters C*, et al.* (2005). Human adult CD34- progenitor cells functionally express the chemokine receptors CCR1, CCR4, CCR7, CXCR5, and CCR10 but not CXCR4. Stem Cells Dev 14, 329-36.

Wapnir IL, Goris M, Yudd A, Dohan O*, et al.* (2004). The Na+/I- symporter mediates iodide uptake in breast cancer metastases and can be selectively down-regulated in the thyroid. Clin Cancer Res 10, 4294-4302.

Willhauck MJ, Mirancea N, Vosseler S, Pavesio A*, et al.* (2007a). Reversion of tumor phenotype in surface transplants of skin SCC cells by scaffold-induced stroma modulation. Carcinogenesis 28, 595-610.

Willhauck MJ, Samani BR, Gildehaus FJ, Wolf I*, et al.* (2007b). Application of 188Re as an Alternative Radionuclide for Treatment of Prostate Cancer following Tumor-Specific Sodium Iodide Symporter Gene Expression. J Clin Endocrinol Metab 92, 4451-8.

Willhauck MJ, Samani BR, Wolf I, Senekowitsch-Schmidtke R*, et al.* (2008a). The potential of 211Astatine for NIS-mediated radionuclide therapy in prostate cancer. Eur J Nucl Med Mol Imaging 35, 1272-81.

Willhauck MJ, Sharif-Samani B, Senekowitsch-Schmidtke R, Wunderlich N*, et al.* (2008b). Functional sodium iodide symporter expression in breast cancer xenografts in vivo after systemic treatment with retinoic acid and dexamethasone. Breast Cancer Res Treat 109, 263-72.

Willhauck MJ, Sharif Samani BR, Klutz K, Cengic N*, et al.* (2008c). Alpha-fetoprotein promoter-targeted sodium iodide symporter gene therapy of hepatocellular carcinoma. Gene Ther 15, 214-23.

Wilmanns C, Fan D, O'brian CA, Bucana CD*, et al.* (1992). Orthotopic and ectopic organ environments differentially influence the sensitivity of murine colon carcinoma cells to doxorubicin and 5-fluorouracil. Int J Cancer 52, 98-104.

Xin H, Kanehira M, Mizuguchi H, Hayakawa T*, et al.* (2007). Targeted delivery of CX3CL1 to multiple lung tumors by mesenchymal stem cells. Stem Cells 25, 1618-26.

Yang JD, Nakamura I, Roberts LR. (2011). The tumor microenvironment in hepatocellular carcinoma: current status and therapeutic targets. Semin Cancer Biol 21, 35-43.

Yao X, Hu JF, Daniels M, Yien H*, et al.* (2003). A novel orthotopic tumor model to study growth factors and oncogenes in hepatocarcinogenesis. Clin Cancer Res 9, 2719-26.

Zacharek A, Chen J, Cui X, Li A*, et al.* (2007). Angiopoietin1/Tie2 and VEGF/Flk1 induced by MSC treatment amplifies angiogenesis and vascular stabilization after stroke. J Cereb Blood Flow Metab 27, 1684-91.

Zhao D, Najbauer J, Annala AJ, Garcia E*, et al.* (2012). Human neural stem cell tropism to metastatic breast cancer. Stem Cells 30, 314-25.

Zischek C, Niess H, Ischenko I, Conrad C*, et al.* (2009). Targeting tumor stroma using engineered mesenchymal stem cells reduces the growth of pancreatic carcinoma. Ann Surg 250, 747-53.

Zlotnik A, Yoshie O. (2000). Chemokines: a new classification system and their role in immunity. Immunity 12, 121-7.

9 Acknowledgments

First, I would like to thank Prof. Dr. Christine Spitzweg who offered me the possibility to work on this exciting project, for providing me with all the equipment and infrastructure needed as well as for her continuous support, encouragement and excellent mentoring throughout my thesis.

Further, I would like to thank Prof. Dr. Ernst Wagner for many helpful discussions and for accepting me as an external PhD student at the Department of Pharmacy, Center of Drug Research, Pharmaceutical Biology-Biotechnology, Ludwig-Maximilians-University, Munich. Also all of his lab members are gratefully acknowledged for their help.

I am also very grateful to Prof. Dr. Peter Nelson from the Department of Clinical Biochemistry, for his scientific support, for his always helpful advice, many fruitful discussions, and for a great collaboration.

Many thanks to all current and former members of the Spitzweg laboratory, Nathalie Schwenk, Katy Schmohl, Andrea Müller, Karoline Kläring, Patrick Dolp, Marie Kolokythas, Dr. Michael Willhauck, Dr. Kathrin Klutz and Dr. Geoffrey Grünwald for assisting, listening, helping, for all the fun we had at night or by day and for so much more. I enjoyed working with you.

I would further like to thank the members of the department of Nuclear Medicine at the Klinikum Großhadern (director: Prof. Dr. Peter Bartenstein) and the department of Clinical Radiology (director: Prof. Dr. Maximilian Reiser) for the great support, personal and technical assistance during imaging and therapy studies. My personal thanks to Matthias Moser for all the fun we had during MR imagings.

I am also grateful to the Members of SFB 824 for their collaboration.

Finally, I want to thank my friends, my family and Rolf Gölfert, who supported me during these years and especially during the final rush, who never stopped believing in me and showed me that life consists of more than science!